CÉLIO CABRAL OLIVEIRA

RGS1 PHOSPHO-BARCODE: DECODING HOW G SIGNALING IS MODULATED IN PLANTS THROUGH THE PHOSPHORYLATION OF ITS COMPONENTS

Thesis submitted to the Applied Biochemistry Graduate Program of the Universidade Federal de Viçosa in partial fulfillment of the requirements for the degree of *Doctor Scientiae*.

Advisor: Pedro Augusto Braga dos Reis

Co-advisors: Elizabeth Pacheco Batista Fontes
Alan M. Jones

VIÇOSA - MINAS GERAIS
2022

Ficha catalográfica elaborada pela Biblioteca Central da Universidade Federal de Viçosa - Campus Viçosa

T
O48c
2022

Oliveira, Célio Cabral, 1995-
RGS1 phospho barcode: decoding how G signaling is modulated in plants through the phosphorylation of its components / Célio Cabral Oliveira. – Viçosa, MG, 2022.
1 tese eletrônica (75 f.): il. (algumas color.).

Texto em inglês.
Orientador: Pedro Augusto Braga dos Reis.
Tese (doutorado) - Universidade Federal de Viçosa, Departamento de Bioquímica e Biologia Molecular, 2022.
Inclui bibliografia.
DOI: https://doi.org/10.47328/ufvbbt.2022.536
Modo de acesso: World Wide Web.

1. Marcadores genéticos. 2. Proteína G. 3. Fosforilação. I. Reis, Pedro Augusto Braga dos, 1985-. II. Universidade Federal de Viçosa. Departamento de Bioquímica e Biologia Molecular. Doutorado em Bioquímica Aplicada. III. Título.

CDD 22. ed. 572.64

Bibliotecário(a) responsável: Euzébio Luiz Pinto CRB-6/3317

CÉLIO CABRAL OLIVEIRA

RGS1 PHOSPHO-BARCODE: DECODING HOW G SIGNALING IS MODULATED IN PLANTS THROUGH THE PHOSPHORYLATION OF ITS COMPONENTS

Thesis submitted to the Applied Biochemistry Graduate Program of the Universidade Federal de Viçosa in partial fulfillment of the requirements for the degree of *Doctor Scientiae*.

APPROVED: August 16, 2022

Assent:

Célio Cabral Oliveira
Author

Pedro Augusto Braga dos Reis
Advisor

ACKNOWLEDGMENTS

This work would not be possible without the support of the best mentors that I could have asked for. I am extremely grateful to my advisor Dr. Pedro Reis, who guided me with his amazing mind for science and with his best efforts to help me on every single moment of this journey. I am also deeply indebted to my co-advisor Dr. Elizabeth Fontes, who has been a reference for me since my undergraduate studies. Thus, words cannot express my gratitude to Dr. Alan Jones, who opened his lab for me and did every single thing that he could to make me feel welcomed.

I am also grateful to the University of North Carolina at Chapel Hill and to the Applied Biochemistry graduate program from the Universidade Federal de Viçosa. Special thanks to my colleagues Dr. Jia Haiyan and Jing Yang for being outstanding coworkers that have a great part in this work. Additionally, I would be remiss in not mentioning Emma, my very first driving instructor and the best company in the world.

I had the pleasure of collaborating with Dr. Daisuke Urano, who contributed with the outstanding evolutionary data presented in here. I really appreciate his efforts. Special thanks to Otto, my best friend since registration day. And to all my friends that stayed by my side over the past years: Amanda, Eduardo, Gabriel, Giovana, Jonatas, Luiz, Nathalia, Paulinha, Victor and many others that I am grateful to have in my life.

I am also thankful to my boyfriend and partner for life Matheus, who was always able to shed a light during my darkest moments. To my mother Claudia and to my brother Cesar, for believing in my dreams.

Finally, I express my gratitude to President Dilma Rousseff and all of the people involved in the creation of the Quota Law, Science Without Borders and many other social programs that allowed me, as a public-school student, to be a research doctor.

This study was financed in part by the Coordenação de Aperfeiçoamento de Pessoal de Nível Superior - Brasil (CAPES) - Finance Code 001. Additional financial support was provided by CNPq, FAPEMIG, NIGMS and NSF.

RESUMO

OLIVEIRA, Célio Cabral, D.Sc. Universidade Federal de Viçosa, Agosto de 2022. **Código de barras de fosforilação de RGS1: decodificando como a sinalização G é modulada em plantas por meio da fosforilação de seus componentes.** Orientador: Pedro Augusto Braga dos Reis. Coorientadores: Alan M. Jones e Elizabeth Pacheco Batista Fontes.

Plantas desencadeiam complexos mecanismos de sinalização celular em respostas a variações ambientais. Neste contexto, vias controladas por proteínas G heterotriméricas desempenham um papel extremamente importante. O complexo G é composto por uma subunidade alfa que se liga a nucleotídeos de guanina, uma subunidade beta e uma subunidade gama. Apesar destas serem conservadas em eucariotos durante o processo evolutivo, plantas, algas verdes e protistas, assim como organismos da base evolutiva, apresentam subunidades alfa capazes de autoativação por meio da troca acelerada de GDP por GTP em seu domínio catalítico. Assim, as proteínas autoativadoras diferem de seus ortólogos na regulação em que, ao invés de serem controladas ao nível de ativação por receptores acoplados a proteínas G (GPCRs), são reguladas através da aceleração da atividade GTPase por proteínas do tipo RGS (reguladores da sinalização G) que contém sete domínios transmembrana (7TM). Diferentemente do mecanismo clássico de ativação por meio da ligação de GTP/GDP em Gα, modificações pós-traducionais em componentes do complexo adicionam uma nova camada de sensibilização, discriminação e propagação de estímulos distintos, estabelecendo um modelo de quatro estados. Embora muitos sítios de fosforilação nos componentes já sejam identificados, os mecanismos envolvidos e a especificidade de cada um deles em vias de sinalização ainda não são elucidados. De maneira a avançar no entendimento deste controle nos componentes do complexo G, como também seu regulador RGS, utilizamos o organismo modelo *Arabidopsis thaliana* e avaliamos o efeito de fosforilação das subunidades G na ativação e distinção de sinal sob diferentes condições. No primeiro capítulo, convergimos dados de fosforilação *in vivo* e *in vitro* de subunidades canônicas e não canônicas, destacando a sua conservação entre eucariotos. Evidenciou-se os receptores do tipo cinase envolvidos e o possível efeito destas modificações na plasticidade de sinal. No segundo capítulo, por meio de mutação sítio dirigida foram gerados mutantes fosfomiméticos e fosfonulos nos resíduos de AtRGS1 que apresentam maior conservação entre espécies e que foram previamente identificados ser fosforilados. Assim, foi avaliado o papel destes resíduos na interação com proteínas do complexo G e com possíveis adaptadores envolvidos em sua localização subcelular. Estes dados, juntamente com dados de microscopia confocal, imunodetecção de proteínas e as mais modernas ferramentas de modelagem estrutural de proteínas, revelam um mecanismo de fosforilação possivelmente

conservado em plantas em que múltiplos resíduos são fosforilados de maneira cooperativa e específica em resposta a diferentes estímulos. Por várias linhas de evidência identificamos o resíduo de serina 278 como importante modulador da função e sinalização mediada por RGS1. Primeiramente, a mutação do resíduo de serina para ácido glutâmico diminui significativamente a interação com proteínas do complexo G e VPS26b (Vacuolar Protein Sorting 26). Segundo, o processo de internalização de RGS1 mediante ao estímulo por flg22 requer a fosforilação do resíduo 278, enquanto, para UDP-glicose, este resíduo é parcialmente requerido. Terceiro, o mutante fosfonulo S278A diminui o recrutamento das proteínas VPS26 mediante a elicitação por flg22. Finalmente, este resíduo é consideravelmente conservado em uma região flexível da proteína capaz de regular o nível de fosforilação de resíduos presentes na cauda C-terminal de ARGS1, assim como de um ou mais resíduos de treonina detectados pela primeira vez *in vivo*. Além disso, em simulações de dinâmica molecular, nota-se o efeito deste resíduo no posicionamento de domínios e flexibilidade de regiões paralelas. Neste contexto, este trabalho apresenta a importância elevada de modificações pós-tradicionais na distinção de sinais desencadeados por sinalização de proteínas G, além de evidenciar a relação dessas modificações com alterações estruturais da proteína RGS1 e que governam suas repostas a estímulos específicos.

Palavras-chave: RGS. Fosforilação. Flg22. Proteína G. 7TM.

ABSTRACT

OLIVEIRA, Célio Cabral, D.Sc. Universidade Federal de Viçosa, August, 2022. **RGS1 phospho-barcode: decoding how G signaling is modulated in plants through the phosphorylation of its components.** Advisor: Pedro Augusto Braga dos Reis. Co-advisors: Alan M. Jones and Elizabeth Pacheco Batista Fontes.

Plants activate complex mechanisms of cellular signaling in response to environmental changes. Thus, signaling pathways controlled by the heterotrimeric G protein play an essential role. The G complex is composed of one guanine nucleotide-binding alpha subunit, one beta and one gamma. In spite of the fact that those proteins were conserved in eukaryotes during the evolution process, plants, algae, and protists, as well as organisms at the evolutionary base, possess self-activating alpha subunits with an accelerated GDP-to-GTP exchange activity at its catalytical domain. Thus, self-activating proteins differ from their orthologs at the activation level that is not controlled by G-protein coupled receptors (GPCRs). Instead, those are regulated by RGS (regulator of G-signaling) proteins with a seven-transmembrane (7TM) domain. Differently from the classical switching mechanism via the GTP/GDP state of Gα, the post-translational modifications on G-core components add a new layer of sensitization, discrimination of recognized stimulus, and propagation of stimulus signaling, which defines a four-state model of G-protein activation. Although several phosphorylation sites have already been identified, the underlying mechanisms and the specificity of each of them on signaling pathways are not fully elucidated. Therefore, to shed a light on this additional control layer in G-protein regulation, as well as on the mechanism of its regulator RGS, we used the model organism *Arabidopsis thaliana* and evaluated the effect of phosphorylation in the G subunits in the signal activation and distinction upon different conditions. In the first chapter, we have crossed *in vivo* and *in vitro* phosphorylation data of canonical and non-canonical subunits, and we highlight the phosphosite conservation among eukaryotes. We pointed out the kinase receptors involved and the potential effect of those modifications on signal plasticity. In the second chapter, through site-direct mutagenesis, we generated phosphomimetics and phosphonull mutants of AtRGS1 residues that presented higher conservation among species and were previously identified by their phosphorylation. Thus, we evaluated the central role of those residues in interacting with G complex proteins and with possible adaptors involved in its subcellular localization. These data, taken together with confocal microscopy results, immunodetection methods, and state-of-the-art protein structural modeling tools, reveal a phosphorylation mechanism that is possibly conserved in plants, in which multiple residues are phosphorylated in a cooperative manner to respond to different stimuli. Several lines of

evidence suggest that the serine 278 residue is an essential modulator of RGS1 function and its signaling pathways. First, mutation on the serine residue to glutamic acid significantly decreases the interaction of RGS with G complex proteins and VPS26b (Vacuolar Protein Sorting 26). Second, the RGS internalization process upon flg22 stimulus requires the 278 residue phosphorylation, which is only partially required upon UDP-glucose stimulus. Third, phosphonull S278A mutation decreases the VPS26 proteins recruitment upon flg22 elicitation. Finally, the serine residue 278 is considerably conserved in a flexible protein region, and it regulates the phosphorylation levels of C-terminal tail residues, and one or more threonine residues that are detected for the first time *in vivo*. Moreover, molecular dynamics simulations evidenced the effect of this residue on domain positioning and flexibility of other regions. Accordingly, this work presents the relevance of post-translational modifications in the signal distinction triggered by G protein signaling, in addition to demonstrating the influence of those modifications on the structural alterations in the RGS proteins, which control their specific stimulus responses.

Keywords: RGS. Phosphorylation. Flg22. G-protein. 7TM.

LIST OF ILLUSTRATIONS

Chapter I

Chapter II

LIST OF TABLES

Chapter I

Chapter II

SUMMARY

GENERAL INTRODUCTION

The classical paradigm for heterotrimeric G-proteins is described in mammalian organisms: they are mainly composed of an alpha GDP/GTP-binding subunit and a beta-gamma dimer that has a higher affinity for the GDP-bound form of alpha, defining an inactive state of the dimer (Milligan and Kostenis, 2006; Gilman 1995; Tang et al., 1992). As animal Gα has an intrinsic GTPase activity that may be accelerated by the cytoplasmic regulator of G-signaling (RGS), its activation consists of a nucleotide exchange event that needs to be activated by G-protein-coupled receptors (GPCRs) with a guanine exchange factor (GEF) activity (Masuho et al., 2020; Doyen et al., 2020; Santos-Otte et al., 2019). Additionally, those receptors possess a seven-transmembrane (7TM) domain and an extracellular N-terminal end, which recognizes a series of signals promoting conformational changes and subsequent G-protein activation inside the cell (Rosenbaum et al., 2009). Although this GEF-receptor mechanism is extensively described for eukaryotes, evolutionary data indicate that animals and other unikonts have evolved from 7TM-RGS-possessing organisms that are near the base of the eukaryotic phylogenetic tree (Bradford et al., 2013).

The bikont organisms that maintain 7TM-RGS proteins mainly comprise of land plants, green algae and protists (Bradford et al., 2013; Mohanasundaram et al., 2022). For instance, the model plant *Arabidopsis thaliana* possesses a self-activating Gα (AtGPA1) with a GDP-to-GTP exchange rate 50 times higher than the fastest one identified in animals (Johnston et al., 2007; Jones et al., 2011). In order to regulate this subunit that has greater affinity for GTP than GDP, the 7TM protein AtRGS1 accelerates the rate of hydrolysis by the coupling with the heterotrimeric G-protein subunits (Chen et al., 2003). The regulation in Arabidopsis also diverges from animals regarding signal distinction and subunit diversity: while animals possess a vast number of G-protein subunit-encoding genes that enable signal diversity by different heterotrimer formation, *Arabidopsis thaliana* genome only codes for one canonical alpha, three non-canonical extra-large alpha proteins (AtXLG1/2/3), one beta (AtAGB1) and three gamma subunits (AtAGG1/2/3) (Jones et al., 2011; Willard and Siderovski, 2004; Chakravorty et al., 2015). Moreover, G-proteins are involved in many pathways (Liang et al., 2016; Petutschnig et al., 2022; Afrin et al., 2021; Smythers et al., 2022; Boonyaves et al., 2022; Tiwari and Bisht, 2022; Li et al., 2019; Chen, 2008), and, although AtRGS1 displays a GPCR-like architecture on its 7TM domain, no consistent data indicated it as being a receptor for a ligand (Li et al., 2016; Chen 2008).

Key components of signal recognition and distinction in plants are receptor-like kinases (RLKs), which are single transmembrane domain-containing enzymes with an extracellular

ligand binding site that regulates the intracellular activation of the kinase domain (Jose et al., 2020). A considerable number of RLKs are described to bind and phosphorylate AtRGS1 and other G-protein subunits (Tunc-Ozdemir et al., 2017; Jia et al., 2019; Liang et al., 2016; Petutschnig et al., 2022; Peng et al., 2018). The correlation between RLKs and G-protein signaling distinction is evidenced by the phosphorylation-dependent uncoupling and endocytosis of AtRGS1, which leaves AtGPA1 free for self-activation and subsequent release of the Gβγ subunit (Urano et al., 2012). For instance, the peptide flg22 is a microbe-associated molecular pattern (MAMP), which is recognized by the receptor FLS2 (FLAGELLIN SENSITIVE 2) and its co-receptor BAK1 (BRI1-ASSOCIATED KINASE 1), both required to trigger the immune response inside the cell (Sun et al., 2013; Gómez-Gómez and Boller, 2000). This complex also interacts with AtGPA1 and its regulator AtRGS1, and, in the presence of the pathogen or its MAMPs, activated BAK1 phosphorylates AtRGS1 and AtGPA1 *in vitro* and *in vivo*, promoting dissociation and G-protein activation (Xue et al., 2020; Liang et al., 2018). In addition to the RLKs' role in signaling, AtRGS1 is also phosphorylated by cytoplasmic kinases as the WITH-NO-LYSINE kinases (WNKs) in response to high concentrations of sugar, which also induces internalization (Cao-Pham et al., 2018; Urano et al., 2012).

While flg22-induced internalization of AtRGS1 occurs via the phosphorylation-dependent clathrin-mediated endocytosis (CME) pathway, the internalization induced by D-glucose also activates the sterol-dependent endocytosis (SDE) pathway, which does not require the phosphorylation of three C-terminal tail sites in AtRGS1 (Watkins et al., 2021). This mechanism is related to the biased signaling theory of GPCR-internalization, in which different phosphorylation patterns at the GPCR C-terminal are able to recruit and activate the adaptor proteins, known as β-arrestins, to act in different pathways (Watkins et al., 2021; Latorraca et al., 2020). As the Arabidopsis genome does not encode any β-arrestin, the candidate adaptors are the retromer proteins VPS26a and VPS26b, which interact with AtRGS1 and are required for its CME-mediated endocytosis (Watkins et al., 2021; Zelazny et al., 2013).

The specific sites of phosphorylation for all Arabidopsis G-protein subunits in the literature are identified on the Chapter I, entitled "G-Protein Phosphorylation: Aspects of Binding Specificity and Function in the Plant Kingdom", which describes the *in vitro* and *in vivo* phosphorylation sites, their potential kinases, and the conservation among eukaryotes. Additionally, the effect of those sites on plant signaling and the most recently described mechanisms for plant G-protein activation, were also covered. This chapter is a published review paper that is available at the International Journal of Molecular Sciences (Oliveira et al., 2022).

Regarding specific phosphosites of AtRGS1, the protein has a cluster of five phosphoserines and three of them are required for AtGPA1 uncoupling during several responses (Watkins et al., 2021). Additionally, one residue at a flexible linker region of AtRGS1 (Ser278) and one residue at the very end of the RGSbox (Ser417) have been reported to be phosphorylated *in vivo* (Oliveira et al., 2022). These data are explored in Chapter II, entitled "RGS1 Global Phosphorylation as a Cooperative Mechanism for G-Protein Regulation", in which we took advantage of *in vivo* phosphomimetic mutations, as well as state-of-the-art in silico structural tools to evaluate the effect of the phosphorylation on AtRGS1 dynamics and function. Consistent data reveal a linked mechanism involving the phosphorylation of multiple residues, including a novel *in vivo* phosphorylation of a threonine residue, and a proposed mechanism of interaction plasticity based on positioning of intracellular domains at the plasma membrane.

REFERENCES

Afrin, T., Costello, C. N., Monella, A. N., Kørner, C. J. and Pajerowska-Mukhtar, K. M. (2022). The interplay of GTP-binding protein AGB1 with ER stress sensors IRE1a and IRE1b modulates Arabidopsis unfolded protein response and bacterial immunity. Plant Signal. Behav. 17, 2018857.

Boonyaves, K., Wu, T.-Y., Dong, Y. and Urano, D. (2022). Interplay between ARABIDOPSIS Gβ and WRKY transcription factors differentiates environmental stress responses. Plant Physiol.

Bradford, W., Buckholz, A., Morton, J., Price, C., Jones, A. M. and Urano, D. (2013). Eukaryotic G protein signaling evolved to require G protein-coupled receptors for activation. Sci. Signal. 6, ra37.

Cao-Pham, A. H., Urano, D., Ross-Elliott, T. J. and Jones, A. M. (2018). Nudge-nudge, WNK-WNK (kinases), say no more? New Phytol. 220, 35–48.

Chakravorty, D., Gookin, T. E., Milner, M. J., Yu, Y. and Assmann, S. M. (2015). Extra-Large G Proteins Expand the Repertoire of Subunits in Arabidopsis Heterotrimeric G Protein Signaling. Plant Physiol. 169, 512–529.

Chen, J.-G. (2008a). Heterotrimeric G-proteins in plant development. Front. Biosci. 13, 3321–3333.

Chen, J.-G. (2008b). Heterotrimeric G-protein signaling in Arabidopsis: Puzzling G-protein-coupled receptor. Plant Signal. Behav. 3, 1042–1045.

Chen, J.-G., Willard, F. S., Huang, J., Liang, J., Chasse, S. A., Jones, A. M. and Siderovski, D. P. (2003). A seven-transmembrane RGS protein that modulates plant cell proliferation. Science 301, 1728–1731.

Doyen, P. J., Beckers, P., Brook, G. A. and Hermans, E. (2020). Regulators of G protein signalling as pharmacological targets for the treatment of neuropathic pain. Pharmacol. Res. 160, 105148.

Gilman, A. G. (1995). Nobel Lecture. G proteins and regulation of adenylyl cyclase. Biosci. Rep. 15, 65–97.

Gómez-Gómez, L. and Boller, T. (2000). FLS2: an LRR receptor-like kinase involved in the perception of the bacterial elicitor flagellin in Arabidopsis. Mol. Cell 5, 1003–1011.

Jia, H., Song, G., Werth, E. G., Walley, J. W., Hicks, L. M. and Jones, A. M. (2019). Receptor-Like Kinase Phosphorylation of Arabidopsis Heterotrimeric G-Protein Gα -Subunit AtGPA1. Proteomics 19, e1900265.

Johnston, C. A., Taylor, J. P., Gao, Y., Kimple, A. J., Grigston, J. C., Chen, J.-G., Siderovski, D. P., Jones, A. M. and Willard, F. S. (2007). GTPase acceleration as the rate-limiting step in Arabidopsis G protein-coupled sugar signaling. Proc Natl Acad Sci USA 104, 17317–17322.

Jones, J. C., Duffy, J. W., Machius, M., Temple, B. R. S., Dohlman, H. G. and Jones, A. M. (2011). The crystal structure of a self-activating G protein alpha subunit reveals its distinct mechanism of signal initiation. Sci. Signal. 4, ra8.

Jose, J., Ghantasala, S. and Roy Choudhury, S. (2020). Arabidopsis Transmembrane Receptor-Like Kinases (RLKs): A Bridge between Extracellular Signal and Intracellular Regulatory Machinery. Int. J. Mol. Sci. 21,.

Latorraca, N. R., Masureel, M., Hollingsworth, S. A., Heydenreich, F. M., Suomivuori, C.-M., Brinton, C., Townshend, R. J. L., Bouvier, M., Kobilka, B. K. and Dror, R. O. (2020). How GPCR Phosphorylation Patterns Orchestrate Arrestin-Mediated Signaling. Cell 183, 1813-1825.e18.

Liang, X., Ding, P., Lian, K., Wang, J., Ma, M., Li, L., Li, L., Li, M., Zhang, X., Chen, S., et al. (2016). Arabidopsis heterotrimeric G proteins regulate immunity by directly coupling to the FLS2 receptor. eLife 5, e13568.

Liang, X., Ma, M., Zhou, Z., Wang, J., Yang, X., Rao, S., Bi, G., Li, L., Zhang, X., Chai, J., et al. (2018). Ligand-triggered de-repression of Arabidopsis heterotrimeric G proteins coupled to immune receptor kinases. Cell Res. 28, 529–543.

Li, B., Makino, S.-I., Beebe, E. T., Urano, D., Aceti, D. J., Misenheimer, T. M., Peters, J., Fox, B. G. and Jones, A. M. (2016). Cell-free translation and purification of Arabidopsis thaliana regulator of G signaling 1 protein. Protein Expr. Purif. 126, 33–41.

Li, L., Su, B., Qi, X., Zhang, X., Song, S. and Shan, X. (2019). JA-Induced Endocytosis of AtRGS1 Is Involved in G-Protein Mediated JA Responses. Int. J. Mol. Sci. 20,.

Masuho, I., Balaji, S., Muntean, B. S., Skamangas, N. K., Chavali, S., Tesmer, J. J. G., Babu, M. M. and Martemyanov, K. A. (2020). A global map of G protein signaling regulation by RGS proteins. Cell 183, 503-521.e19.

Milligan, G. and Kostenis, E. (2006). Heterotrimeric G-proteins: a short history. Br. J. Pharmacol. 147 Suppl 1, S46-55.

Mohanasundaram, B., Dodds, A., Kukshal, V., Jez, J. M. and Pandey, S. (2022). Distribution and the evolutionary history of G-protein components in plant and algal lineages. Plant Physiol. 189, 1519–1535.

Oliveira, C. C., Jones, A. M., Fontes, E. P. B. and Reis, P. A. B. D. (2022). G-Protein Phosphorylation: Aspects of Binding Specificity and Function in the Plant Kingdom. Int. J. Mol. Sci. 23,.

Peng, Y., Chen, L., Li, S., Zhang, Y., Xu, R., Liu, Z., Liu, W., Kong, J., Huang, X., Wang, Y., et al. (2018). BRI1 and BAK1 interact with G proteins and regulate sugar-responsive growth and development in Arabidopsis. Nat. Commun. 9, 1522.

Petutschnig, E., Anders, J., Stolze, M., Meusel, C., Hacke, R., Much, L., Schwier, M., Gippert, A.-L., Kroll, S., Fasshauer, P., et al. (2022). EXTRA LARGE G-PROTEIN2 mediates cell

death and hyperimmunity in the chitin elicitor receptor kinase 1-4 mutant. Plant Physiol. 189, 2413–2431.

Rosenbaum, D. M., Rasmussen, S. G. F. and Kobilka, B. K. (2009). The structure and function of G-protein-coupled receptors. Nature 459, 356–363.

Santos-Otte, P., Leysen, H., van Gastel, J., Hendrickx, J. O., Martin, B. and Maudsley, S. (2019). G Protein-Coupled Receptor Systems and Their Role in Cellular Senescence. Comput. Struct. Biotechnol. J. 17, 1265–1277.

Smythers, A. L., Bhatnagar, N., Ha, C., Majumdar, P., McConnell, E. W., Mohanasundaram, B., Hicks, L. M. and Pandey, S. (2022). Abscisic acid-controlled redox proteome of Arabidopsis and its regulation by heterotrimeric Gβ protein. New Phytol.

Sun, Y., Li, L., Macho, A. P., Han, Z., Hu, Z., Zipfel, C., Zhou, J.-M. and Chai, J. (2013). Structural basis for flg22-induced activation of the Arabidopsis FLS2-BAK1 immune complex. Science 342, 624–628.

Tang, W. J., Iñiguez-Lluhi, J. A., Mumby, S. and Gilman, A. G. (1992). Regulation of mammalian adenylyl cyclases by G-protein alpha and beta gamma subunits. Cold Spring Harb. Symp. Quant. Biol. 57, 135–144.

Tiwari, R. and Bisht, N. C. (2022). The multifaceted roles of heterotrimeric G-proteins: lessons from models and crops. Planta 255, 88.

Tunc-Ozdemir, M., Li, B., Jaiswal, D. K., Urano, D., Jones, A. M. and Torres, M. P. (2017). Predicted functional implications of phosphorylation of regulator of G protein signaling protein in plants. Front. Plant Sci. 8, 1456.

Urano, D., Phan, N., Jones, J. C., Yang, J., Huang, J., Grigston, J., Taylor, J. P. and Jones, A. M. (2012). Endocytosis of the seven-transmembrane RGS1 protein activates G-protein-coupled signalling in Arabidopsis. Nat. Cell Biol. 14, 1079–1088.

Watkins, J. M., Ross-Elliott, T. J., Shan, X., Lou, F., Dreyer, B., Tunc-Ozdemir, M., Jia, H., Yang, J., Oliveira, C. C., Wu, L., et al. (2021). Differential regulation of G protein signaling in Arabidopsis through two distinct pathways that internalize AtRGS1. Sci. Signal. 14,.

Willard, F. S. and Siderovski, D. P. (2004). Purification and in vitro functional analysis of the Arabidopsis thaliana regulator of G-protein signaling-1. Meth. Enzymol. 389, 320–338.

Xue, J., Gong, B.-Q., Yao, X., Huang, X. and Li, J.-F. (2020). BAK1-mediated phosphorylation of canonical G protein alpha during flagellin signaling in Arabidopsis. J. Integr. Plant Biol. 62, 690–701.

Zelazny, E., Santambrogio, M. and Gaude, T. (2013). Retromer association with membranes: plants have their own rules! Plant Signal. Behav. 8,.

CHAPTER I

G-PROTEIN PHOSPHORYLATION: ASPECTS OF BINDING SPECIFICITY AND FUNCTION IN THE PLANT KINGDOM

Published article
Celio Cabral Oliveira, Alan M. Jones, Elizabeth Pacheco Batista Fontes, Pedro Augusto Braga dos Reis (2022). G-Protein Phosphorylation: Aspects of Binding Specificity and Function in the Plant Kingdom. International Journal of Molecular Sciences. 23(12):6544. doi: 10.3390/ijms23126544.

Pages 18 to 34

International Journal of
Molecular Sciences

MDPI

Review

G-Protein Phosphorylation: Aspects of Binding Specificity and Function in the Plant Kingdom

Celio Cabral Oliveira [1,2,3], Alan M. Jones [3,4], Elizabeth Pacheco Batista Fontes [1,2] and Pedro A. Braga dos Reis [1,2,*]

[1] Department of Biochemistry and Molecular Biology, Universidade Federal de Viçosa, Viçosa 36570, Brazil; celio.oliveira@ufv.br (C.C.O.); bbfontes@ufv.br (E.P.B.F.)
[2] National Institute of Science and Technology in Plant-Pest Interactions, Bioagro, Viçosa 36570, Brazil
[3] Department of Biology, University of North Carolina at Chapel Hill, Chapel Hill, NC 27599, USA; alanjones@bio.unc.edu
[4] Department of Pharmacology, University of North Carolina at Chapel Hill, Chapel Hill, NC 27599, USA
* Correspondence: pedroreis@ufv.br

Abstract: Plant survival depends on adaptive mechanisms that constantly rely on signal recognition and transduction. The predominant class of signal discriminators is receptor kinases, with a vast member composition in plants. The transduction of signals occurs in part by a simple repertoire of heterotrimeric G proteins, with a core composed of α-, β-, and γ-subunits, together with a 7-transmembrane Regulator G Signaling (RGS) protein. With a small repertoire of G proteins in plants, phosphorylation by receptor kinases is critical in regulating the active state of the G-protein complex. This review describes the in vivo detected phosphosites in plant G proteins and conservation scores, and their in vitro corresponding kinases. Furthermore, recently described outcomes, including novel arrestin-like internalization of RGS and a non-canonical phosphorylation switching mechanism that drives G-protein plasticity, are discussed.

Keywords: phosphorylation; G protein; RGS; GPA1; AGB1; XLG; AGG; kinase; structure; regulation

Citation: Oliveira, C.C.; Jones, A.M.; Fontes, E.P.B.; Reis, P.A.B.d. G-Protein Phosphorylation: Aspects of Binding Specificity and Function in the Plant Kingdom. *Int. J. Mol. Sci.* **2022**, *23*, 6544. https://doi.org/10.3390/ijms23126544

Academic Editor: Karl-Josef Dietz

Received: 24 May 2022
Accepted: 9 June 2022
Published: 11 June 2022

Publisher's Note: MDPI stays neutral with regard to jurisdictional claims in published maps and institutional affiliations.

1. Introduction

Plants lack the mobility mechanisms observed in other kingdoms; hence, their survival depends on adaptive mechanisms that constantly rely on signal perception and transduction [1]. Among the main signaling molecules, the heterotrimeric G proteins play an essential role. They are composed of α-, β-, and γ-subunits, modulated by nucleotide-binding status. The activation/inactivation of the complex occurs through the GTP/GDP binding process. The Gα-GDP binding maintains the complex in an inactive form, and Gα remains associated with Gβ and Gγ proteins. During the activation process, GDP is replaced by GTP, which promotes the dissociation of Gα from Gβγ proteins and, in turn, triggers the downstream signaling [2,3]. The modulation of the Gα protein to GDP-bound or GTP-bound is a precise and specific process. In mammals, the modulation of the GDP-to-GTP exchange mechanism is performed by G-protein-coupled receptors (GPCRs) that act as guanine nucleotide exchange factors (GEFs). Gα protein has intrinsic GTPase activity, but with a slow rate of hydrolysis. Therefore, it requires some factor(s) to accelerate the GTPase activity to modulate the signaling to a steady state (Figure 1) [4,5].

In metazoans, many molecules activate different pathways through G proteins [6]. The signal distinction is mainly explained by a vast combination of subunits and GPCRs present in their genome [7]. On the other hand, plant genomes encode a few subunits; for example, the *Arabidopsis thaliana* genome encodes only one canonical Gα subunit (AtGPA1), three atypical Gα subunits (AtXLG1-3), one beta (AtAGB1), and three gamma (AtAGG1-3) subunits, one RGS regulator (AtRGS1), and no characterized GPCR [8]. This limited number of protein components does not correlate with the complexity of the

signaling events mediated by G protein in plants [9]. The multiplicity of propagated signals from plant G proteins relies on the different activator receptors and various post-translational modifications on the G subunits, rather than the number of components [10]. Moreover, in plants, algae, and protists, Gα presents GPCR-independent nucleotide exchange, and some species are heavily regulated by the atypical seven-transmembrane (7TM) Regulator of G-signaling 1 (RGS1) (Figure 1) [11–13]. As cytoplasmic kinases and receptor-like kinases (RLKs) are consistently linked to G-protein mediation [14–16], here, we discuss the mapping of phosphorylation events and outcomes regarding the G-signaling core in plants.

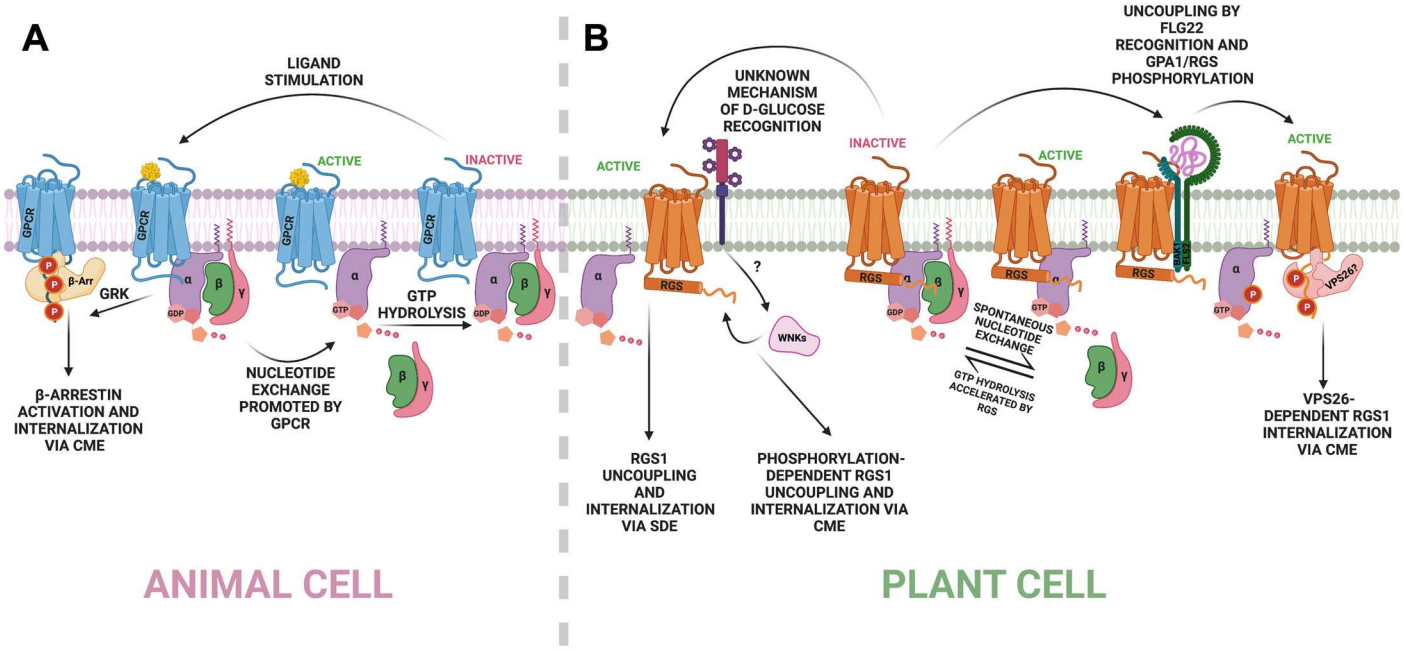

Figure 1. Conserved and non-conserved G-protein activation mechanisms in plants and animals. (**A**) An animal cell recognizes an extracellular signal via GPCR that promotes nucleotide exchange at the alpha subunit. GTP-bound Gα releases G$\beta\gamma$ for downstream signaling. Inactivation occurs under GTP hydrolysis and phosphorylation-induced GPCR internalization. (**B**) Nucleotide exchange is spontaneous in plant cells with no characterized GPCR. Negative regulation via GTPase acceleration activity is promoted by 7TM-RGS proteins. D-glucose activates endocytosis via two different mechanisms: RGS1 is phosphorylated by the WNKs and internalized in a VPS26-independent module via clathrin-mediated endocytosis (CME), or RGS1 is internalized in a phosphorylation-independent mechanism via sterol-dependent endocytosis (SDE). Flg22 is recognized by the BAK1/FLS2 complex, and multiple phosphorylation occurs at GPA1 and at the C-terminus of RGS1. The phosphorylated core is uncoupled, and downstream signaling is activated. Flg22-induced RGS1 internalization occurs via CME in a β-arrestin-like mechanism mediated by the VPS26 proteins. Created with BioRender.com (Publication license OL240ET01G. Accessed on 7 June 2022).

2. Phosphorylation and Internalization of RGS1 in an Arrestin-Like Mechanism

G-protein-coupled receptors are composed of an extracellular N-terminus, a 7TM domain with intra- and extracellular loops, and a disordered cytoplasmic C-terminal domain [17]. GPCRs bind agonists, leading to activation through a conformational change that relays the signal to the Gα subunit regulation by accelerating the release of bound GDP [18]. GPCRs are phosphorylated by GPCR kinases (GRKs), initiating the recruitment and activation of adaptor proteins, β-arrestins, that precede clathrin binding and endocytosis [19]. B-arrestins affect signaling by internalizing the GPCR away from its G-protein complex, and they also propagate signaling by interacting with effector proteins [20]. Different phosphorylation patterns at the V2 vasopressin receptor (V_2R) C-tail

promote different levels of β-arrestin1 binding and activation via conformational changes. Those findings suggest a "phosphorylation barcode" reading in which the spatial arrangement of phosphate groups determines the recruitment and activation of β-arrestins, rather than the number of phosphorylated residues at the receptor (Figure 1) [21].

The structure of the Arabidopsis regulator, AtRGS1, has a hybrid architecture of GPCR topology and an animal RGS protein [22]. The prototype contains a GPCR-like seven-transmembrane barrel domain at the N-terminus, followed by a disordered linker region that may contain a short helix, a conserved RGS domain, and an unstructured C-terminal tail, which harbors several di-serines typical of GPCRs (Figure 2) [23]. AtRGS1 undergoes endocytosis under high concentrations of D-glucose within a few minutes in a Gβ-dependent manner. The C-terminus of the 7TM regulator possesses a cluster of serine residues (Ser428, Ser430, Ser431, Ser435, and Ser436) that resemble the ones found in mammalian organisms. Although GRKs have not been identified in plant genomes, several WNKs (WITH NO LYSINE KINASE) [24] interact with AtRGS1 and phosphorylate the C-tail residues Ser428 and Ser435 or Ser436 in vitro. The inactivation of those phosphosites (Ser → Ala mutation) and the deletion of some *WNK* genes reduce glucose-induced internalization of AtRGS1 [14].

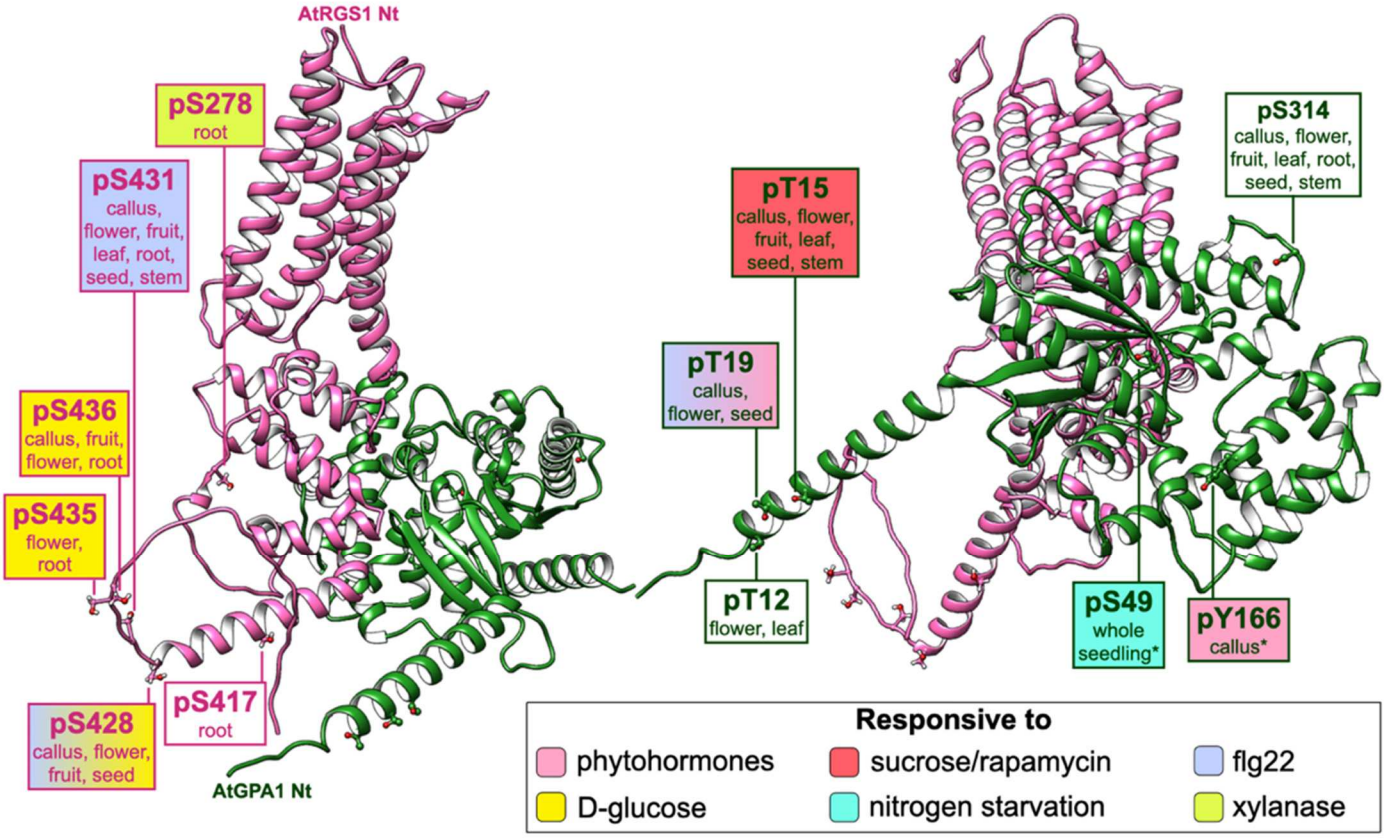

Figure 2. Experimental phosphorylation map of AtRGS1 and AtGPA1 dimer. Structural models of AtRGS1 (hot pink) and AtGPA1 (forest green) are shown. Xylanase-induced phosphorylation is detected at serine 278, which constitutes the linker region of AtRGS1 [25,26]. Phosphorylation occurs at the C-terminal tail of AtRGS1 in the serine residues 417, 428, 430, 431, 435, and 436 [26]. D-glucose-induced phosphorylation of AtRGS1 occurs at Ser428/435/436 [14], and phosphorylation under flg22 treatment is Ser428/431-dependent [27]. AtGPA1 is phosphorylated at the N-terminal threonine residues 12, 15, and 19 [26,28–32]. pThr19 has a reduced phosphorylation signal with flg22 treatment but is induced by ABA. Tyrosine residue 166 is at the all-alpha helical domain interface and responds to several phytohormones [29,33]. Phosphorylation occurs at the catalytic domain of the serine residues 49 and 314, and pSer49 is induced by sugar exposure [26,29,34]. Top-ranked models were obtained using AlphaFold2 [35], and the dimer complex was predicted by overlapping the

models with the crystal structure of the heterodimeric complex of human RGS1 and activated Gi alpha 1 (PDB 2GTP). Phosphosites are represented as balls and sticks. Experimental data were obtained from both the PhosphAt database (https://phosphat.uni-hohenheim.de, accessed on 20 May 2022) and ATHENA (http://athena.proteomics.wzw.tum.de, accessed on 20 May 2022). ATHENA was used to identify tissue-specific phosphorylation, which is pointed out below residue identification. Color filling indicates experimental treatment. Asterisks indicate residues that were not mapped in all tissues.

The peptide flg22, a bacterial elicitor of host responses, binds to its receptor FLS2 (FLAGELLIN-SENSITIVE 2) and co-receptor BAK1 (BRI1-ASSOCIATED RECEPTOR KINASE 1), leading to the induction of specific response genes, ROS production, and calcium signaling [36,37]. However, the deletion of the *AtRGS1* gene impairs the flg22-mediated responses, indicating a genetic interaction between *AtRGS1* and FLS2 signaling [27,38,39]. Furthermore, other biotic pathways (e.g., anti-fungal responses elicited by chitin) are affected by AtRGS1, and bacterial infection in *rgs1-2* plants is attenuated compared to that in the wild type [27]. Since flg22 and chitin act as external signals, it is reasonable to assume that elicitor-modulated RLKs interact with and phosphorylate AtRGS1. Accordingly, BAK1 and its interacting partners FLS2, BIK1, PEPR1, and BIR1 have been shown to phosphorylate RGS1 in vitro [40]. Furthermore, genetic and biochemical assays indicate that RLK BRI1-LIKE 3 (BRL3) also interacts with AtRGS1 to control ROS production and plant development during flg22 and sugar responses [38]. Phosphorylation of 7TM-RGS also occurs in soybean, where the Nod factor receptor 1 (NFR1) phosphorylates GmRGS2 in vitro to control nodule formation. Interestingly, three of the five NFR1-induced phosphorylated residues are localized at the predicted linker region of GmRGS2, and one of them (Ser277) is conserved in AtRGS1 (Ser278) (Table 1) [41]. Likewise, this linker residue has been shown to be phosphorylated in xylanase-treated root cell cultures [25].

Table 1. MS-detected phosphorylation sites from the Arabidopsis G-protein core.

Protein	Residue	Detected In Vivo?	In Vitro Kinase	Conservation Score (Plants Only) *	Conservation Score (Eukaryotes, Excluding Plants) *
AtRGS1	Ser278	Yes [25]	BRL3, BIK1, PBL1 [15,27]	−0.861	
	Ser339	No [15]	BRL3 [15]	0.714	−1.131
	Ser365	No [15]	BRL3 [15]	−1.373	0.444
	Thr375	No [15]	BRL3 [15]	−1.016	−0.162
	Thr379	No [15]	BRL3 [15]	−0.582	0.483
	Ser405	No [15]	BRL3 [15]	−0.981	0.959
	Ser406	No [15]	BRL3 [15]	−1.139	−0.559
	Ser417	Yes [26]	BRL3, BIK1 [15,27]	1.798	
	Ser428	Yes [26]	BRL3, PEPR1, WNK8, BIK1, PBL1 [11,14,27]	−0.211	
	Ser430	Yes [26,27]	BRL3, BIK1, PBL1 [15,27]	−1.116	
	Ser431	Yes [26,27]	BRL3, BIK1, PBL1 [15,27]	−0.853	
	Ser435	Yes [26]	BRL3, WNK8 [11,14,27]	−1.048	
	Ser436	Yes [26]	BRL3, WNK8 [11,14]	−0.097	
	Ser450	Yes [27]	BIK1, PBL1 [27]	1.297	
	Ser452	Yes [27]	BIK1, PBL1 [27]	1.897	
	Ser453	Yes [27]	BRL3, BIK1, PBL1 [15,27]	0.429	
AtGPA1	Ser8	No [16]	BAK1, PSY1R, PEPR1, BRL3, BRI1, XIP1, AT2G19230, AT2G37050, AT5G62710 [16]	1.567	−0.741
	Thr12	Yes [28,31]	BAK1, SERK1, PSY1R, PEPR1, BRL3, XIP1, AT2G19230, AT2G37050, AT5G62710 [16]	2.432	2.226

	Thr15	Yes [30,32]	BAK1, SERK1, PSY1R, BRI1, XIP1, AT2G19230, AT2G37050, AT5G62710 [16]	3.816	0.489
	Thr19	Yes [29]	BAK1, SERK1, PSY1R, BRL3, BRI1, XIP1, AT2G19230, AT2G37050, AT5G62710 [16]	1.349	0.949
	Ser49	Yes [42]		−0.658	−0.908
	Ser52	No [16]	BRL3, AT2G19230, AT5G62710 [16]	−0.167	−0.945
	Thr53	No [16]	BRI1 [16]	−0.974	−0.942
	Ser73	No [16]	BAK1 [16]	0.293	0.322
	Thr85	No [16]	BAK1, PSY1R, BRL3, BRI1, AT2G19230, AT5G62710 [16]	−0.588	−0.792
	Thr93	No [16]	BAK1, SERK1, PSY1R, BRL3, BRI1, XIP1, AT2G19230 [16]	0.609	−0.700
	Thr101	No [16]	BAK1, XIP1 [16]	5.029	0.514
	Ser103	No [16]	AT2G19230 [16]	−0.179	1.321
	Ser109	No [16]	BAK1, SERK1, BRL3, AT5G62710 [16]	−0.428	1.116
	Ser110	No [16]	BRI1 [16]	5.031	0.509
	Ser112	No [16]	SERK1, AT2G19230, AT2G37050, AT5G62710 [16]	0.333	−0.266
	Thr141	No [16]	BAK1, BRL3 [16]	0.345	1.160
	Thr164	No [16]	SERK1, XIP1, AT5G10290, AT2G37050, AT5G62710 [16]	−0.007	−0.847
	Tyr166	Yes [29]		−0.673	−0.929
	Ser175	No [16]	AT5G62710 [16]	−0.464	0.857
	Thr193	No [16]	BRI1 [16]	−0.985	−0.942
	Thr194	No [16]	BRI1 [16]	−0.680	−0.807
	Ser314	Yes [26]	BAK1, AT5G62710 [16]	0.146	0.303
	Ser315	No [16]	BAK1, AT5G62710 [16]	0.349	−0.304
	Thr339	No [16]	BAK1 [16]	0.079	1.063
	Thr353	No [16]	BRI1 [16]	−0.311	−0.898
AtAGB1	Ser2	Yes [26]		−0.301	1.319
	Ser4	Yes [26]		2.106	1.568
	Thr14	No [43]	BRI1 [43]	1.347	−0.356
	Thr16	No [43]	BRI1 [43]	0.838	−0.137
	Thr34	No [43]	BRI1 [43]	−0.110	−0.003
	Ser40	No [43]	BRI1 [43]	0.520	0.002
	Thr46	No [43]	BRI1 [43]	2.140	0.422
	Ser49	No [43]	BRI1 [43]	1.972	0.304
	Thr53	No [43]	BRI1 [43]	0.048	1.096
	Thr65	No [43]	BRI1 [43]	0.034	−0.538
	Ser70	No [43]	BRI1 [43]	−0.421	−0.529
	Ser82	No [43]	BRI1 [43]	−1.179	−0.624
	Thr100	No [43]	BRI1 [43]	0.228	−0.127
	Thr243	No [43]	BRI1 [43]	−0.687	−0.561
	Thr253	No [43]	BRI1 [43]	0.776	−0.327
AtAGG2	Ser6	Yes [26]		1.889	−0.927
	Ser8	Yes [25]		0.223	−0.428
	Ser9	Yes [42]		1.827	0.045
AtAGG3	Ser21	No [43]	BRI1 [43]	−0.967	1.287
	Ser22	No [43]	BRI1 [43]	−0.933	0.097
	Ser37	Yes [26]	BRI1 [43]	−1.522	1.643
	Ser78	No [43]	BRI1 [43]	1.621	−2.114
	Thr92	No [43]	BRI1 [43]	0.913	−1.267

AtXLG1	Ser462	Yes [26]		1.114	3.103
	Ser471	Yes [26]		0.233	1.061
	Tyr876	Yes [42]		1.458	2.004
	Tyr879	Yes [42]		0.231	1.367
	Tyr887	Yes [42]		−0.188	−0.128
AtXLG2	Ser13	Yes [30,41,44]		0.644	
	Ser23	Yes [30,45,46]		1.892	
	Ser38	Yes [26]		−0.937	
	Ser69	Yes [47]		0.404	
	Ser71	Yes [48]		0.556	
	Ser72	Yes [47]		0.542	
	Ser75	Yes [30,44]		0.689	
	Ser141	Yes [26]		1.825	
	Ser148	Yes [47]	BIK1 [47]	−0.079	
	Ser150	Yes [47]	BIK1 [47]	1.152	
	Ser151	Yes [30,44]		1.467	
	Ser154	Yes [30,44]		1.143	
	Ser156	Yes [47]		1.919	
	Ser169	Yes [30,44,46,48–50]		0.681	
	Ser191	Yes [47]		0.865	
	Ser194	Yes [26]		1.539	
	Ser489	Yes [47]		−0.520	−1.243
	Ser530	Yes [51]		0.991	0.644
	Thr773	Yes [47]		0.655	0.550
	Ser774	Yes [47]		0.190	−0.397
AtXLG3	Ser78	Yes [26]		1.823	
	Ser82	Yes [26]		−0.216	
	Ser85	Yes [26]		0.112	
	Ser99	Yes [26]		1.173	
	Ser101	Yes [26]		1.432	
	Ser103	Yes [26]		−0.082	
	Ser107	Yes [26]		−0.421	
	Ser243	Yes [26]		−0.533	
	Ser416	Yes [26]		0.247	−1.125
	Ser506	Yes [52,53]		0.846	−1.221

* Normalized conservation score obtained from the ConSurf server. A lower score indicates higher residue conservation. Sequences were obtained using the BLAST tool (https://blast.ncbi.nlm.nih.gov/Blast.cgi?PAGE=Proteins), and representative sequences were selected using CD-HIT (http://weizhong-lab.ucsd.edu/cdhit_suite/, accessed on 20 May 2022) with a sequence identity cut-off of 0.9. MSA was obtained with ClustalOmega (https://www.ebi.ac.uk/Tools/msa/clustalo/, accessed on 20 May 2022). For non-plant eukaryotic conservation, RGS (PF00615) and Gγ (PF00631) family sequences were obtained from Pfam. AtRGS1 and XLGs' non-conserved regions were excluded from the final analysis.

While the C-terminal serine cluster phosphorylation in response to sugar and pathogens has been confirmed, the specific phosphorylation sites are still unclear because distinguishing the mass spectrometry (MS) signals of neighbor phosphoserines is not an easy task [14,27]. The inactivation of Ser431 alone (AtRGS1^{S431A}) inhibits the C-terminal phosphorylation induced by flg22, Elf18, chitin, and Pep9. Flg22-induced dissociation of RGS1/XLG2 and RGS1/FLS2 complexes is also inhibited by a single Ser431 mutation, while a quadruple phosphomimetic mutation at the cluster (AtRGS1$^{S428/431/435/436D}$) causes defective binding of both complexes [27].

Consistent with the GPCR internalization mechanism and the biased signaling theory, in which different signal/receptor interactions trigger different pathways [54], AtRGS1 is internalized by two phosphorylation-dependent endocytosis pathways. Flg22 induces AtRGS1 internalization via clathrin-mediated endocytosis (CME), while D-glucose triggers both CME and sterol-dependent endocytosis (SDE). The recruitment of the

CME endocytic machinery towards GPCRs requires prior β-arrestin binding and activation, but plant genomes do not encode these proteins [55,56]. Nevertheless, Arabidopsis has three proteins with arrestin folds that bind as heterodimers to AtRGS1 and are required for endocytosis [55]. These include the vacuolar sorting proteins 26 (VPS26)—AtVPS26a, AtVPS26b, and AtVPS26-like components of the retromer [57], well-known in animals for their role in endosomal to plasma membrane anterograde trafficking [58]. VPS26 appears to moonlight as β-arrestins in plants, and because some GPCR endocytosis does not require β-arrestins [59], VPS26 proteins may serve the same role in animals.

The candidate adaptor VPS26b forms a homodimer or a heterodimer with VPS26a, both required for flg22-mediated internalization of AtRGS1. However, those genes are not involved in AtRGS1 internalization that is induced by high concentrations of glucose [55]. Additionally, the inactivation of three cluster sites (AtRGS1$^{S428/435/436A}$) completely abolishes flg22-induced internalization but only partially affects the glucose-mediated internalization of AtRGS1 [55]. Furthermore, a phosphatase is also required for AtRGS1 stability, and its presence reduces the in vitro identified phosphorylation by the WNKs [60]. These findings suggest an animal-like mechanism in which the phosphorylation patterns are the key for recruitment and posterior signal distinction and transduction.

3. Phosphorylation as a Switch Mechanism of AtGPA1

Eukaryotic organisms encode over 100 guanine nucleotide-binding proteins (GNBPs), represented by heterotrimeric G proteins, small Ras-related proteins, and translation elongation factors [61]. Besides the high sequence identity, those GNBPs share a common structural core composed of six beta-sheet strands, five alpha-helices, and five highly conserved loop regions that bind to GDP/GTP. Each of the five loops is responsible for phosphate binding, guanine ring binding, or Mg^{2+} binding and coordination [62]. Upon binding, GTP hydrolysis occurs with a subunit-specific intrinsic rate. A conformational change brings the two switch regions (Switch I and Switch II) to a non-flexible conformation that orientates the magnesium ion in order to facilitate the reaction [33,61]. The canonical alpha subunit of heterotrimeric G proteins contains the small Ras-like domain and an all-alpha helical domain that, in animals, is involved in guanine exchange factor (GEF) binding, nucleotide release inhibition, and ubiquitination processes (Figure 3) [62–66].

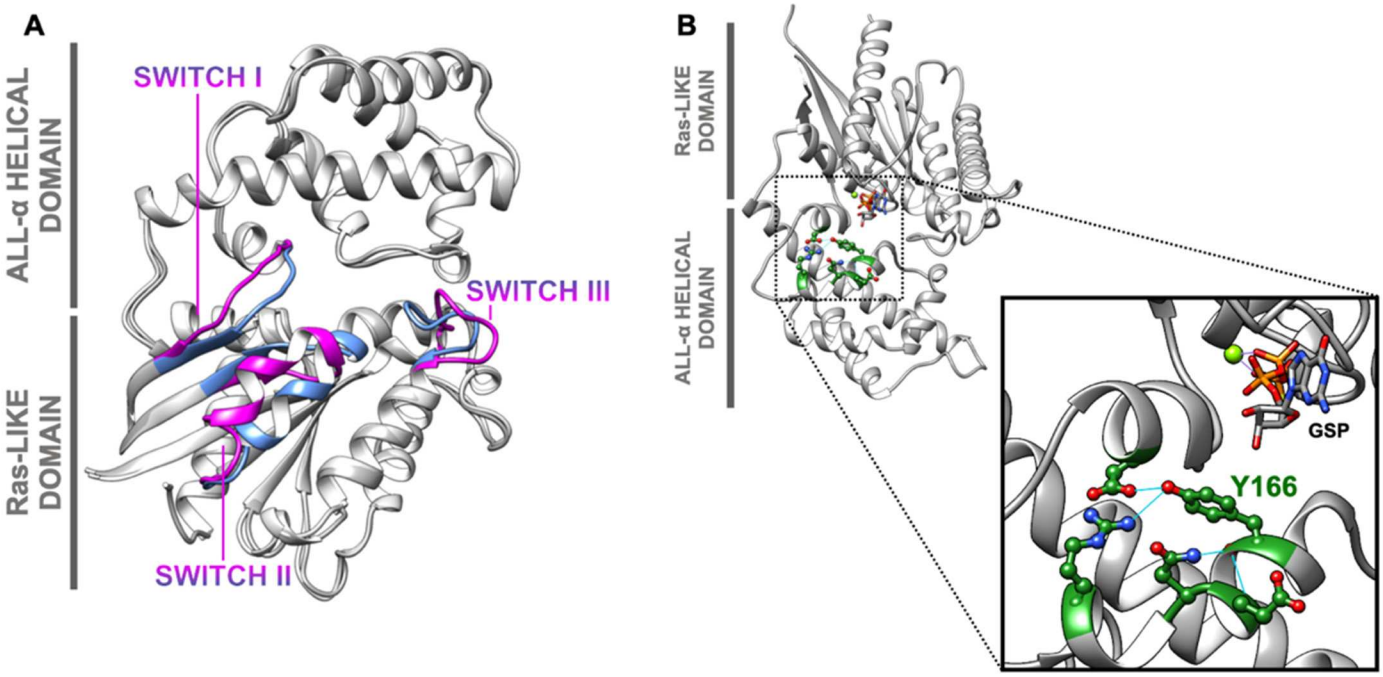

Figure 3. Switching mechanism of Gα. (**A**) The animal Gα activation mechanism. Transducin alpha.GDP (grey and magenta, PDB 1TAG) and transducin alpha.GTP (grey and light blue, PDB 1TND) from *Bos taurus* were selected in order to show nucleotide-induced conformational change in animals. Structures were overlapped, and switch regions of both states were colored in pink and blue, as indicated. Adapted from [67]. (**B**) The plant Gα "phosphoswitch" region. AtGPA1 is phosphorylated at tyrosine 166 in order to affect AtRGS1 interaction and its accelerated GTPase cycle. The crystal structure of AtGPA1 (PDB 2XTZ) is represented in grey with forest green highlights. Tyr166 is at the interface of the two conserved domains and forms hydrogen bonds (cyan) with neighbor residues (balls and sticks). A GTP molecule with Mg^{2+} is near this residue, and they are represented as sticks and as a light green sphere, respectively. Adapted from [68].

The *Arabidopsis thaliana* Gα subunit (AtGPA1) has a spontaneous nucleotide exchange activity about 50 times higher than that of $G\alpha_{oA}$ (G protein alpha subunit o), the fastest exchanging Gα identified in mammalians [13,22]. Even though AtRGS1 maintains AtGPA1 in a resting state by increasing the GTP hydrolysis rate, the endocytosis of the regulator requires prior G-protein activation. Thus, the balance of cycling and hydrolysis within AtGPA1 is crucial for downstream signaling activation [40,68]. There are examples in animals and yeast regarding activation by phosphorylation of Gα. Phosphorylation of the bovine Gsα (Gs alpha subunit) by epidermal growth factor receptor (EGFR) is exclusive to tyrosine residues and promotes adenylate cyclase [69]. In *Saccharomyces cerevisiae*, the alpha subunit Gpa2 is phosphorylated by glycogen synthase kinase (GSK), increasing its localization on the plasma membrane and activating protein kinase A (PKA) at a higher level [70]. Nevertheless, the characterized phosphorylation sites from these events are not conserved among plant components [68].

Although only a small amount (4.3%) of phosphopeptides are phosphotyrosines, and there is no evidence of bona fide tyrosine kinases in Arabidopsis [28,71], phosphoproteomics studies have demonstrated a phosphorylation signal at tyrosine 166 of AtGPA1 (Figures 2 and 3B). Furthermore, this residue is one of the BAK1 substrates and has been found to be differentially phosphorylated under abscisic acid (ABA), indole-3-acetic acid (IAA), gibberellic acid (GA), jasmonate (JA), and kinetin treatments [29,68]. The Tyr166 phosphosite is localized in the interface of the two domains, and it is predicted to regulate AtRGS1 binding by forming a salt bridge in this region. AtRGS1 has a higher affinity for the transitional state of alpha, but a phosphomimetic mutation that changes Tyr166 enables AtRGS1 to bind to its GDP-bound state [68]. This new mechanism is dubbed tyrosine phosphoswitching, in which the function of the AtRGS1 protein switches from a GAP (GTPase activating protein) function to a GDI (GDP dissociation inhibitor) function based on the phosphorylation state of its substrate AtGPA1 (Figure 3B). Moreover, flg22 treatment promotes the phosphorylation of AtGPA1 at Thr19, which is essential for RGS1 binding regulation during biotic signaling, and it is also differentially phosphorylated under ABA treatment (Figure 2) [29,33].

The phosphorylation of AtGPA1 under biotic stress and hormone treatment is consistent with the fact that both AtGPA1 and AGB1 interact with the JA signaling regulators TCP14 and JAZ3, transcription factors that are stabilized in the nucleus by both G-subunits [29, 52, internal data]. The stabilization of those transcription factors is favored by the phosphorylation of both Tyr166 and the N-terminal residues Ser8, Thr12, Thr15, and Thr19, which promotes the dissociation of AtGPA1 from both AGB and RGS proteins. This mechanism evidences the role of phosphorylated GPA1 during biotic responses and hormone crosstalk, unveiling a novel mechanism of G-protein subunit sequestering for transcriptional regulation [internal data]. Except for Ser8, all involved phosphoresidues were detected in vivo by MS analysis, and Y166 is the most conserved among plants and other eukaryotes (Table 1).

Finally, about 24 residues inside the Ras-like and helical domains have been demonstrated to be phosphorylated in vitro by 11 different RLKs (Table 1). Interestingly, some residues are phosphorylated by different kinases depending on the state of AtGPA1,

raising the hypothesis that nucleotide-dependent AtGPA1 conformation is crucial for substrate accessibility and, consequently, for RLK specificity [16].

4. Stress Responses through XLG Phosphorylation

The non-canonical Gα subunits called extra-large G proteins (XLGs) are unique to plants [72]. The C-terminal halves of XLG proteins are homologous to those of the canonical alpha subunits. The non-conserved N-terminal halves of XLG proteins contain a nuclear localization signal (NLS) and a cysteine-rich region [73]. This semi-conserved domain lacks many key residues for nucleotide binding, resulting in poor nucleotide affinity and slow GTP hydrolysis [74,75]. In addition, the Arabidopsis XLGs (XLG1, XLG2, and XLG3) can interact with the Gβγ dimer and AtRGS1 under some conditions but with no evidence of an associated GAP activity [72,74].

Multiple data indicate that genetic ablation of *XLGs* results in the opposite effect of ablation of *AtGPA1* regarding pathogen susceptibility, lateral root proliferation, salt stress, and stomatal density [72,73,75,76]. The extra-large subunits are also genetically linked to tunicamycin and D-glucose sensitivity, while *gpa1* mutants display a wild-type phenotype under such treatments [72]. Even though these proteins are thought to be negative regulators of AtGPA1 by sequestering Gβγ or RGS1 from the canonical complex, they may act parallelly during ABA responses and root development [76].

Regarding biotic responses, *xlg2* null mutants have impaired flg22 responses, and both *AtXLG2* and *AtXLG3* genes are induced by this elicitor. In addition, XLG2 and XLG3 interact with BIK1, FLS2, and RbohD (NADPH/respiratory burst oxidase protein D), and the complementation of knockout plants with AtXLG2$^{S141/148/150/151A}$ expression abolishes flg22-induced phosphorylation and lowers ROS response compared to that in wild-type plants [47]. In contrast, XLG2 signaling with CERK1 (CHITIN ELICITOR RECEPTOR KINASE 1) under chitin elicitation is not affected by the same N-terminal mutations [77].

In proteomics studies, XLG2 has several in vivo detected phosphosites: five N-terminal residues respond to ionizing radiation and six respond to "end-of-day" conditions [30,44]. Among these residues, Ser13 responds to osmotic stress, and Ser71/169 respond to nitrate starvation [45,46,48–50]. Ser13 and Ser38 display increased phosphorylation signals 15 minutes after flg22 exposure, while serine residues 75, 185, 190, 191, 194, and 198 show decreased signals after 3 or 15 minutes of exposure [60]. In addition to the four mutated N-terminal serine residues, XLG2 is differentially phosphorylated at the helical domain (Ser530) by flg22 [51]. Several other phosphorylated sites in the non-conserved region are constitutively detected in different tissues (Table 1). XLG3 has nine N-terminal tissue-specific phosphoresidues under normal conditions [26]. Like XLG2-Ser530 phosphorylation, Ser506 of the XLG3 helical domain is differentially phosphorylated under ABA, sucrose, mannitol, and short cold treatments [42,51–53], and it is detected with a reduced signal in the first minutes of flg22 exposure [60].

Although XLG1 has a nuclear localization signal, its localization is partner-dependent [78,79], and it is not phosphorylated at the N-terminus. Instead, it is phosphorylated right after the NLS in the serines 462 and 471 [26,72]. Atypical tyrosine phosphorylation (Y876/879/887) may occur at the end of helix G5 in isoxaben-treated seedlings [42]. Taken together, these data indicate a similar phosphorylation-mediated regulation mechanism between XLG2 and XLG3 under stress responses, but not XLG1, which may be related to its different subcellular localization.

5. Gβγ Specificity and Function

In contrast to being only a negative regulator of Gα signaling, AGB1 is a crucial signaling component in plants [80] like in yeast [81]. Among other phenotypes, *agb1* null mutants exhibit dwarf morphology, impaired abiotic responses, reduced ROS burst under flg22 elicitation, and higher susceptibility to pathogen attack [80,82–85]. This susceptibility is directly related to the upregulation of JA responsive genes on *agb1* plants, indicating that JA signaling may be negatively regulated by AGB1 [internal data].

Genetic data indicate that AGB1 requires the gamma subunit for signaling. Only AGG1 is linked to pathogen defense, while both AGG1 and AGG2 are involved in auxin-mediated signaling via different mechanisms. The inhibition of germination by D-glucose or osmotic stress is independently mediated by AGG2 or AGG1, respectively [86]. On top of that, AtAGG3 and its rice homologs mediate ion channel regulation, seed, and organ development [87,88]. Consistently with the signaling module, alpha-binding to AGB1 is also gamma-dependent, displaying distinct functions according to its binding partners. While GPA1 has a binding preference for AGB1/AGG3, the interaction of XLG1 and XLG2 with AGB1 depends similarly on AGG1 and AGG2 [72,89]. Additionally, XLG3 binds equally to all three heterodimers and competes with GPA1 for Gβ interaction [72].

The phosphorylation events likely regulate dimer preference and signal specificity since AGB1, AGG2, and AGG3 have MS-confirmed phosphorylation sites [26,42]. The receptor-like kinase complex BAK1/BRI1 interacts with both AGG3 and AGB1, and the latter interaction is increased under 2% D-glucose treatment. Both subunits are phosphorylated by BRI1 in vitro, and inactivation of the corresponding MS-detected sites leads to impaired sugar response in planta [43]. The receptor-like kinase AtZAR1 (ZYGOTIC ARREST 1) has a calmodulin-binding domain, interacts with Gβ, and may integrate Ca^{2+} signaling with the heterotrimeric G-protein pathway [90].

The N-terminal domain of AGB1 has predicted target motifs for glycogen synthase kinase 3/SHAGGY-like protein kinases (GSKs) and interacts with the GSK BIN2. The 3/SHAGGY motifs are present within 46–358 residues, and in vivo phosphorylation of AGB1 has only been detected at Ser2 and Ser4 [26,91]. On top of beta phosphorylation, AGG2 is differentially phosphorylated at non-distinguished serine residues 6, 8, and 9 in response to sucrose and xylanase treatments [25,26,42]. Like in XLG2, an AGG3 phosphosite is identified at Ser37 in response to end-of-day conditions and ionizing radiation (Table 1) [30,44]. Finally, the same site displays an enhanced phosphorylation signal after 15 minutes of anti-bacterial immunity elicitation [60].

Molecular protein modeling mapped the beta phosphorylation at or near the Gβγ interaction interface with close (+)-charged residues [35]. Moreover, AGG2 and AGG3 are phosphorylated near these sites and close to the Gα interface. AGG3 shows a long non-structured C-terminal tail (res. 116–251) far from the interface that was excluded from the model for visualization purposes. This structural estimation indicates that phosphorylation may affect the interaction dynamics of the trimer and, therefore, signal specificity (Figure 4).

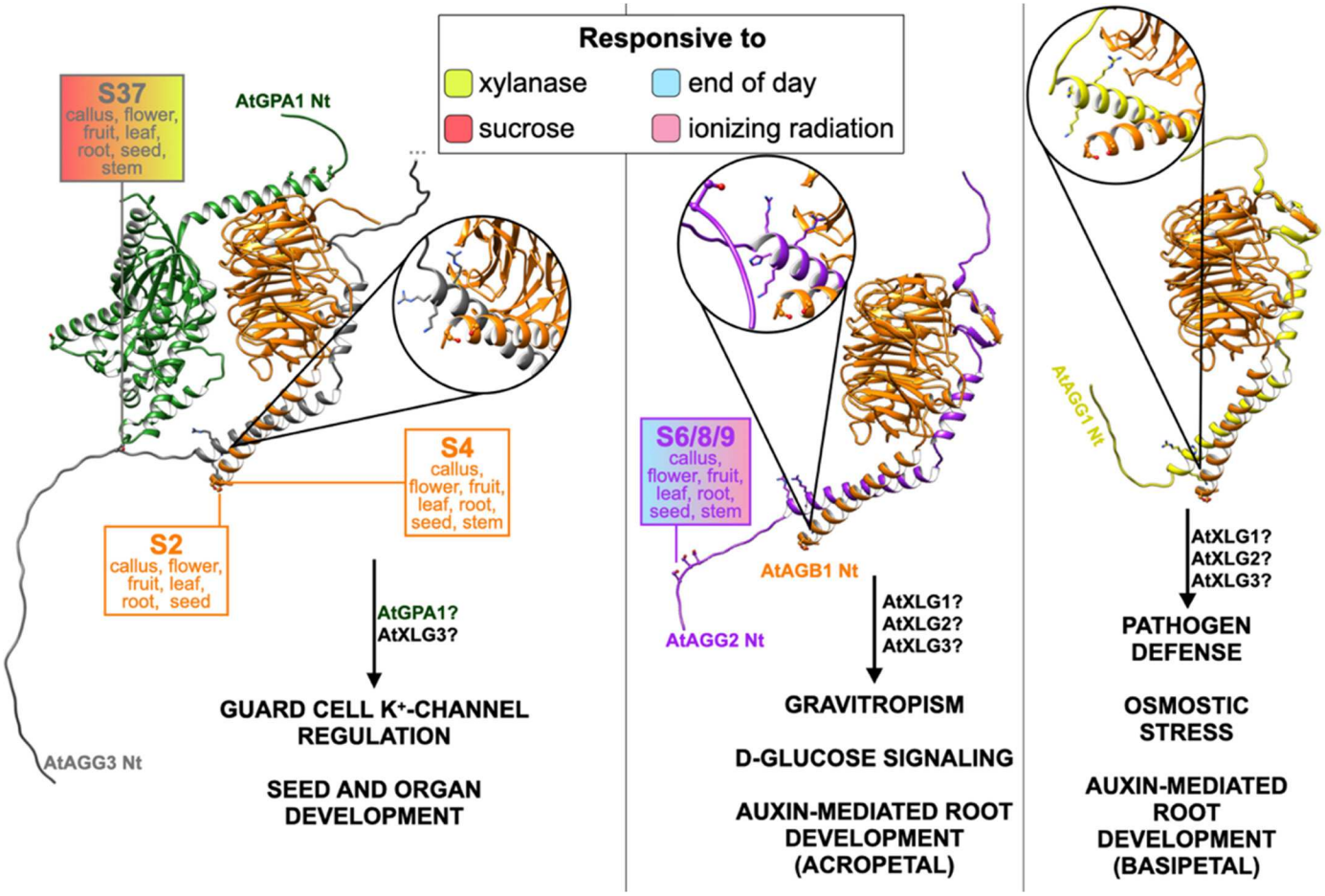

Figure 4. Gβγ specificity and function distinction. AtGPA1 (forest green) binds preferentially to AGB1 (orange) when dimerized with AGG3 (grey), which regulates ion transport, seed, and organ development [72,87–89]. β-dimerized AGG2 (purple) binds to the XLGs in order to regulate gravitropism, sugar responses, and root development [72,86]. Phosphorylation occurs in vivo at the N-terminal portions of AGB1, AGG2, and AGG3 [26,42,60]. Beta-gamma complex models were created using AlphaFold2, and top-ranked models were selected for analysis [35]. The heterotrimeric complex was created by overlapping the models with the crystal structure of the heterotrimeric G-protein complex of Bos taurus (PDB 1GOT). Experimental data were obtained from the PhosphAt database (https://phosphat.uni-hohenheim.de, accessed on 23 May 2022) and ATHENA (http://athena.proteomics.wzw.tum.de, accessed on 23 May 2022). AGG3 unmodeled C-terminal regions were removed for better visualization. ATHENA was used to identify tissue-specific phosphorylation, which is pointed out below residue identification. Phosphosites are represented as balls and sticks. Candidate AGB1pS37-interacting residues are represented as sticks only. Color filling indicates experimental treatments.

6. G-Paradox and Four-State Model

The nucleotide state of animal Gα modulates the heterotrimer formation from a "switch off" (GDP-bound) to a "switch on" (GTP-bound) structure (Figure 3A) [67]. Thus, it is controversial that, in plants, no structural difference was detected within the trimer during the two nucleotide states of AtGPA1 [92]. Furthermore, genetic complementation of the rice dwarf mutant d1 (OsRGA1-defective) with a constitutive GTP-bound alpha mutant (OsRGA1^{Q223L}) rescued the normal development phenotype, suggesting that on–off cycling is not required [93]. Adding XLGs and their functions to the plant G-protein repertoire has moved the plant signaling module even further from the established animal module [72]. Both AtGPA1 and XLGs present nucleotide independency for most functions and structural plasticity [74,89,94].

Another observation is that AtRGS1 strongly controls the complex state in vitro, but *rgs1* plants present subtle phenotypes compared to other G-protein mutants [95]. Furthermore, one of the few *rgs1* strong phenotypes is its poor capability of photosynthetic adjustment under dynamic or excessive irradiation, even though the behavior is wild-type-like during constant light conditions [96]. The RLK phosphorylation over several subunits also differs from the animal paradigm [16,38].

Therefore, to provide a solution to this paradox, the current plant model consists of four described states of Gα—Gα-GTP, Gα-GDP, pGα-GDP, and pGα-GTP—in which only the phosphorylated forms are signaling competent. In addition, RLKs are activated by an external stimulus and phosphorylate RGS1, resulting in an altered GTP/GDP state of the switch. The switch is also phosphorylated by the RLKs, independent of its nucleotide state [95]. Finally, phosphorylation is highlighted as a crucial regulation component, and the post-translational state of the subunits may explain inconsistencies in reverse genetic studies.

7. Conclusions

The phosphorylation at threonine/serine/tyrosine residues modulates many aspects of protein function and, consequently, is a highly regulated process. Advances in protein modeling, genetic data, and phosphoproteomic analysis have provided a direct link between phosphorylation status and G-signaling activation and triggering specificity. Flg22 elicitation induces phosphorylation at Ser428/431 residues on AtRGS1 proteins [27], while glucose induces phosphorylation at Ser428/435/436 [14]. These distinct phosphorylation patterns are implicated in specific cell responses modulated by G-protein activation through different RLKs. AtWNK8 phosphorylates at least two serine residues at the RGS protein upon glucose induction, and this phosphorylation event promotes G-signaling activation and RGS endocytosis [14]. However, FLS2 and its coreceptor BAK1 trigger the phosphorylation of RGS on Ser428/431, promoting its dissociation from FLS2 and Gα [27]. AtGPA1 shows dynamic phosphorylation upon flg22 elicitation, which reduces the phosphorylation level of Thr19, implicating a specific role of this AtGPA1 residue in plant signaling responses to flg22 [33], although the same phosphoresidue is induced by hormone treatment [29]. Therefore, the signaling discrimination relies on a specific combination of phosphorylation between RGS and GPA1 proteins, a regulatory mechanism that may be expanded to form atypical core conformations that include the XLGs and different gamma subunits.

Herein, we reviewed the phosphorylation status of the G-protein signaling components and its ability to regulate their binding affinity, localization, and stability, thus controlling their function on signal transduction and propagation. However, the characterization of the underlying G-protein phosphorylation status is still in its infancy; hence, the identification of different protein kinase phosphosites might shed light on signal discrimination and G-signaling activation. Furthermore, understanding the underlying mechanism of specific residue phosphorylation can be exploited as a marker for G-protein distinct signaling. Finally, the intricated mechanism of G-protein dynamism in plants does not rely only on a defined composition of the complex or its nucleotide-binding status, but rather is regulated by the phosphorylation status of the main components, RLKs, and other interacting partners, creating a complex post-translational G code for signal transduction.

Author Contributions: C.C.O., conceptualization, writing—original draft preparation; A.M.J., E.P.B.F. and P.A.B.d.R., writing—review and editing, supervision and funding acquisition; P.A.B.d.R., project administration. All authors have read and agreed to the published version of the manuscript.

Funding: This work at UFV was partially funded by CAPES (finance code 001), FAPEMIG, and CNPq (403819/2021-0 to E.P.B.F./P.A.B.R.). The work at UNC was supported by NIGMS (GM065989)

and NSF (MCB-1713880 and IOS 2034929) to A.M.J.; C.C.O. is a recipient of a CAPES graduate fellowship.

Institutional Review Board Statement: Not applicable.

Informed Consent Statement: Not applicable.

Data Availability Statement: The in vivo data analyzed in this study is available online at the Arabidopsis Protein Phosphorylation Site Database and at the Arabidopsis THaliana ExpressioN Atlas.

Conflicts of Interest: The authors declare no conflict of interest.

Glossary

GPA1	Heterotrimeric G-protein Alpha Subunit
AGB1	Heterotrimeric G-protein Beta Subunit
AGG	Heterotrimeric G-protein Gamma Subunit
RGS	Regulator of G Signaling
XLG	Extra-Large G Protein
CME	Clathrin-Mediated Endocytosis
SDE	Sterol-Dependent Endocytosis
GPCR	G-Protein-Coupled Receptor
GEF	Guanine Nucleotide Exchange Factor
RLK	Receptor-Like Kinase
V_2R	V2 Vasopressin Receptor
GRK	GPCR Kinase
FLS2	FLAGELLIN-SENSITIVE 2
BAK1	BRI1-ASSOCIATED RECEPTOR KINASE 1
NFR1	Nod Factor Receptor 1
ABA	Abscisic Acid
VPS26	Vacuolar Sorting Proteins 26
WNK	WITH NO LYSINE KINASE
GNBP	Guanine Nucleotide-Binding Protein
EGFR	Epidermal Growth Factor Receptor
GSK	Glycogen Synthase Kinase
PKA	Protein Kinase A
IAA	Indole-3-Acetic Acid
CERK1	Chitin Elicitor Receptor Kinase 1
JA	Jasmonic Acid
GA	Gibberellic Acid
GAP	GTPase Activating Protein
MS	Mass Spectrometry

References

1. Žádníková, P.; Smet, D.; Zhu, Q.; Van Der Straeten, D.; Benková, E. Strategies of seedlings to overcome their sessile nature: Auxin in mobility control. *Front. Plant Sci.* **2015**, *6*, 218. https://doi.org/10.3389/fpls.2015.00218.
2. Kaziro, Y.; Itoh, H.; Kozasa, T.; Nakafuku, M.; Satoh, T. Structure and function of signal-transducing GTP-binding proteins. *Annu. Rev. Biochem.* **1991**, *60*, 349–400. https://doi.org/10.1146/annurev.bi.60.070191.002025.
3. Ross, E.M. Coordinating speed and amplitude in G-protein signaling. *Curr. Biol.* **2008**, *18*, R777–R783. https://doi.org/10.1016/j.cub.2008.07.035.
4. McCudden, C.R.; Hains, M.D.; Kimple, R.J.; Siderovski, D.P.; Willard, F.S. G-protein signaling: Back to the future. *Cell. Mol. Life Sci.* **2005**, *62*, 551–577. https://doi.org/10.1007/s00018-004-4462-3.
5. Oldham, W.M.; Hamm, H.E. Heterotrimeric G protein activation by G-protein-coupled receptors. *Nat. Rev. Mol. Cell Biol.* **2008**, *9*, 60–71. https://doi.org/10.1038/nrm2299.
6. Temple, B.R.; Jones, C.D.; Jones, A.M. Evolution of a signaling nexus constrained by protein interfaces and conformational states. *PLoS Comp. Biol.* **2110**, *6*, e1000962. https://doi.org/10.1371/journal.pcbi.1000962.
7. de Mendoza, A.; Sebé-Pedrós, A.; Ruiz-Trillo, I. The evolution of the GPCR signaling system in eukaryotes: Modularity, conservation, and the transition to metazoan multicellularity. *Genome Biol. Evol.* **2014**, *6*, 606–619. https://doi.org/10.1093/gbe/evu038.
8. Trusov, Y.; Botella, J.R. Plant G-Proteins Come of Age: Breaking the Bond with Animal Models. *Front. Chem.* **2016**, *4*, 24. https://doi.org/10.3389/fchem.2016.00024.

9. Urano, D.; Jones, A.M. Heterotrimeric G protein-coupled signaling in plants. *Annu. Rev. Plant Biol.* **2014**, *65*, 365–384. https://doi.org/10.1146/annurev-arplant-050213-040133.
10. Chakravorty, D.; Assmann, S. G protein subunit phosphorylation as a regulatory mechanism in heterotrimeric G protein signaling in mammals, yeast, and plants. *Biochem. J.* **2018**, *475*, 3331–3357. https://doi.org/10.1042/BCJ20160819.
11. Jones, J.C.; Temple, B.R.S.; Jones, A.M.; Dohlman, H.G. Functional reconstitution of an atypical G protein heterotrimer and regulator of G protein signaling protein (RGS1) from *Arabidopsis thaliana*. *J. Biol. Chem.* **2011**, *286*, 13143–13150. https://doi.org/10.1074/jbc.M110.190355.
12. Bradford, W.; Buckholz, A.; Morton, J.; Price, C.; Jones, A.M.; Urano, D. Eukaryotic G protein signaling evolved to require G protein-coupled receptors for activation. *Sci. Signal*. **2013**, *6*, ra37. https://doi.org/10.1126/scisignal.2003768.
13. Urano, D.; Fu, Y.; Jones, A.M. Activation of an unusual G-protein in the simple protist Trichomonas vaginalis. *Cell Cycle* **2013**, *12*, 3127–3128. https://doi.org/10.4161/cc.26350.
14. Urano, D.; Phan, N.; Jones, J.C.; Yang, J.; Huang, J.; Grigston, J.; Taylor, J.P.; Jones, A.M. Endocytosis of the seven-transmembrane RGS1 protein activates G-protein-coupled signalling in Arabidopsis. *Nat. Cell Biol.* **2012**, *14*, 1079–1088. https://doi.org/10.1038/ncb2568.
15. Tunc-Ozdemir, M.; Li, B.; Jaiswal, D.K.; Urano, D.; Jones, A.M.; Torres, M.P. Predicted functional implications of phosphorylation of regulator of G protein signaling protein in plants. *Front. Plant Sci.* **2017**, *8*, 1456. https://doi.org/10.3389/fpls.2017.01456.
16. Jia, H.; Song, G.; Werth, E.G.; Walley, J.W.; Hicks, L.M.; Jones, A.M. Receptor-Like Kinase Phosphorylation of Arabidopsis Heterotrimeric G-Protein Gα -Subunit AtGPA1. *Proteomics* **2019**, *19*, e1900265. https://doi.org/10.1002/pmic.201900265.
17. Latorraca, N.R.; Venkatakrishnan, A.J.; Dror, R.O. GPCR dynamics: Structures in motion. *Chem. Rev.* **2017**, *117*, 139–155. https://doi.org/10.1021/acs.chemrev.6b00177.
18. Mahoney, J.P.; Sunahara, R.K. Mechanistic insights into GPCR-G protein interactions. *Curr. Opin. Struct. Biol.* **2016**, *41*, 247–254. https://doi.org/10.1016/j.sbi.2016.11.005.
19. Carman, C.V.; Benovic, J.L. G-protein-coupled receptors: Turn-ons and turn-offs. *Curr. Opin. Neurobiol.* **1998**, *8*, 335–344. https://doi.org/10.1016/S0959-4388(98)80058-5.
20. Peterson, Y.K.; Luttrell, L.M. The Diverse Roles of Arrestin Scaffolds in G Protein-Coupled Receptor Signaling. *Pharmacol. Rev.* **2017**, *69*, 256–297. https://doi.org/10.1124/pr.116.013367.
21. Latorraca, N.R.; Masureel, M.; Hollingsworth, S.A.; Heydenreich, F.M.; Suomivuori, C.-M.; Brinton, C.; Townshend, R.J.L.; Bouvier, M.; Kobilka, B.K.; Dror, R.O. How GPCR Phosphorylation Patterns Orchestrate Arrestin-Mediated Signaling. *Cell* **2020**, *183*, 1813–1825.e18. https://doi.org/10.1016/j.cell.2020.11.014.
22. Johnston, C.A.; Taylor, J.P.; Gao, Y.; Kimple, A.J.; Grigston, J.C.; Chen, J.-G.; Siderovski, D.P.; Jones, A.M.; Willard, F.S. GTPase acceleration as the rate-limiting step in Arabidopsis G protein-coupled sugar signaling. *Proc. Natl. Acad. Sci. USA* **2007**, *104*, 17317–17322. https://doi.org/10.1073/pnas.0704751104.
23. Chen, J.-G.; Jones, A.M. AtRGS1 function in *Arabidopsis thaliana*. *Methods Enzymol.* **2004**, *389*, 338–350. https://doi.org/10.1016/S0076-6879(04)89020-7.
24. Cao-Pham, A.H.; Urano, D.; Ross-Elliott, T.J.; Jones, A.M. Nudge-nudge, WNK-WNK (kinases), say no more? *New Phytol.* **2018**, *220*, 35–48. https://doi.org/10.1111/nph.15276.
25. Benschop, J.J.; Mohammed, S.; O'Flaherty, M.; Heck, A.J.R.; Slijper, M.; Menke, F.L.H. Quantitative phosphoproteomics of early elicitor signaling in Arabidopsis. *Mol. Cell. Proteom.* **2007**, *6*, 1198–1214. https://doi.org/10.1074/mcp.M600429-MCP200.
26. Mergner, J.; Frejno, M.; List, M.; Papacek, M.; Chen, X.; Chaudhary, A.; Samaras, P.; Richter, S.; Shikata, H.; Messerer, M.; et al. Mass-spectrometry-based draft of the Arabidopsis proteome. *Nature* **2020**, *579*, 409–414. https://doi.org/10.1038/s41586-020-2094-2.
27. Liang, X.; Ma, M.; Zhou, Z.; Wang, J.; Yang, X.; Rao, S.; Bi, G.; Li, L.; Zhang, X.; Chai, J.; et al. Ligand-triggered de-repression of Arabidopsis heterotrimeric G proteins coupled to immune receptor kinases. *Cell Res.* **2018**, *28*, 529–543. https://doi.org/10.1038/s41422-018-0027-5.
28. Sugiyama, N.; Nakagami, H.; Mochida, K.; Daudi, A.; Tomita, M.; Shirasu, K.; Ishihama, Y. Large-scale phosphorylation mapping reveals the extent of tyrosine phosphorylation in Arabidopsis. *Mol. Syst. Biol.* **2008**, *4*, 193. https://doi.org/10.1038/msb.2008.32.
29. Chen, Y.; Hoehenwarter, W.; Weckwerth, W. Comparative analysis of phytohormone-responsive phosphoproteins in *Arabidopsis thaliana* using TiO2-phosphopeptide enrichment and mass accuracy precursor alignment. *Plant J.* **2010**, *63*, 39. https://doi.org/10.1111/j.1365-313X.2010.04218.x.
30. Roitinger, E.; Hofer, M.; Köcher, T.; Pichler, P.; Novatchkova, M.; Yang, J.; Schlögelhofer, P.; Mechtler, K. Quantitative phosphoproteomics of the ataxia telangiectasia-mutated (ATM) and ataxia telangiectasia-mutated and rad3-related (ATR) dependent DNA damage response in *Arabidopsis thaliana*. *Mol. Cell. Proteom.* **2015**, *14*, 556–571. https://doi.org/10.1074/mcp.M114.040352.
31. Nakagami, H.; Sugiyama, N.; Mochida, K.; Daudi, A.; Yoshida, Y.; Toyoda, T.; Tomita, M.; Ishihama, Y.; Shirasu, K. Large-scale comparative phosphoproteomics identifies conserved phosphorylation sites in plants. *Plant Physiol.* **2010**, *153*, 1161–1174. https://doi.org/10.1104/pp.110.157347.
32. Van Leene, J.; Han, C.; Gadeyne, A.; Eeckhout, D.; Matthijs, C.; Cannoot, B.; De Winne, N.; Persiau, G.; Van De Slijke, E.; Van de Cotte, B.; et al. Capturing the phosphorylation and protein interaction landscape of the plant TOR kinase. *Nat. Plants* **2019**, *5*, 316–327. https://doi.org/10.1038/s41477-019-0378-z.

33. Xue, J.; Gong, B.-Q.; Yao, X.; Huang, X.; Li, J.-F. BAK1-mediated phosphorylation of canonical G protein alpha during flagellin signaling in Arabidopsis. *J. Integr. Plant Biol.* **2020**, *62*, 690–701. https://doi.org/10.1111/jipb.12824.
34. Engelsberger, W.R.; Schulze, W.X. Nitrate and ammonium lead to distinct global dynamic phosphorylation patterns when re-supplied to nitrogen-starved Arabidopsis seedlings. *Plant J.* **2012**, *69*, 978–995. https://doi.org/10.1111/j.1365-313X.2011.04848.x.
35. Jumper, J.; Evans, R.; Pritzel, A.; Green, T.; Figurnov, M.; Ronneberger, O.; Tunyasuvunakool, K.; Bates, R.; Žídek, A.; Potapenko, A.; et al. Highly accurate protein structure prediction with AlphaFold. *Nature* **2021**, *596*, 583–589. https://doi.org/10.1038/s41586-021-03819-2.
36. Sun, Y.; Li, L.; Macho, A.P.; Han, Z.; Hu, Z.; Zipfel, C.; Zhou, J.-M.; Chai, J. Structural basis for flg22-induced activation of the *Arabidopsis* FLS2-BAK1 immune complex. *Science* **2013**, *342*, 624–628. https://doi.org/10.1126/science.1243825.
37. Marcec, M.J.; Tanaka, K. Crosstalk between Calcium and ROS Signaling during Flg22-Triggered Immune Response in Arabidopsis Leaves. *Plants* **2021**, *11*, 14. https://doi.org/10.3390/plants11010014.
38. Tunc-Ozdemir, M.; Jones, A.M. BRL3 and AtRGS1 cooperate to fine tune growth inhibition and ROS activation. *PLoS ONE* **2017**, *12*, e0177400. https://doi.org/10.1371/journal.pone.0177400.
39. Ghusinga, K.R.; Paredes, F.; Jones, A.M.; Colaneri, A. Reported differences in the flg22 response of the null mutation of AtRGS1 correlates with fixed genetic variation in the background of Col-0 isolates. *Plant Signal. Behav.* **2021**, *16*, 1878685. https://doi.org/10.1080/15592324.2021.1878685.
40. Tunc-Ozdemir, M.; Urano, D.; Jaiswal, D.K.; Clouse, S.D.; Jones, A.M. Direct Modulation of Heterotrimeric G Protein-coupled Signaling by a Receptor Kinase Complex. *J. Biol. Chem.* **2016**, *291*, 13918–13925. https://doi.org/10.1074/jbc.C116.736702.
41. Choudhury, S.R.; Pandey, S. Phosphorylation-Dependent Regulation of G-Protein Cycle during Nodule Formation in Soybean. *Plant Cell* **2015**, *27*, 3260–3276. https://doi.org/10.1105/tpc.15.00517.
42. Durek, P.; Schmidt, R.; Heazlewood, J.L.; Jones, A.; MacLean, D.; Nagel, A.; Kersten, B.; Schulze, W.X. PhosPhAt: The *Arabidopsis thaliana* phosphorylation site database. An update. *Nucleic Acids Res.* **2010**, *38*, D828–D834. https://doi.org/10.1093/nar/gkp810.
43. Peng, Y.; Chen, L.; Li, S.; Zhang, Y.; Xu, R.; Liu, Z.; Liu, W.; Kong, J.; Huang, X.; Wang, Y.; et al. BRI1 and BAK1 interact with G proteins and regulate sugar-responsive growth and development in Arabidopsis. *Nat. Commun.* **2018**, *9*, 1522. https://doi.org/10.1038/s41467-018-03884-8.
44. Al-Momani, S.; Qi, D.; Ren, Z.; Jones, A.R. Comparative qualitative phosphoproteomics analysis identifies shared phosphorylation motifs and associated biological processes in evolutionary divergent plants. *J. Proteom.* **2018**, *181*, 152–159. https://doi.org/10.1016/j.jprot.2018.04.011.
45. Bhaskara, G.B.; Wen, T.-N.; Nguyen, T.T.; Verslues, P.E. Protein Phosphatase 2Cs and Microtubule-Associated Stress Protein 1 Control Microtubule Stability, Plant Growth, and Drought Response. *Plant Cell* **2017**, *29*, 169–191. https://doi.org/10.1105/tpc.16.00847.
46. Reiland, S.; Finazzi, G.; Endler, A.; Willig, A.; Baerenfaller, K.; Grossmann, J.; Gerrits, B.; Rutishauser, D.; Gruissem, W.; Rochaix, J.-D.; et al. Comparative phosphoproteome profiling reveals a function of the STN8 kinase in fine-tuning of cyclic electron flow (CEF). *Proc. Natl. Acad. Sci. USA* **2011**, *108*, 12955–12960. https://doi.org/10.1073/pnas.1104734108.
47. Liang, X.; Ding, P.; Lian, K.; Wang, J.; Ma, M.; Li, L.; Li, L.; Li, M.; Zhang, X.; Chen, S.; et al. Arabidopsis heterotrimeric G proteins regulate immunity by directly coupling to the FLS2 receptor. *eLife* **2016**, *5*, e13568. https://doi.org/10.7554/eLife.13568.
48. Wang, X.; Bian, Y.; Cheng, K.; Gu, L.-F.; Ye, M.; Zou, H.; Sun, S.S.-M.; He, J.-X. A large-scale protein phosphorylation analysis reveals novel phosphorylation motifs and phosphoregulatory networks in Arabidopsis. *J. Proteom.* **2013**, *78*, 486–498. https://doi.org/10.1016/j.jprot.2012.10.018.
49. Menz, J.; Li, Z.; Schulze, W.X.; Ludewig, U. Early nitrogen-deprivation responses in Arabidopsis roots reveal distinct differences on transcriptome and (phospho-) proteome levels between nitrate and ammonium nutrition. *Plant J.* **2016**, *88*, 717–734. https://doi.org/10.1111/tpj.13272.
50. Reiland, S.; Messerli, G.; Baerenfaller, K.; Gerrits, B.; Endler, A.; Grossmann, J.; Gruissem, W.; Baginsky, S. Large-scale Arabidopsis phosphoproteome profiling reveals novel chloroplast kinase substrates and phosphorylation networks. *Plant Physiol.* **2009**, *150*, 889–903. https://doi.org/10.1104/pp.109.138677.
51. Mithoe, S.C.; Boersema, P.J.; Berke, L.; Snel, B.; Heck, A.J.R.; Menke, F.L.H. Targeted quantitative phosphoproteomics approach for the detection of phospho-tyrosine signaling in plants. *J. Proteome Res.* **2012**, *11*, 438–448. https://doi.org/10.1021/pr200893k.
52. Wang, P.; Xue, L.; Batelli, G.; Lee, S.; Hou, Y.-J.; Van Oosten, M.J.; Zhang, H.; Tao, W.A.; Zhu, J.-K. Quantitative phosphoproteomics identifies SnRK2 protein kinase substrates and reveals the effectors of abscisic acid action. *Proc. Natl. Acad. Sci. USA* **2013**, *110*, 11205–11210. https://doi.org/10.1073/pnas.1308974110.
53. Xue, L.; Wang, P.; Wang, L.; Renzi, E.; Radivojac, P.; Tang, H.; Arnold, R.; Zhu, J.-K.; Tao, W.A. Quantitative measurement of phosphoproteome response to osmotic stress in arabidopsis based on Library-Assisted eXtracted Ion Chromatogram (LAXIC). *Mol. Cell. Proteom.* **2013**, *12*, 2354–2369. https://doi.org/10.1074/mcp.O113.027284.
54. Bologna, Z.; Teoh, J.-P.; Bayoumi, A.S.; Tang, Y.; Kim, I.-M. Biased G Protein-Coupled Receptor Signaling: New Player in Modulating Physiology and Pathology. *Biomol. Ther.* **2017**, *25*, 12–25. https://doi.org/10.4062/biomolther.2016.165.
55. Watkins, J.M.; Ross-Elliott, T.J.; Shan, X.; Lou, F.; Dreyer, B.; Tunc-Ozdemir, M.; Jia, H.; Yang, J.; Oliveira, C.C.; Wu, L.; et al. Differential regulation of G protein signaling in Arabidopsis through two distinct pathways that internalize AtRGS1. *Sci. Signal.* **2021**, *14*, eabe4090. https://doi.org/10.1126/scisignal.abe4090.

56. Laporte, S.A.; Miller, W.E.; Kim, K.-M.; Caron, M.G. beta-Arrestin/AP-2 interaction in G protein-coupled receptor internalization: Identification of a beta-arrestin binging site in beta 2-adaptin. *J. Biol. Chem.* **2002**, *277*, 9247–9254. https://doi.org/10.1074/jbc.M108490200.
57. Zelazny, E.; Santambrogio, M.; Gaude, T. Retromer association with membranes: Plants have their own rules! *Plant Signal. Behav.* **2013**, *8*, e25312. https://doi.org/10.4161/psb.25312.
58. Gallon, M.; Clairfeuille, T.; Steinberg, F.; Mas, C.; Ghai, R.; Sessions, R.B.; Teasdale, R.D.; Collins, B.M.; Cullen, P.J. A unique PDZ domain and arrestin-like fold interaction reveals mechanistic details of endocytic recycling by SNX27-retromer. *Proc. Natl. Acad. Sci. USA* **2014**, *111*, E3604–E3613. https://doi.org/10.1073/pnas.1410552111.
59. van Koppen, C.J.; Jakobs, K.H. Arrestin-independent internalization of G protein-coupled receptors. *Mol. Pharmacol.* **2004**, *66*, 365–367. https://doi.org/10.1124/mol.104.003822.
60. Watkins, J.M.; Clark, N.M.; Song, G.; Oliveira, C.C.; Mishra, B.; Brachova, L.; Seifert, C.M.; Mitchell, M.S.; dos Reis, P.A.B.; Urano, D.; et al. Phosphorylation dynamics in a flg22-induced, heterotrimeric G-protein dependent signaling network in *Arabidopsis thaliana* reveals a candidate PP2A phosphatase involved in AtRGS1 trafficking. *BioRxiv* **2021**. https://doi.org/10.1101/2021.12.06.471472.
61. Vetter, I.R.; Wittinghofer, A. The guanine nucleotide-binding switch in three dimensions. *Science* **2001**, *294*, 1299–1304. https://doi.org/10.1126/science.1062023.
62. Sprang, S.R. G protein mechanisms: Insights from structural analysis. *Annu. Rev. Biochem.* **1997**, *66*, 639–678. https://doi.org/10.1146/annurev.biochem.66.1.639.
63. Simanshu, D.K.; Nissley, D.V.; McCormick, F. RAS proteins and their regulators in human disease. *Cell* **2017**, *170*, 17–33. https://doi.org/10.1016/j.cell.2017.06.009.
64. Chen, Z.; Singer, W.D.; Sternweis, P.C.; Sprang, S.R. Structure of the p115RhoGEF rgRGS domain-Galpha13/i1 chimera complex suggests convergent evolution of a GTPase activator. *Nat. Struct. Mol. Biol.* **2005**, *12*, 191–197. https://doi.org/10.1038/nsmb888.
65. Mittal, V.; Linder, M.E. The RGS14 GoLoco domain discriminates among Galphai isoforms. *J. Biol. Chem.* **2004**, *279*, 46772–46778. https://doi.org/10.1074/jbc.M407409200.
66. Marotti, L.A.; Newitt, R.; Wang, Y.; Aebersold, R.; Dohlman, H.G. Direct identification of a G protein ubiquitination site by mass spectrometry. *Biochemistry* **2002**, *41*, 5067–5074. https://doi.org/10.1021/bi015940q.
67. Van Eps, N.; Oldham, W.M.; Hamm, H.E.; Hubbell, W.L. Structural and dynamical changes in an alpha-subunit of a heterotrimeric G protein along the activation pathway. *Proc. Natl. Acad. Sci. USA* **2006**, *103*, 16194–16199. https://doi.org/10.1073/pnas.0607972103.
68. Li, B.; Tunc-Ozdemir, M.; Urano, D.; Jia, H.; Werth, E.G.; Mowrey, D.D.; Hicks, L.M.; Dokholyan, N.V.; Torres, M.P.; Jones, A.M. Tyrosine phosphorylation switching of a G protein. *J. Biol. Chem.* **2018**, *293*, 4752–4766. https://doi.org/10.1074/jbc.RA117.000163.
69. Poppleton, H.; Sun, H.; Fulgham, D.; Bertics, P.; Patel, T.B. Activation of Gsalpha by the epidermal growth factor receptor involves phosphorylation. *J. Biol. Chem.* **1996**, *271*, 6947–6951. https://doi.org/10.1074/jbc.271.12.6947.
70. Huang, S.; Benben, A.; Green, R.; Cheranda, N.; Lee, G.; Joseph, B.; Keaveney, S.; Wang, Y. Phosphorylation of the Gα protein Gpa2 promotes protein kinase A signaling in yeast. *J. Biol. Chem.* **2019**, *294*, 18836–18845. https://doi.org/10.1074/jbc.RA119.009609.
71. Rudrabhatla, P.; Reddy, M.M.; Rajasekharan, R. Genome-wide analysis and experimentation of plant serine/ threonine/tyrosine-specific protein kinases. *Plant Mol. Biol.* **2006**, *60*, 293–319. https://doi.org/10.1007/s11103-005-4109-7.
72. Chakravorty, D.; Gookin, T.E.; Milner, M.J.; Yu, Y.; Assmann, S.M. Extra-Large G Proteins Expand the Repertoire of Subunits in Arabidopsis Heterotrimeric G Protein Signaling. *Plant Physiol.* **2015**, *169*, 512–529. https://doi.org/10.1104/pp.15.00251.
73. Lee, Y.R.; Assmann, S.M. *Arabidopsis thaliana* "extra-large GTP-binding protein" (AtXLG1): A new class of G-protein. *Plant Mol. Biol.* **1999**, *40*, 55–64. https://doi.org/10.1023/a:1026483823176.
74. Lou, F.; Abramyan, T.M.; Jia, H.; Tropsha, A.; Jones, A.M. An atypical heterotrimeric Gα protein has substantially reduced nucleotide binding but retains nucleotide-independent interactions with its cognate RGS protein and Gβγ dimer. *J. Biomol. Struct. Dyn.* **2020**, *38*, 5204–5218. https://doi.org/10.1080/07391102.2019.1704879.
75. Heo, J.B.; Sung, S.; Assmann, S.M. Ca2+-dependent GTPase, extra-large G protein 2 (XLG2), promotes activation of DNA-binding protein related to vernalization 1 (RTV1), leading to activation of floral integrator genes and early flowering in Arabidopsis. *J. Biol. Chem.* **2012**, *287*, 8242–8253. https://doi.org/10.1074/jbc.M111.317412.
76. Urano, D.; Maruta, N.; Trusov, Y.; Stoian, R.; Wu, Q.; Liang, Y.; Jaiswal, D.K.; Thung, L.; Jackson, D.; Botella, J.R.; et al. Saltational evolution of the heterotrimeric G protein signaling mechanisms in the plant kingdom. *Sci. Signal.* **2016**, *9*, ra93. https://doi.org/10.1126/scisignal.aaf9558.
77. Petutschnig, E.; Anders, J.; Stolze, M.; Meusel, C.; Hacke, R.; Schwier, M.; Gippert, A.-L.; Kroll, S.; Fasshauer, P.; Wiermer, M.; et al. EXTRA LARGE G-PROTEIN 2 (XLG2) mediates cell death and hyperimmunity via a novel, apoplastic ROS-independent pathway in *Arabidopsis thaliana*. *BioRxiv* **2021**. https://doi.org/10.1101/2021.10.08.463358.
78. Kamal, M.M.; Ishikawa, S.; Takahashi, F.; Suzuki, K.; Kamo, M.; Umezawa, T.; Shinozaki, K.; Kawamura, Y.; Uemura, M. Large-Scale Phosphoproteomic Study of Arabidopsis Membrane Proteins Reveals Early Signaling Events in Response to Cold. *Int. J. Mol. Sci.* **2020**, *21*, 8631. https://doi.org/10.3390/ijms21228631.
79. Liang, Y.; Gao, Y.; Jones, A.M. Extra Large G-Protein Interactome Reveals Multiple Stress Response Function and Partner-Dependent XLG Subcellular Localization. *Front. Plant Sci.* **2017**, *8*, 1015. https://doi.org/10.3389/fpls.2017.01015.

80. Lease, K.A.; Wen, J.; Li, J.; Doke, J.T.; Liscum, E.; Walker, J.C. A mutant Arabidopsis heterotrimeric G-protein beta subunit affects leaf, flower, and fruit development. *Plant Cell* **2001**, *13*, 2631–2641. https://doi.org/10.1105/tpc.010315.
81. Clapham, D.E.; Neer, E.J. G protein beta gamma subunits. *Annu. Rev. Pharmacol. Toxicol.* **1997**, *37*, 167–203. https://doi.org/10.1146/annurev.pharmtox.37.1.167.
82. Gao, Y.; Wang, S.; Asami, T.; Chen, J.-G. Loss-of-function mutations in the Arabidopsis heterotrimeric G-protein alpha subunit enhance the developmental defects of brassinosteroid signaling and biosynthesis mutants. *Plant Cell Physiol.* **2008**, *49*, 1013–1024. https://doi.org/10.1093/pcp/pcn078.
83. Cho, Y.; Yu, C.-Y.; Iwasa, T.; Kanehara, K. Heterotrimeric G protein subunits differentially respond to endoplasmic reticulum stress in Arabidopsis. *Plant Signal. Behav.* **2015**, *10*, e1061162. https://doi.org/10.1080/15592324.2015.1061162.
84. Ma, Y.; Chen, M.; Xu, D.; Fang, G.; Wang, E.; Gao, S.; Xu, Z.; Li, L.; Zhang, X.; Min, D.; et al. G-protein β subunit AGB1 positively regulates salt stress tolerance in Arabidopsis. *J. Integr. Agric.* **2015**, *14*, 314–325. https://doi.org/10.1016/S2095-3119(14)60777-2.
85. Maruta, N.; Trusov, Y.; Brenya, E.; Parekh, U.; Botella, J.R. Membrane-localized extra-large G proteins and Gbg of the heterotrimeric G proteins form functional complexes engaged in plant immunity in Arabidopsis. *Plant Physiol.* **2015**, *167*, 1004–1016. https://doi.org/10.1104/pp.114.255703.
86. Trusov, Y.; Rookes, J.E.; Tilbrook, K.; Chakravorty, D.; Mason, M.G.; Anderson, D.; Chen, J.-G.; Jones, A.M.; Botella, J.R. Heterotrimeric G protein gamma subunits provide functional selectivity in Gbetagamma dimer signaling in Arabidopsis. *Plant Cell* **2007**, *19*, 1235–1250. https://doi.org/10.1105/tpc.107.050096.
87. Chakravorty, D.; Trusov, Y.; Zhang, W.; Acharya, B.R.; Sheahan, M.B.; McCurdy, D.W.; Assmann, S.M.; Botella, J.R. An atypical heterotrimeric G-protein γ-subunit is involved in guard cell K^+-channel regulation and morphological development in *Arabidopsis thaliana*. *Plant J.* **2011**, *67*, 840–851. https://doi.org/10.1111/j.1365-313X.2011.04638.x.
88. Li, S.; Liu, W.; Zhang, X.; Liu, Y.; Li, N.; Li, Y. Roles of the Arabidopsis G protein γ subunit AGG3 and its rice homologs GS3 and DEP1 in seed and organ size control. *Plant Signal. Behav.* **2012**, *7*, 1357–1359. https://doi.org/10.4161/psb.21620.
89. Maruta, N.; Trusov, Y.; Chakravorty, D.; Urano, D.; Assmann, S.M.; Botella, J.R. Nucleotide exchange-dependent and nucleotide exchange-independent functions of plant heterotrimeric GTP-binding proteins. *Sci. Signal.* **2019**, *12*, eaav9526. https://doi.org/10.1126/scisignal.aav9526.
90. Yu, T.-Y.; Shi, D.-Q.; Jia, P.-F.; Tang, J.; Li, H.-J.; Liu, J.; Yang, W.-C. The arabidopsis receptor kinase ZAR1 is required for zygote asymmetric division and its daughter cell fate. *PLoS Genet.* **2016**, *12*, e1005933. https://doi.org/10.1371/journal.pgen.1005933.
91. Tsugama, D.; Liu, S.; Takano, T. Arabidopsis heterotrimeric G protein β subunit, AGB1, regulates brassinosteroid signalling independently of BZR1. *J. Exp. Bot.* **2013**, *64*, 3213–3223. https://doi.org/10.1093/jxb/ert159.
92. Adjobo-Hermans, M.J.W.; Goedhart, J.; Gadella, T.W.J. Plant G protein heterotrimers require dual lipidation motifs of Galpha and Ggamma and do not dissociate upon activation. *J. Cell Sci.* **2006**, *119*, 5087–5097. https://doi.org/10.1242/jcs.03284.
93. Oki, K.; Fujisawa, Y.; Kato, H.; Iwasaki, Y. Study of the constitutively active form of the alpha subunit of rice heterotrimeric G proteins. *Plant Cell Physiol.* **2005**, *46*, 381–386. https://doi.org/10.1093/pcp/pci036.
94. Maruta, N.; Trusov, Y.; Urano, D.; Chakravorty, D.; Assmann, S.M.; Jones, A.M.; Botella, J.R. GTP binding by Arabidopsis extra-large G protein 2 is not essential for its functions. *Plant Physiol.* **2021**, *186*, 1240–1253. https://doi.org/10.1093/plphys/kiab119.
95. Ghusinga, K.R.; Elston, T.C.; Jones, A.M. Towards resolution of a paradox in plant G-protein signaling. *Plant Physiol.* **2022**, *188*, 807–815. https://doi.org/10.1093/plphys/kiab534.
96. Liao, K.-L.; Jones, R.D.; McCarter, P.; Tunc-Ozdemir, M.; Draper, J.A.; Elston, T.C.; Kramer, D.; Jones, A.M. A shadow detector for photosynthesis efficiency. *J. Theor. Biol.* **2017**, *414*, 231–244. https://doi.org/10.1016/j.jtbi.2016.11.027.

CHAPTER II

RGS1 GLOBAL PHOSPHORYLATION AS A COOPERATIVE MECHANISM FOR G-PROTEIN REGULATION

ABSTRACT

RGS1 global phosphorylation as a cooperative mechanism for G-protein regulation

Multiple pathways in the plant cell are mediated by the self-activating heterotrimeric G-proteins. Therefore, one of the major steps of regulation at the alpha subunit requires the presence of GTPase-activating proteins (GAPs) that, in plants, algae, and protists, are found to be seven-transmembrane (7TM) proteins with a conserved RGSbox cytoplasmic domain. The Arabidopsis regulator of G-signaling (AtRGS1) is phosphorylated in response to several stimuli as for the bacterial peptide flg22 and the nucleotide sugar UDP-glucose, leading to the uncoupling from the alpha subunit AtGPA1. Here we take advantage of the split luciferase technique, immunodetection assays, confocal microscopy, and *in silico* simulations to evaluate the effect of phosphomimetic and phosphonull versions of AtRGS1 on its structure and function. Quantitative data indicated that multiple phosphorylation events on the C-terminal tail serine cluster of AtRGS1 are required for G-protein activation and recruitment of the endocytic machinery. Consistently, plant-conserved linker residue (Ser278) promotes Gα, Gβ and adaptor protein dissociation, while it regulates the flexibility, contacts, and phosphorylation levels of distal phosphosites, including the cluster serines and one or more threonine residues predicted at the RGSbox. Additionally, the inactivation of the phosphosite by a serine-to-alanine mutation abolished the internalization of AtRGS1 on flg22-treated seedlings, but no change was observed under UDP-glucose addition. Collectively with the presented evolutionary data, we propose plant-conserved mechanism of regulation based on multiple phosphorylation events regulating protein flexibility, plasma membrane positioning, thus interface availability.

Keywords: RGS1. Phosphorylation. Flg22. G-protein. Linker. Cluster.

INTRODUCTION

The plant adaptation process to adverse environmental conditions requires the activation and coordination of specific responses that modulate the cell signaling and its metabolism to guarantee energy availability and plant survival (Bohnert and Sheveleva, 1998). For instance, drought and salinity conditions lead to differential stomatal opening that affects CO_2 uptake, and, as a consequence, the photorespiratory cycle (Bohnert and Sheveleva, 1998; Nelson et al., 1998; Ingram and Bartels, 1996; Pirasteh-Anosheh et al., 2016). Thus, a combination of external signal perception, signal transduction, hormone regulation, and gene expression is crucial for maintaining plant homeostasis (Waadt et al., 2022; Li et al., 2022; Belkhadir et al., 2014).

Cell signaling relies on different and complex mechanisms that may specifically recognize a signal and trigger a precise response to its activation. In this context, the heterotrimeric G-protein signaling plays an essential role through the modulation of distinct cell responses (Jiang et al., 2022). Its general and conserved activation/inactivation mechanism is mainly based on the GTP/GDP binding to the alpha subunit, and, consequently, its affinity to the dimer Gβγ (Clapham and Neer, 1997). The regulation of multiple pathways via heterotrimeric G-proteins acts as a bottleneck for cellular signaling in plants, while in animals, a vast combination of alpha, beta and gamma subunits is modulated by different G-protein-coupled-receptors (GPCRs) (Oldham and Hamm, 2008; Hurowitz et al., 2000). *Arabidopsis thaliana* genome only codes one canonical alpha (AtGPA1), one beta (AtAGB1) and three gamma (AtAGG1/2/3) subunits and has no characterized GPCR (Urano and Jones, 2014; Chen and Jones, 2004). Additionally, three non-canonical extra-large Gα proteins (XLGs) are identified in Arabidopsis, and a regulator of G-signaling (AtRGS1) has been widely studied (Chen et al., 2003; Chakravorty et al., 2015). Even though the classical paradigm in animals involves RGS proteins, which are found to be soluble proteins in a group of GTPase-accelerating proteins (GAPs) (Exton 2013), plant RGS proteins present an architecture that comprises a seven-transmembrane (7TM) GPCR-like domain at the N-terminal portion, a flexible linker region, and a conserved RGSbox domain followed by a non-conserved C-terminal tail (Figure 1A) (Oliveira et al., 2022; Siderovski and Willard, 2005; Jumper et al., 2021). Moreover, plants, algae, and protists possess Gα subunits that are able to exchange GDP to GTP in a GPCR-independent mechanism, and a limited number of those are regulated by 7TM-RGS proteins. The presence of 7TM-GAPs on the eukaryotic base indicates that ancestral regulators of G-proteins were GAP-functioning receptors (Bradford et al., 2013).

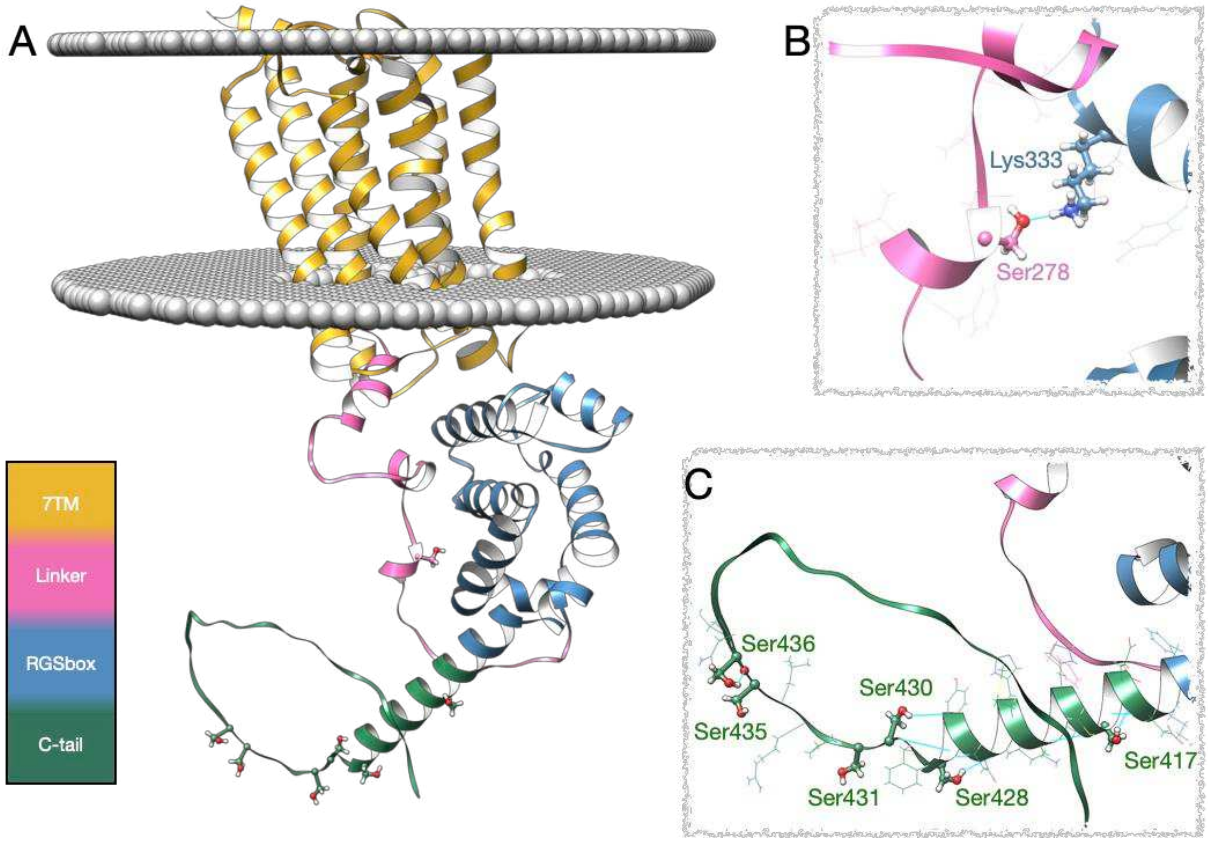

Figure 1 - AtRGS1 structural model at the plasma membrane. (A) Top-ranked AlphaFold2 protein structural model predicts that full-length AtRGS1 has seven transmembrane domains (yellow), a flexible linker region (pink) followed by a conserved RGSbox domain (blue), and a disordered C-terminal tail (green). **(B)** Ser278 is predicted in a small helix segment, and it displays a plausible hydrogen bond with the RGSbox residue Lys333. **(C)** *In vivo*-detected C-terminal tail residues are composed of Ser417 and five other residues (Ser428, Ser430, Ser 431, Ser435 and Ser436) clustered after the RGSbox. Predicted hydrogen bonds are represented as cyan lines. Serine phosphosites and Lys333 are indicated as ball and sticks. Neighbor residues are represented as wires. Plasma membrane lipids are represented as grey balls. Domains and regions are separated by color as indicated.

In addition to the nucleotide exchange activity, animal G-signaling is negatively regulated by GPCR C-tail phosphorylation and β-arrestin-mediated signaling (Gurevich and Gurevich, 2019). The phosphorylation is promoted by GPCR kinases (GRKs) at the cytoplasmic portion, which results in β-arrestin recruitment and activation (Jean-Charles et al., 2017). Activated β-arrestin may desensitize G-signaling with or without receptor internalization, or it acts as a scaffold protein for specific arrestin signaling (Xiao and Sun, 2018; Jean-Charles et al., 2017). The concept of biased signaling on GPCRs reflects a barcoding where multiple serine and threonine residues are phosphorylated in a specific manner to drive arrestin binding, conformation, and, as a consequence, its function on cellular signaling (Liggett 2011; Latorraca et al., 2020). On the other side, AtRGS1 is phosphorylated *in vivo* and *in vitro* at multiple serine

residues that include a cluster of five residues at the C-terminal tail, one serine (Ser417) at the end of the RGSbox and one at the linker region (Ser278) (Figure 1); while predicted and *in vitro* detected sites include two threonine residues at the RGSbox (Oliveira et al., 2022; Tunc-Ozdemir et al., 2017).

In sugar production and signaling, photosynthetic efficiency depends not only on night/day conditions, but also on other environmental factors, and this makes sugar concentration drastically vary from a few minutes to hours (Deuschle et al., 2006; Fu et al., 2014). Thus, plants present dose-duration reciprocity for sugar sensing and signaling, where a coordinated response is similarly activated under transient, low-intensity or high-intensity sugar signals (Fu et al., 2014). In order to regulate plant metabolism and growth, D-glucose is able to activate several sensors, as one glycolysis-independent pathway mediated by the hexokinase (HXK) enzymes, one glycolysis-dependent pathway linked to the SNF1-related Protein Kinase 1 (SNK1), and one G-protein-dependent pathway, where AtRGS1 is phosphorylated and internalized under high concentrations of the monosaccharide (Fu et al., 2014; Urano et al., 2012; Smeekens et al., 2010). Finally, the sugar-induced phosphorylation of AtRGS1 is mediated by the atypical enzymes WITH-NO-LYSINE kinases (WNKs) (Cao-Pham et al., 2018; Urano et al., 2012).

Recent data suggests that UDP-glucose may be the main signal on AtRGS1-mediated sugar responses: (1) UDP-glucose is able to induce the phosphorylation of the AtRGS1 serine cluster residues *in vivo*; (2) the sucrose synthase enzymes SuS1 and SuS4 are AtRGS1 interacting partners and are required for D-glucose- and sucrose-induced internalization, but not UDP-glucose induced internalization (unpublished) (Klopffleisch et al., 2011; Oliveira et al., 2022).

Immune responses in plants can be elicited by flg22, a peptide that contains 22 amino acid residues from the N-terminal portion of bacterial flagellin (Zipfel et al., 2004; Gómez-Gómez et al., 1999). Flg22 is recognized by its receptor FLS2 (FLAGELLIN-SENSITIVE 2), a leucine-rich repeat (LRR) receptor-like kinase (RLK) (Gómez-Gómez and Boller, 2000). Under elicitation, FLS2 forms a complex with other LRR-RLK BAK1 (BRASSINOSTEROID INSENSITIVE 1-associated receptor kinase 1) and with the cytoplasmic kinase BIK1 (BOTRYTIS-INDUCED KINASE 1) (Zipfel et al., 2004; Lu et al., 2010). BIK1 is transphosphorylated by the complex and released to regulate downstream responses as RbohD-mediated ROS (reactive oxygen species) production, MAPK (mitogen-activated protein kinase) cascade activation, and calcium burst (Lu et al., 2010; Zhou et al., 2019). The defense process under flg22 elicitation, and for other biotic stressors, leads to a growth attenuation that is

mediated by several phytohormones, including the brassinosteroids (BRs). Accordingly, BAK1 also dimerizes with the BR receptor BRI1 (BRASSINOSTEROID INSENSITIVE 1), leading to BR pathway activation and immune response attenuation that is downstream of BAK1 dimerization (Peres et al., 2019). This mechanism was first described as unidirectional, as PTI (PAMP-triggered immunity) activation did not affect the analyzed steps of BR signaling pathways (Albrecht et al., 2012), but it has been shown that flg22 elicitation is able to suppress BR biosynthesis-related genes in a pathway that is independent of BR recognition, unveiling an indirect and bidirectional crosstalk (Jiménez-Góngora et al., 2015). A reverse modulation of antiviral and flg22 signaling is also explored in the literature, in which the LRR-RLK NIK1 mediates the crosstalk with its plasma membrane interacting partners FLS2 and BAK1 (Li et al., 2019).

Under flg22-activated signaling, AtRGS1 interacts with the FLS2/BAK1/BIK1 complex and the phosphorylation at the serine cluster is required for further AtRGS1 internalization and G-protein uncoupling (Liang et al., 2016; Liang et al., 2018; Tunc-Ozdemir et al., 2016). Since Arabidopsis genome does not encode any β-arrestin, the proposed adaptors are two of the vacuolar protein sorting 26 (VPS26a/b), which interact with AtRGS1 and are both required for flg22-induced internalization via clathrin-mediated endocytosis (CME) (Watkins et al., 2021; Zelazny et al., 2013). Similar to the immune responses, at high sugar concentrations AtVPS26a and AtVPS26b mediate a phosphorylation-dependent internalization of AtRGS1 via CME, but another pathway is also activated, internalizing AtRGS1 via sterol-dependent endocytosis (SDE) (Watkins et al., 2021). Furthermore, the D-glucose-activated SDE pathway does not depend on cluster phosphorylation, unveiling two distinct endocytic pathways that modulate G-protein in Arabidopsis (Watkins et al., 2021; Urano et al., 2012). Finally, VPS26 proteins have an arrestin-like folding, and these findings are consistent with the β-arrestin biased signaling described in mammals (Watkins et al., 2021; Bologna et al., 2017).

Those molecular findings are consistent with several phenotypes observed in *rgs1-2* plants, as it displays lower pathogen colonization rate comparing to wild-type plants, higher flg22-related gene induction, abolished flg22-induced Ca^{2+} release, and impaired reactive oxygen species (ROS) burst under immune elicitation (Liang et al., 2018; Marcec and Tanaka, 2021; Tunc-Ozdemir and Jones, 2017; Ghusinga et al., 2021; Watkins et al., 2021). Furthermore, *rgs1-2* plants have higher germination/growth rate under high concentrations D-glucose and NaCl, while 35S::RGS1 transformed plants show higher tolerance to drought compared to the Columbia ecotype (Urano et al., 2012; Colaneri et al., 2014; Huang et al., 2015; Chen et al., 2006).

The absence of GPCRs in plants may be explained by the regulation performed by receptor-like kinases (RLKs), which recognize the signal and triggers the modulation of the G-complex in a phosphorylation-dependent mechanism. With the exception of AtAGG1, all other G-protein subunits were also found to be phosphorylated *in vivo* (Oliveira et al., 2022). AtGPA1 has a novel mechanism in G-signaling where phosphorylation at the Tyrosine residue 166 is required for activation rather than the nucleotide state alone (Li et al., 2018). In a plausible coordination with other N-terminal residues, Tyr166 is required for BAK1-mediated phosphorylation of AtGPA1, and the phosphomimetic mutation AtGPA1^{Y166E} leads to weaker AtRGS1 interaction, attenuating the GTPase activity (Li et al., 2018; Xue et al., 2020).

Although several residues are involved in the AtRGS1-mediated pathways for flg22 and D-glucose (Liang et al., 2018; Urano et al., 2012; Watkins et al., 2021), the effects of the signal-specific cluster residues, and other two phosphosites located outside of the cluster (Ser278 and Ser417) are still unclear. Here, we took advantage of the multiple AtRGS1 phosphomimetic mutations and molecular dynamics (MD) simulations to shed light in the RGS1 mechanisms through its phosphorylation pattern, which drives and discriminates the G-protein binding, activation, and stress responses. Moreover, we explore different evolutionary aspects of 7TM-RGS proteins across plant and algae species, including a novel concept - evolutionary constraint based on phosphosite-driven domain orientation.

MATERIAL AND METHODS

Plasmid construction and site-directed mutagenesis

Entry clones were generated using the Gateway™ technology. The coding region of *AtRGS1* (AT3G26090) was amplified from *Arabidopsis thaliana* cDNA and inserted on pDONR221 by BP Clonase (Invitrogen) reaction. *HiBiT*-tagged *AtRGS1* entry clone was generated by inserting the short coding sequence at the Reverse primer (Table 1) and inserted on pENTR/D-TOPO vector (Invitrogen). For site-directed mutagenesis, Q5® High-Fidelity DNA Polymerase (New England Biolabs) was used for end-to-end amplification of the entry vector. Mutagenesis oligonucleotides were designed for single or multiple codon modification and a free phosphate group was added to the 5' end of each primer (Table 1). The linear vector was then ligated using the T4 DNA Ligase enzyme (Invitrogen). New clones were generated by transforming into E. coli DH5α and confirmed by sequencing. Cloned genes were subjected to LR Clonase (Invitrogen) reaction and transferred to the plant expression vectors pEarleyGate 101, pK7FWG2 and pCAMBIA-NLuc. Clones from *AtGPA1*, *AtAGB1*, *AtVPS26a* and *AtVPS26b* on pCAMBIA-CLuc vectors, as well as TAP-tagged AtRGS1 overexpressing lines,

were obtained from Jones Lab stocks at The University of North Carolina at Chapel Hill (US) (Watkins et al., 2021; Urano et al., 2012).

Structural modeling and molecular dynamics simulation

Tridimensional structural models from single chains and complexes were obtained using the AlphaFold2 algorithm (Jumper et al., 2021; Mirdita et al., 2022). Five models were generated, relaxed with the AMBER embedded tool, and top ranked models were chosen based on pLDDT score for proteins or pTM score for complexes. Top 1 models were then subjected to membrane positioning using the PPM 3.0 Web Server (Lomize et al., 2021)**,** where plant plasma membrane parameters were selected and the N-terminal of AtRGS1 was placed at the extracellular portion of the membrane.

For single AtRGS1 structures, discrete molecular dynamics (DMD) simulations of C-alpha atoms were performed with the MDWeb tool at 295K for 500 ns (Hospital et al., 2012). Conformational variability of phosphomimetic and alanine mutants were analyzed by calculating Cα Root Mean Square Deviation (RMSD) of the whole protein along the trajectory or per residue. Dynamic residue correlation was extracted from the trajectory with the MDM-TASK tool (Sheik Amamuddy et al., 2021). For AtRGS1-AtGPA1 complexes and AtRGS1 intrachain contacts, we analyzed the interchain residue contact network using the CABS-flex 2.0 tool for an all-atom simulation of 10 ns (Kuriata et al., 2018). UCSF Chimera was used for structure handling and representation (Pettersen et al., 2004).

Split-luciferase complementation assay

CLuc-tagged and HiBiT-NLuc-tagged genes were transferred into GV3101 *Agrobacterium* cells and leaf co-infiltration was performed on 5-week-old *Nicotiana benthamiana* plants. About 6 leaf disks from each of the 16 biological replicates were collected 2 days after infiltration and mixed in 96-well plate with 1 mM D-Luciferin or HiBiT reaction mix (Promega). Reaction was maintained in the dark for 10 minutes and light intensity was measured at 570 nm. Luciferase activity was normalized by the HiBiT expression level average in each leaf. For treated leaf disks, 1 mM D-Luciferin was mixed with 1 μM flg22 and the reaction was maintained in the dark for 25 minutes before measurement.

Plant transformation and growth conditions

Arabidopsis thaliana rgs1-2 allele was obtained from the Arabidopsis Biological Resource Center (ABRC) and confirmed by RT-qPCR (Table 1) (Chen et al., 2003). The ecotype Columbia (Col-0) was used as the wild-type control. Phosphomimetic and phosphonull versions of AtRGS1 on pEarleyGate 101 vector were transferred to *Agrobacterium tumefaciens*

cells and transformed into *rgs1-2* plants by the floral dip method (Zhang et al., 2006). Single-insertion homozygous lines were selected by BASTA resistance and its related survival rate.

For normal growth, Arabidopsis plants were maintained in a growth chamber under short-day conditions (21°C, 8h/light, 16h/dark). Seedlings for RT-qPCR and western blot analysis were germinated on ¼ strength liquid Murashige and Skoog (MS) medium and grown for 7 days under low constant light conditions. For confocal microscopy, seedlings were placed on ¼ strength liquid MS and etiolated under dark conditions.

Nicotiana benthamiana plants were germinated on soil and kept in a half-day photoperiod (25°C, 12h/day, 22°C, 12h/night) for 5 weeks before infiltration. Dark treatment was applied for 24 hours post-infiltration.

RGS1-YFP internalization

Since the overexpression of a membrane protein may activate endocytic pathways, plants with a wild-type-like expression of YFP-tagged AtRGS1^{WT} (#112), AtRGS1^{S278A} (#345), AtRGS1^{S431A} and AtRGS1$^{S428/431/435/436A}$ (quadA, #290) (Figure S1) were kept under light for 4 hours and transferred to dark conditions. After 3 days of germination, elongated hypocotyl cells were subjected to 15 minutes of 100 nM flg22 exposure or 30 minutes of 123 µM UDP-glucose exposure. Single cells were then observed in a Zeiss LSM880 microscope (C-Apochromat 40x/1.2NA water immersion objective) and YFP signal was recorded from several Z-layers. Image processing and quantification was performed as described in the literature (Watkins et al., 2021).

Immunoblotting analysis of RGS1

For phosphorylation detection, 7-day-old seedlings from overexpressing lines (Figure S1) were subjected to 100 nM flg22 treatment for 3 minutes. Total protein was extracted with RGS1 extraction buffer (50 mM Tris-HCl, pH 7.5, 20% glycerol, 1% Triton X-100, 1 mM EDTA,150 mM NaCl, 50 mM Tris-HCl, pH 7.5, 1 mM PMSF, and 1x Sigma protease and phosphatase inhibitor cocktail). YFP-tagged AtRGS1, AtRGS1^{S278E}, AtRGS1^{S278A} and AtRGS1$^{S428/431/435/436A}$ were purified using µMACS GFP Isolation Kit (Miltenyi Biotec). Purified proteins were separated in 10-12% acrylamide gels and transferred to nitrocellulose or PVDF membranes. Total RGS was detected with HRP anti-GFP antibody (Abcam, ab6663) or anti-AtRGS1 antibody. Phosphorylation was detected using anti-phospho-serine and anti-phospho-threonine antibodies, and cluster phosphorylation at the specific residues Ser428, Ser435 and Ser436 using the anti-phospho-AtRGS1 antibody (Urano et al., 2012).

cDNA preparation and quantitative PCR

Genotyping of complemented lines were performed in 7-day-old seedlings growth under low constant light conditions. Frozen material was ground, and RNA was extracted using the GeneJET Plant RNA Purification Mini Kit (Thermo Scientific). cDNA was synthesized by M-MLV (Thermo Scientific) reaction after DNAse I (Thermo Scientific) treatment. Relative quantification was performed in a CFX Connect Real-Time PCR Detection System (BioRad). The $2^{-\Delta\Delta Ct}$ method was applied using the endogenous control UBQ10 (AT4G05320).

Phylogenetic analysis

We manually collected 7TM-RGS sequences from diverse plants covering streptophyte algae to flowering plants; XP_002267857.1 (*Vitis vinifera*), GAQ79965.1 (*Klebsormidium nitens*), XP_024539565.1 (*Selaginella moellendorffii*), GBG89443.1 (*Chara braunii*), NP_189238.2 (*Arabidopsis thaliana*). These initial sequences were aligned with CLUSTAL W and employed to perform HMMER search against UniProtKB database with the e-value threshold of 10^{-10}. The HMMER search yielded 307 sequences from green plants (Taxonomy Identifier: 33090).

The 307 sequences were pre-processed by removing redundant sequences and/or sequences shorter than 420 residues. The remaining sequences were aligned using the MAFFT version 7, followed by the removal of gapped positions containing ≥10% gaps. We also removed highly similar sequences that showed 75% or higher identity to other sequences and sequences that contain a gap region (≥7 consecutive gaps). The finalized sequence set (28 sequences with 445 positions) was used for phylogenetic analysis by PhyML with the JTT substitution model and 160 bootstrap iterations. The ConSurf server (Ashkenazy et al., 2016) was used to visualize the evolutionary conservation at the AtRGS1 structural model.

RESULTS

Phosphorylation of AtRGS1 at Ser278 regulates G-protein binding

RGS1 phosphorylation by RLKs has been implicated as an important mechanism of signaling triggered in a specific ligand-dependent activation. Therefore, distinct RGS1 phosphorylation patterns might drive the direction and specificity of each signal. In order to test if unique phosphorylation sites have any influence on G-protein binding, VPS26 recruitment and stress responses, we have created multiple phosphomimetic mutants of AtRGS1 from the most conserved *in vivo*-detected sites (Oliveira et al., 2022). Moreover, to test the individual influence of a single phosphomimetic at the cluster region, we generated a quintuple mutant where one site was replaced by an aspartic acid or glutamic acid residue, while the remaining serines were replaced by alanine residues. Ser278 and Ser417 were individually

replaced, once those are the only two *in vivo* sites outside the cluster (Figure 1) (Oliveira et al., 2022).

Using transient expression in *Nicotiana benthamiana* plants, we have determined the binding affinity changes of AtRGS1 phosphomimetic mutants in comparison with the wild-type form of the protein. Single-residue mutations at the C-terminal serine cluster did not affect AtGPA1 binding, and only the quintuple AtRGS1$^{S428E/S430/431/435/436A}$ affected Gβ binding (Figure 2A). Regarding the adaptors VPS26a and VPS26b, single cluster phosphomimicking did not promote any increase in binding. Instead, adding a negative charge at Ser428 and Ser435 decreased the affinity for VPS26a, while AtRGS1$^{S431E/S428/430/435/436A}$ drastically reduced VPS26b binding (Figure 2A). The present data suggests that a null or negative effect of single point phosphomimetic mutations at the serine cluster is not significant enough to promote Gα dissociation or adaptor recruiting.

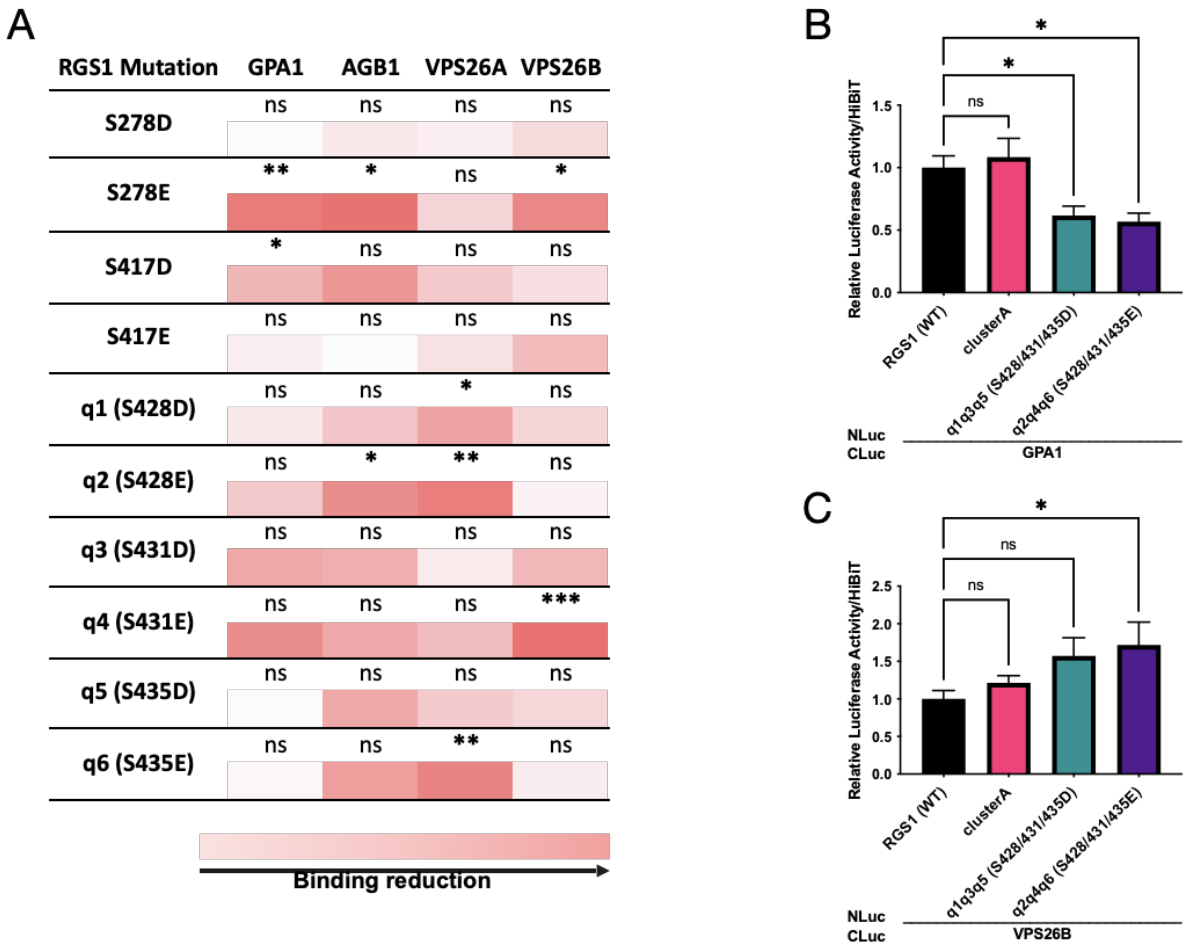

Figure 2 - Phosphomimetic effects on AtRGS1 interactions. (A) Split-luciferase data summary of AtRGS1 phosphomimetics and its interaction levels compared to the wild-type protein. Transiently expressed Gα, Gβ, and candidate adaptor proteins were tested against AtRGS1 variants in *Nicotiana benthamiana* leaves. Fold-variation comparing to the non-mutated AtRGS1 is represented as a white and red gradient. White indicates no change in

luciferase signal. Red indicates signal depletion comparing to the wild-type protein. **(B-C)** Multiple phosphomimetic mutations at the cluster are required for GPA1 activation and VPS26B recruitment. Split-luciferase data is normalized by RGS1 expression levels. Error bars = SEM, n ≈ 16. Significance levels: * <0.05, ** <0.01, *** <0.001, ns = not significant as determined by a two-way ANOVA with post-hoc Tukey multiple comparison test.

AtRGS1^{S417D} slightly reduces AtRGS1-AtGPA1 complex, but changing the linker residue Ser278 to a glutamic acid residue promotes Gα, Gβ and VPS26b dissociation (Figure 2A). As Ser278 is a substrate for BIK1, AVRPPHB SUSCEPTIBLE1 (PBS1)-like 1 (PBL1) and BRI1-LIKE 3 (BRL3) (Tunc-Ozdemir et al., 2017; Liang et al., 2018; Oliveira et al., 2022), this phosphorylation may be required for the crosstalk between growth and immune responses that is mediated by AtRGS1.

Multiple cluster phosphorylation leads to G-protein dissociation and adaptor recruitment

Since single-point mutations at the C-terminal tail did not promote Gα dissociation and subsequent activation, we have decided to test a combination of a triple phosphomimetic mutant over a double alanine mutation background. The sites Ser428, Ser431and Ser435 were chosen based on neighbor residue distance, function, and conservation, respectively. Both AtRGS1$^{S428/431/435E/S430/436A}$ and AtRGS1$^{S428/431/435D/S430/436A}$ promoted AtGPA1 dissociation (Figure 2B), but only AtRGS1$^{S428/431/435D/S430/436A}$ had a significant increase on VPS26b binding (Figure 2C). Aside from the wild-type control, we have also tested a S428/430/431/435/436A mutation (hereafter clusterA) that did not affect binding, as expected for non-phosphorylatable form (Figure 2B-C). In the arrestin-GPCR signaling pathways, the β-arrestin binding is not directly proportional to its activation levels (Latorraca et al., 2020). Thus, the ability of the two mutants to promote Gα dissociation and partial adaptor recruitment suggests a mechanism where phosphorylation induces G-protein activation prior to adaptor recruitment, and AtRGS1 may be internalized to avoid possible phosphatase binding and subsequent AtGPA1 inactivation.

Ser278 is required for flg22-induced internalization of AtRGS1

RGS1 endocytosis in a ligand-dependent manner promotes the desensitization and increases signaling duration. The internalization of AtRGS1-YFP is observed within 15 minutes of flg22 exposure or 30 minutes of 6% D-glucose treatment, and C-tail phosphorylation is required or partially required for this process (Watkins et al., 2021). Using a UDP molecule, the SuS enzymes are able to convert sucrose in UDP-D-glucose and D-frutose (Kleczkowski 1996), and, while concentrations above 6% of D-glucose are optimal to induce the

internalization of the 7TM protein, only 123 nM of UDP-glucose is able to promote efficient internalization of RGS1-YFP (unpublished).

In order to test the effect of pSer278 in those pathways, we have used *rgs1-2* plants complemented with AtRGS1-YFP, AtRGS1^{S278A}-YFP or AtRGS1$^{S428/431/435/436A}$-YFP (hereafter quadA) for single-cell internalization quantification. UDP-glucose was used as the sugar signal since it induces C-terminal phosphorylation. Dark-induced elongated hypocotyl cells were treated and observed over time, picture was taken after 15 or 30 minutes and internal YFP signal was quantitated over membrane-located YFP.

Our data shows that phosphorylation of Ser278 is required for flg22-mediated internalization, but only partially required for UDP-glucose signaling (Figure 3A), which is consistent with AtRGS1 being internalized by two different pathways under D-glucose treatment (Watkins et al., 2021), the candidate precursor of UDP-glucose in G-protein signaling. Interestingly, the quadA mutant presented abolished flg22-mediated internalization as expected, but UDP-glucose signaling was completely ablated as well. The inconsistence of UDP-glucose with D-glucose published results (Watkins et al., 2021) may be explained by two experimental differences: (1) D-glucose and UDP-glucose balance may be regulated by the SuS-RGS binding, resulting in different mechanisms for the two sugar signals, or (2) quadA has an extra alanine mutation than the one published for D-glucose (3SA/AtRGS1$^{S428/435/436A}$). Thus, the presence of the C-terminal with a specific residue combination may be required for complete ablation of sugar-induced AtRGS1-YFP internalization (Watkins et al., 2021).

Although Ser431 is described as being required for the flg22-induced internalization of AtRGS1 (Liang et al., 2018), our data indicates wild-type-like internalization levels for AtRGS1^{S431A}. Thus, we have demonstrated that a single cluster phosphosite inactivation, or a single phosphomimetic mutation alone, are not able to promote changes in RGS1 internalization and G-protein activation.

AtRGS1 phosphorylation at the linker is required for flg22-induced binding change

To evaluate if flg22 is able to recruit the candidate adaptors to the membrane, we tested if AtRGS1 and AtRGS1^{S278A} interactions with both VPS26a and VPS26b would be affected by the addition of an immune response elicitor in the reaction buffer. Curiously, the addition of flg22 at high concentrations (1 μM) drastically reduced the wild-type RGS1 interactions with both proteins after 25 minutes of treatment (Figure 3B-C). This may be explained by: (1) Arabidopsis-specific components that may not be conserved in the transiently expressed *Nicotiana benthamiana* leaves; (2) the time of the treatment that may be too long for a time-

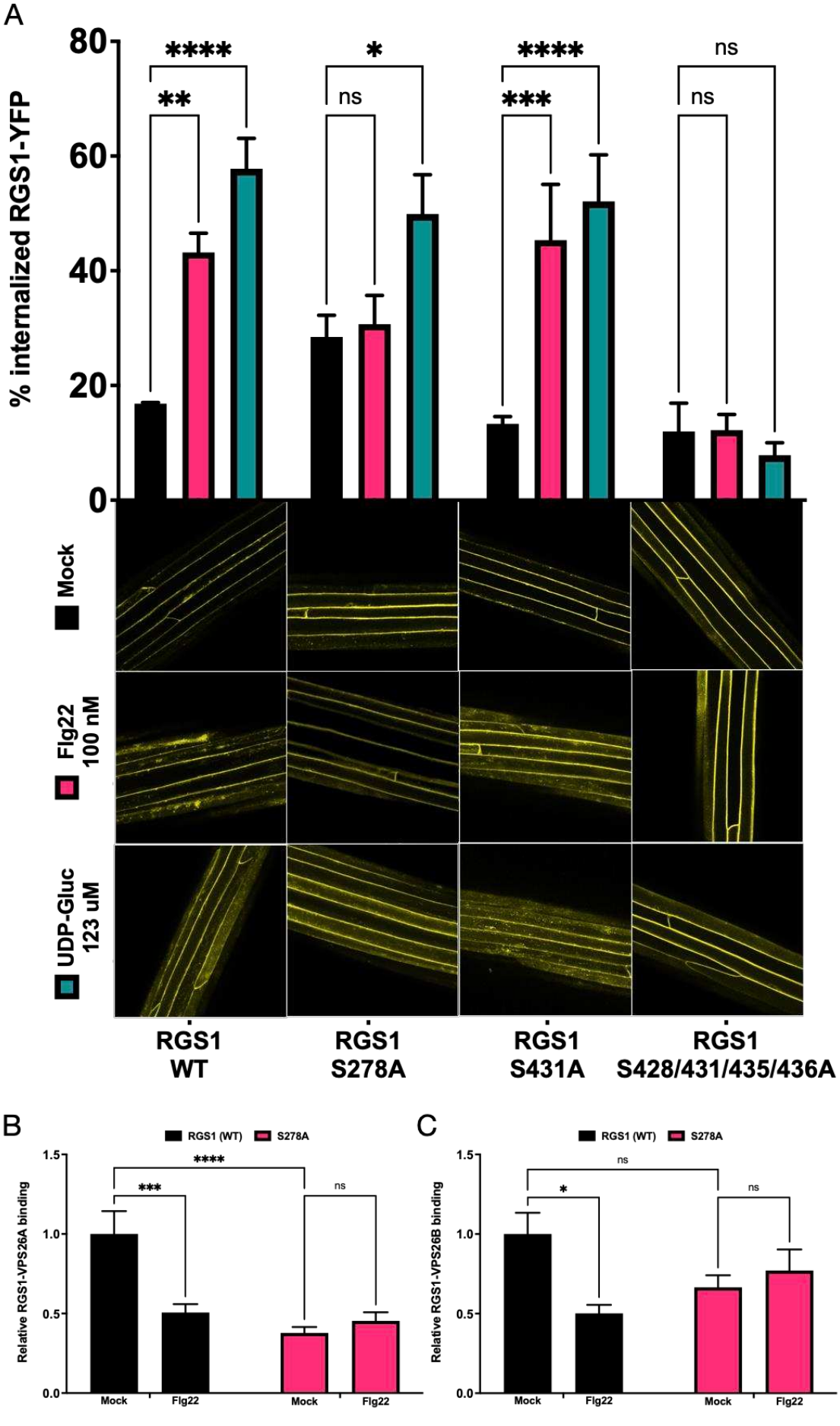
A
% internalized RGS1-YFP
80
60
40
20
0
****
**
*
ns
****
***
ns
ns
Mock
Flg22
100 nM
UDP-Gluc
123 uM
RGS1
WT
RGS1
S278A
RGS1
S431A
RGS1
S428/431/435/436A
B
RGS1 (WT)
S278A
Relative RGS1-VPS26A binding
1.5
1.0
0.5
0.0
****
***
ns
Mock
Flg22
Mock
Flg22
C
RGS1 (WT)
S278A
Relative RGS1-VPS26B binding
1.5
1.0
0.5
0.0
ns
*
ns
Mock
Flg22
Mock
Flg22

Figure 3 - Ser278 phosphorylation is required for flg22 signaling. (A) RGS1-YFP internalization on dark-induced elongated hypocotyls under flg22 and UDP-glucose treatments. n ≈ 5. **(B-C)** Split-luciferase normalized data indicates that RGS1^{S278A} is insensitive to 1 μM flg22-induced binding changes with the candidate adaptors VPS26A and VPS26B. n ≈ 16. Error bars = SEM. Significance levels: * <0.05, ** <0.01, *** <0.001, **** <0.0001, ns = not significant as determined by a two-way ANOVA with post-hoc Tukey multiple comparison test.

limited interaction; (3) signal depletion could be due to conformational change and not to affinity reduction, once both parameters are not proportionally related (Latorraca et al., 2020).

AtRGS1^{S278A} presented lower binding affinity to both VPS26 proteins in comparison with the wild-type form of AtRGS1. However, the addition of flg22 did not show a significant impact on the interactions (Figure 3B-C). These data indicate a coordinated mechanism in which phospho-Ser278 is linked with the required cluster phosphorylation that regulates flg22-induced binding change, whether it is recruitment or release is still unclear.

Ser278 dynamics correlates to C-terminal tail phosphosites and RGSbox residues

Since the top ranked AtRGS1 model indicates a plausible hydrogen bond between Ser278 and the RGSbox residue Lys333, we have decided to investigate how those residues would move in an aqueous environment using DMD simulation. After 500 ns of simulation, we generated a dynamic residue cross correlation map (Figure 4A) and extracted the specific numbers of Ser278 (Figure 4B) in order to evaluate which residues have a movement correlation with the linker region. Consistent with the static model, Lys333 is positively correlated to Ser278 dynamics. Moreover, C-tail phosphosites present a stronger correlation with the same linker region (Figure 4A-B).

Even though the static models of phosphomimetic mutants did not differ from the wild-type version of AtRGS1, molecular dynamics simulations are necessary to identify changes on the contacts and flexibility of the protein. Residue flexibility was evaluated on AtRGS1 Ser278 phosphomimetic and phosphonull structural models by obtaining the RMSD per residue along the trajectory. While flexibility of the linker region had an RMSD peak on the S278E and S278A mutants, it is clear that both phosphomimetic models S278E and S278D presented increased flexibility at the beginning of the C-terminal tail, where the other phosphosites are located (Figure 4C).

This data, taken together with the split luciferase (Figure 2) and internalization results (Figure 3), may suggests that the phosphorylation of the linker is either upstream or concomitant with cluster phosphorylation. Furthermore, the exclusive impairment of flg22 signaling on AtRGS1^{S278A} is consistent with the fact that cluster phosphorylation is required for flg22-

induced internalization of AtRGS1-YFP, but only partially for sugar signaling (Watkins et al., 2021).

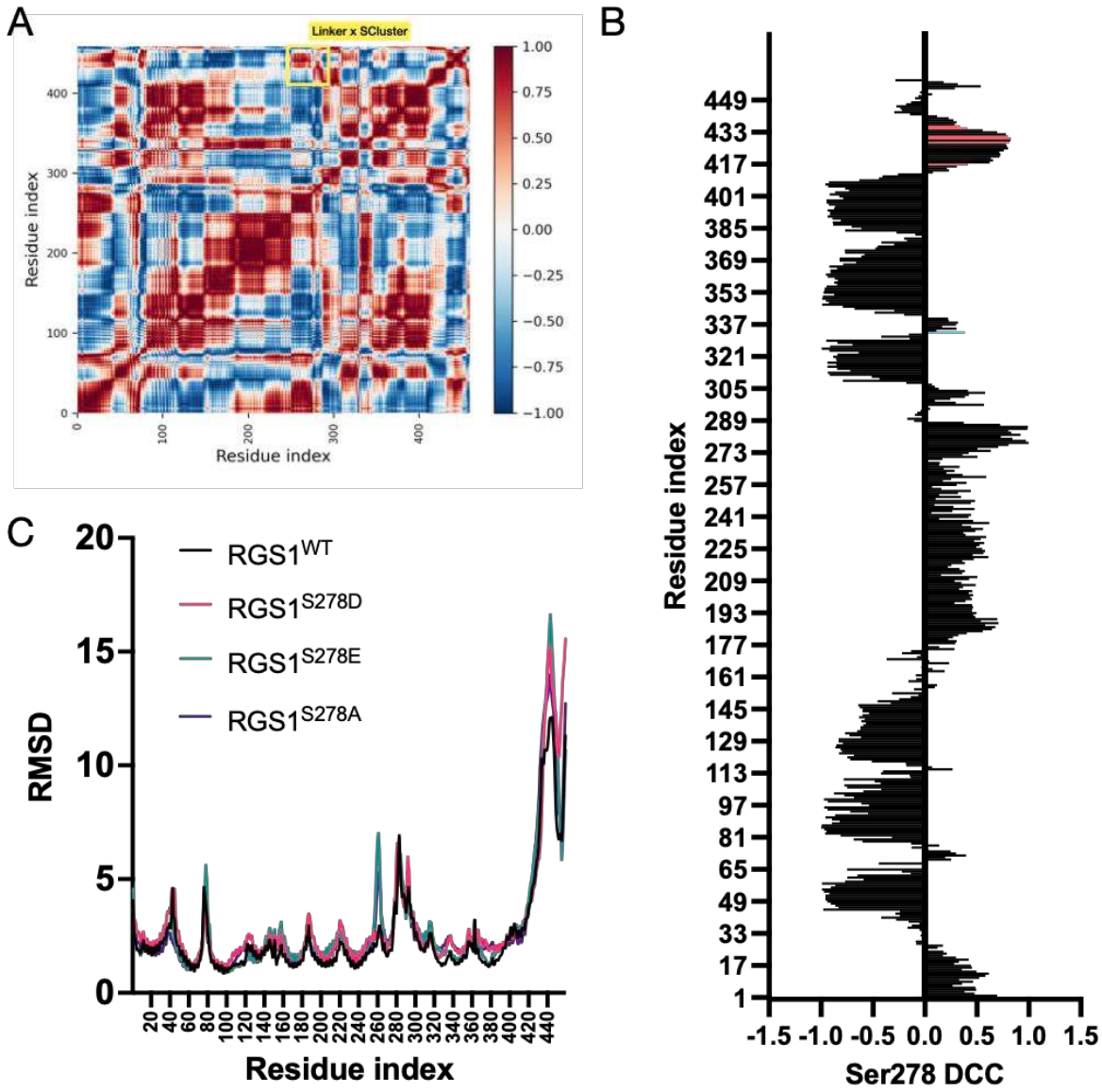

Figure 4 - Serine cluster dynamics is linked to Ser278 trajectory. (A) Dynamic residue cross correlation of wild-type AtRGS1 during 500 ns of C-alpha DMD simulation. Linker region and C-tail serine cluster correlation is highlighted in a yellow box. **(B)** Ser278 dynamics is positively correlated with the Lys333 (blue) and *in vivo* detected phosphosites (red). **(C)** Root-mean-square deviation of AtRGS1 mutants. S278D (pink) and S278E (aqua green) phosphomimetic mutations increase cluster flexibility during the simulation.

AtRGS1^{S278E} promotes AtGPA1 dissociation *in silico*

Once AtRGS1-AtGPA1 dimer is attenuated *in vivo* by the S278E substitution, we have tested how the structural model of the dimer would behave in a water solution by an all-atom MD simulation. The initial static model created with AlphaFold2 was similar to the human crystal of non-TM RGS proteins in dimerization with the Gi alpha 1 subunit (PDB 2GTP)

(Figure S2) (Soundararajan et al., 2008). Even though the static model of AtRGS1^{S278E}-GPA1 did not show many visual changes, it is clear that the contacts of the C-terminal tail phosphosites in AtRGS1 were completely lost with the N-terminal helix of AtGPA1 and with multiple intrachain residues (Figure 5).

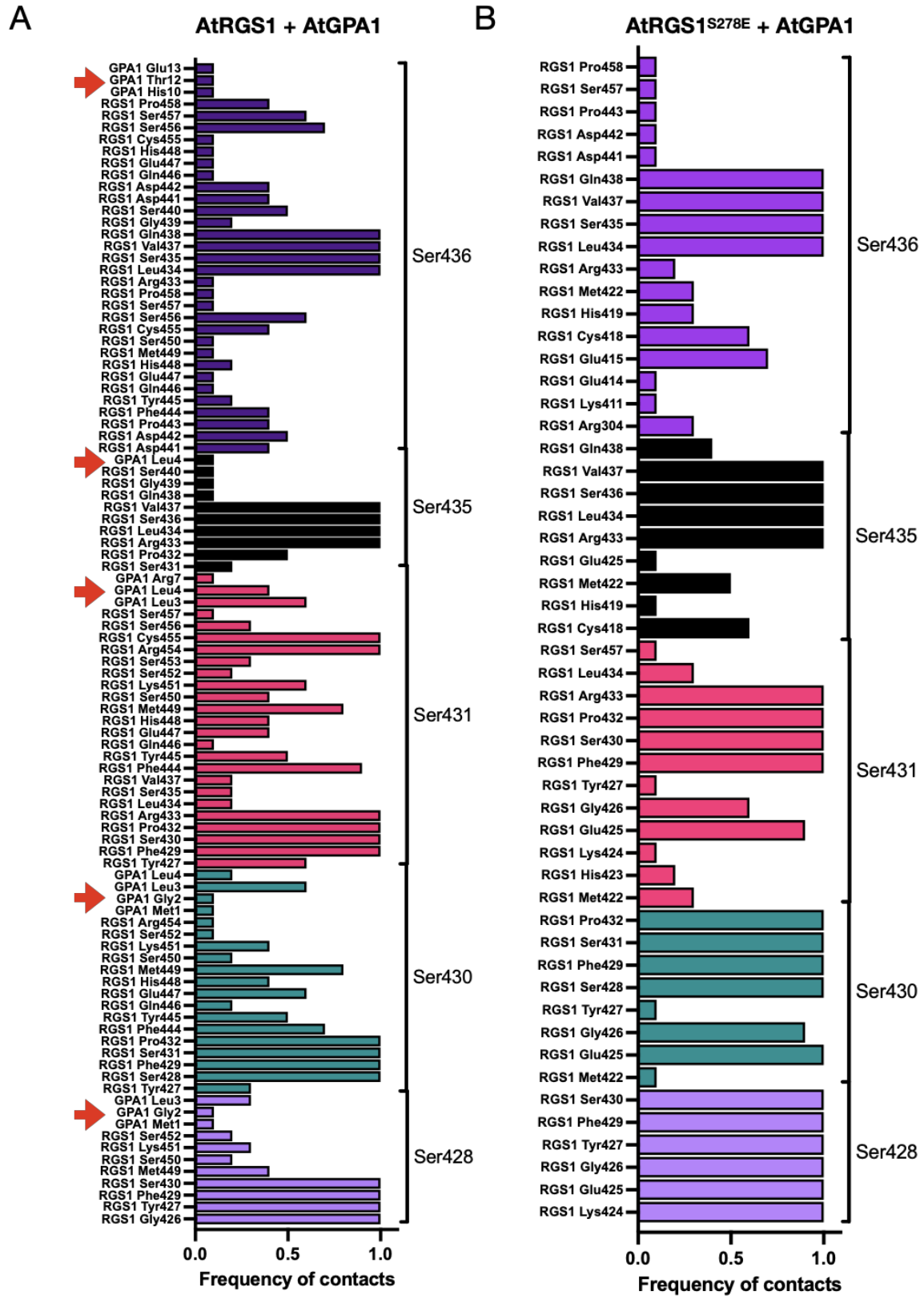

Figure 5 - AtRGS1^{S278E} induces AtGPA1 dissociation *in silico*. (A) Frequency of contacts of wild-type AtRGS1 maintains contacts the C-terminal phosphorylation sites near AtGPA1 N-terminal helix. **(B)** Ser278 phosphomimetic mutation ablates C-terminal proximity of AtGPA1 first helix. AtRGS1 analyzed sites are pointed on the left Y axis, while GPA1 (red arrows) and intrachain contacts are indicated on the right Y axis. Frequency of contacts indicates the ratio of representative models with close residues during the all-atom simulation.

Interestingly, AtGPA1 N-terminal helix has several phosphosites that are induced by flg22 or other treatments (Oliveira et al., 2022; Xue et al., 2020), which suggests a multiple phosphorylation mechanism in both components that would promote lower affinity and higher activation levels during certain atypical conditions.

Ser278 mutations impair serine cluster phosphorylation

The *in silico* correlation of Ser278 with the C-tail serine cluster sites may implicate a direct modulation effect in the phosphorylation pattern of those specific residues and, therefore, the phosphomimetics or phosphonull mutants would present a distinct pattern. To evaluate the *in vivo* phosphorylation, we took advantage of specific AtRGS1 antibodies that recognize the phosphorylated cluster sites pS428, pS435 and pS436. As expected, the wild-type version of the protein displayed an increased flg22-induced-phosphorylation at one or more of the three tested sites (Figure 6A-B), which may be due to Ser428, one of the two sites described as required for flg22 signaling (Liang et al., 2018). But, due to mass spectrometry (MS) limitations on distinguishing neighbor residues, we do not discard the possibility that the other two sites (Ser435/436) are also differentially phosphorylated with the treatment.

The quadA mutant, that cannot be phosphorylated on those sites, did not present any signal. Curiously, S278A and S278E presented similar phosphorylation patterns on the quantification, with no change on the serine cluster phosphorylation status under elicitation (Figure 6A-B). Although the quantification of S278E indicated weak cluster phosphorylation, no visual band was observed on the western blot repetitions, while S278A had a subtle signal (Figure 6A). Thus, we do not discard the fact that other additional sites that are not covered by the antibody specificity are differentially phosphorylated on those mutants, which may include Ser430/431.

AtRGS1 displays Ser278-linked threonine phosphorylation mechanism

Although many phosphosites have been identified *in vitro*, their characterization *in vivo* is still unclear, and only Serine residues are identified in phosphoproteomics studies (Tunc-Ozdemir et al., 2017; Oliveira et al., 2022). For that matter, we have tested the purified AtRGS1 variants for threonine and tyrosine phosphorylation. Although no phosphotyrosine signal was detected, phosphothreonine signal was evident on AtRGS1^{WT}, but weaker on other mutants

with no apparent change on the tested exposure time and concentration of flg22 (Fig. 6A-C). To this date, AtRGS1 has no *in vivo* detected threonine phosphosites, but two residues of the RGSbox (Thr375/379) have been identified *in vitro* (Tunc-Ozdemir et al., 2017; Oliveira et al., 2022). Those sites are BRL3 targets, a receptor-like kinase that controls ROS burst and root growth inhibition during flg22 and sugar responses, respectively (Tunc-Ozdemir and Jones, 2017).

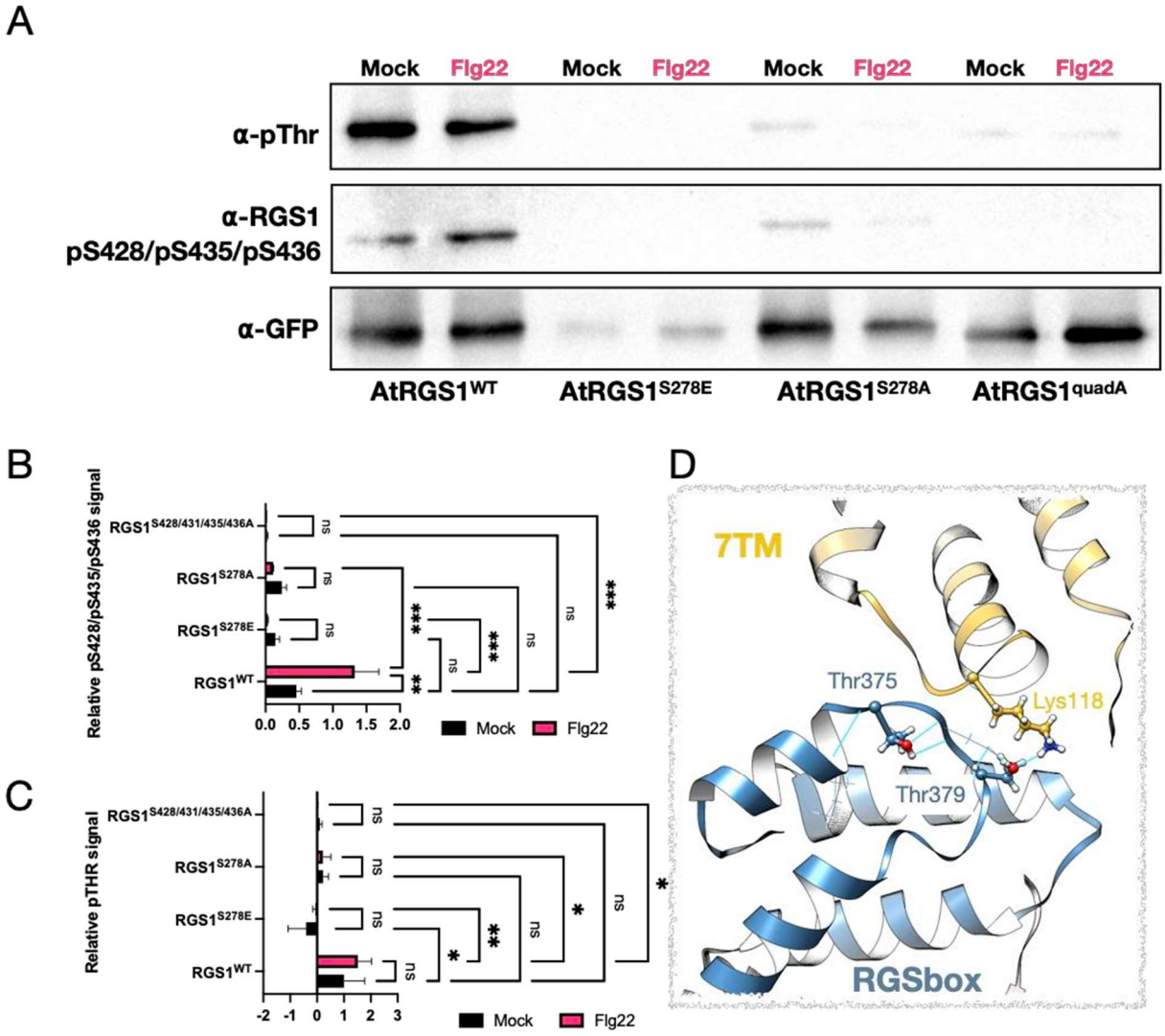

Figure 6 - Ser278 regulates AtRGS1 global phosphorylation. (A) Immunoblot analysis of *rgs1-2* lines complemented with wild-type, S278E, S278A, or S428/431/435/436A (quadA) versions of 35S::AtRGS1-YFP under 3 minutes of 100 nM flg22 treatment. Purified proteins were probed for **(B)** the phosphoserine cluster sites (pS436/pS435/pS436) and **(C)** phosphothreonine. Error bars = SEM, n = 3. Significance levels: * <0.05, ** <0.01, *** <0.001, ns = not significant as determined by a two-way ANOVA with post-hoc Šidák multiple comparison test. **(D)** AlphaFold2 model of AtRGS1 indicates that *in vitro* threonine phosphorylation sites are linked to the 7TM domain (yellow) of the regulator. Predicted hydrogen bonds are represented as a cyan line. Phosphosites and Lys118 are indicated as ball and sticks. Neighbor residues are represented as wires.

On the AlphaFold2 static model is possible to predict a hydrogen bond between Ser479 and the 7TM residue Lys118, which is in the cytoplasmic turn of the domain (Figure 6D). Additionally, a 10 ns all-atom MD with AtRGS1^{WT} and AtRGS1^{S278E} had different contact parameters not only on the linker region (Figure 7A), but also on the contacts of the two RGSbox residues (Figure 7B-C). Glu278 on the S278E mutant was able to maintain a considerable distance from the Lys333 in most models, but most contacts of the residue with the helix that precedes RGSbox lysine were abolished. In contrast, Thr379 was mostly apart from the Lys118 on the AtRGS1^{S278E} trajectory, while plausible contacts were detected in most representative models of the wild-type protein. The difference on the frequency of contacts on the linker, RGSbox and 7TM residues corroborate with the hypothesis that domain orientation and interface availability may be controlled by the phosphorylation status of Ser278. Moreover, different *in vivo* phosphorylation levels for the variants indicate that global phosphorylation of the protein is a coordinated process with the linker being upstream or concomitant not only to the cluster, but also to the RGSbox novel *in vivo* kinase targets.

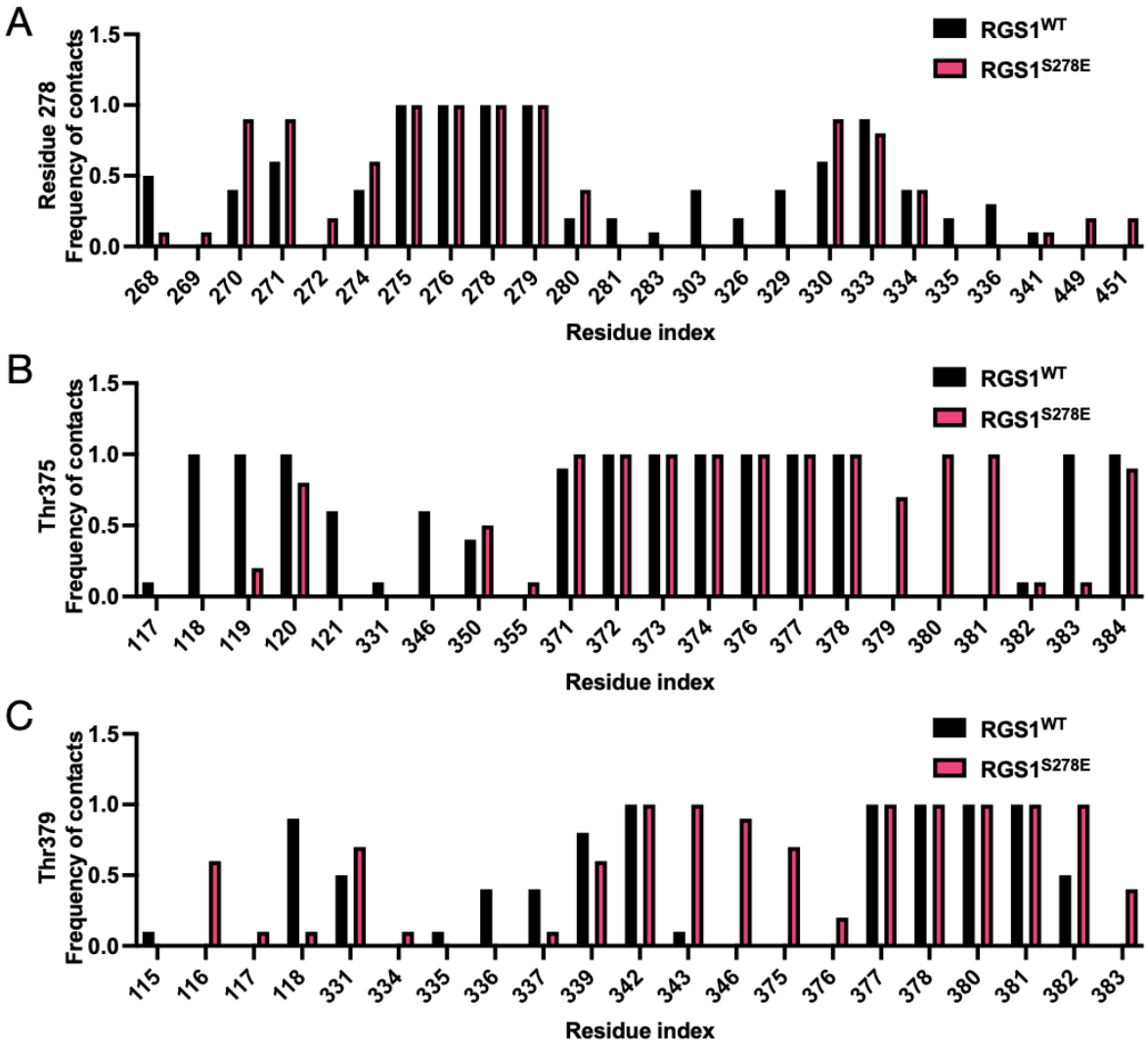

Figure 7 - AtRGS1^{S278E} induces different dynamics of threonine-containing RGSbox region. Cabs-FLEX all-atom simulation of AtRGS1 monomer. Frequency of contacts of wild-type (black) and S278E (pink) AtRGS1 specific residues during the simulation are indicated on the Y axis. **(A)** Mutation of the linker residue changes its contacts and the orientation of RGSbox phosphosites **(B)** Thr375 and **(C)** Thr379.

Key residues are conserved among plant 7TM-RGS proteins

While most eukaryotic groups possess RGS proteins, it has been proposed that ancestor organisms' Gα were GEF-independent and regulated by 7TM-GAP proteins, while superior organisms evolved to be GEF-dependent regarding G-protein activation (Bradford et al., 2013). A phylogenetic analysis using diverse plants 7TM-RGS protein sequences as query, groups AtRGS1 with other eudicot members, followed by magnoliids, monocots, lycophytes, and algae, respectively (Figure 8B). The generated MSA (Figure S3) was also used as a conservation reference to generate a structure colored by residue conservation, which evidenced a considerable conservation on the flexible regions of the land plant proteins, including phosphosites and possible interacting residues (Figure 8A).

For MD comparison, we have picked the structural models of the most related AtRGS1 ortholog, from *Medicago truncatula*, and of the most distant one, from the *Klebsormidium nitens*. A 500 ns C-alpha MD simulation at 295K revealed a similar RMSD profile of the aligned residues, with the most divergent specie presenting higher flexibility levels on the linker region that englobes Ser278 on AtRGS1 (Figure 8C). The main difference on domain flexibility among distant species may be explained by the fact that key residues, including a linker phosphosite and other plant-conserved islands of the region, are not present on the earlier species (Figure S3). This suggests a novel regulation mechanism on higher plants, in which key sites are phosphorylated in order to drive domain positioning, interface availability and, as a consequence, G-protein activation.

DISCUSSION

The few heterotrimeric G-protein subunits found in Arabidopsis are required to the majority of phosphorylation events inside the plant cell, defying a strong link with pathways that include flg22-activated signaling (Song et al., 2018; Watkins et al., 2021). Moreover, the atypical regulation mediated by 7TM-RGS proteins is strongly influenced by several phosphoresidues at the C-terminal tail, but little is known about the effect of individual residues on protein interactions and G-signaling activation (Urano et al., 2012; Liang et al., 2018). Other than the cluster sites, two phosphoserines are detected *in vivo* at the linker region and at the very end of the RGSbox domain (Oliveira et al., 2022).

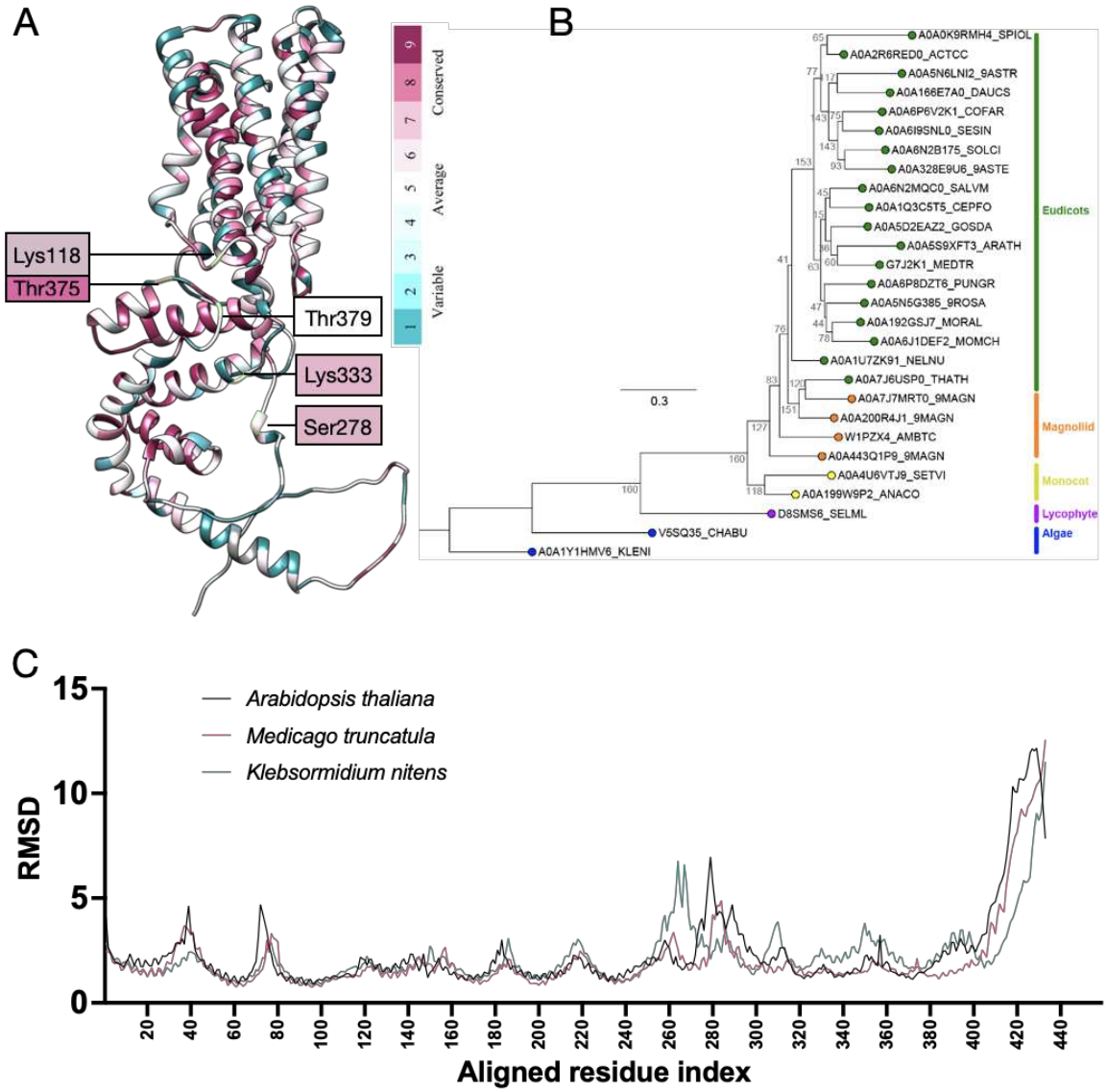

Figure 8 - Key residues are conserved among 7TM-GAP containing species. (A) ConSurf AtRGS1 model colored by residue conservation from the most (pink) to the least conserved (cyan). Key residues are highlighted and colored as indicated in the model. **(B)** JTT substitution model-based phylogenetic of 7TM-RGS proteins across plants and green algae groups related species that are indicated on the left. **(C)** Residue RMSD of AtRGS1 homologs during a 500 ns C-alpha DMD simulation. Data indicates that the most distant organism (*Klebsormidium nitens*, aqua green) differs the most from AtRGS1 (black) and its closer relative (*Medicago truncatula*, pink) on the linker region and RGSbox regarding flexibility.

An extensive interaction mapping of AtRGS1 phosphomimetic mutants using the split luciferase quantitative method allowed us to understand the effect of single sites on the interactions with AtGPA1, AtAGB1 and the two candidate adaptors AtVPS26a and AtVPS26b. As a single phosphomimetic mutant, AtRGS1S^{278E} promoted stronger dissociation of Gα, Gβ and VPS26b interactions compared to the wild-type protein, pointing it out as a strong candidate

on G-protein activation and, possibly, AtRGS1 endocytosis. Thus, none of the versions of AtRGS1 with one cluster residue phosphomimicked over a quadruple alanine mutation promoted Gα activation or adaptor recruitment. Instead, phosphomimicking the residues Ser428 and Ser435 affected VPS26a binding drastically, while the mutant q4 (S431E/clusterA) affected VPS26b binding (Figure 2A).

Adding negative charges to three cluster residues (Ser428/431/435), at the same time as the inactivation of two other sites (Ser430/436), promoted Gα dissociation and VPS26b recruitment, indicating that multiple phosphorylation events at the cluster are required (Figure 2B-C). Curiously, treating infiltrated *N. benthamiana* leaves with 1 μM flg22 promoted VPS26 dissociation from AtRGS1 comparing to the mock treatment (Figure 3B-C). This may be inconsistent with the VPS26 requirement for flg22-mediated internalization of AtRGS1 (Watkins et al., 2021), and it can be explained by experimental parameters discussed in the results section, or by the fact that, like the β-arrestin mechanism, adaptor binding is not directly related to activation (Latorraca et al., 2020). The *rgs1-2* plants complemented with AtRGS1$^{S428/430/435/436A}$ had no flg22- or D-glucose-induced RGS1-YFP internalization (Figure 3A). Thus, the inactivation of three of those sites (S428/S435/436A) is described to affect only the SDE-mediated internalization induced by D-glucose, but not the complete internalization (Watkins et al., 2021). Therefore, Ser431 inactivation alone did not affect the CME pathway and further studies with specific endocytosis inhibitors and multiple phosphosite combinations are necessary.

The Nod factor receptor 1α from soybean (GmNFR1α) is able to phosphorylate three linker residues of GmRGS2 *in vitro*, but no consistent data was presented for the specific phosphorylation of these sites *in vivo* (Choudhury and Pandey, 2015). Other than that, Arabidopsis is a non-leguminous plant and does not present root nodulation. Furthermore, the inactivation of the Arabidopsis site by a serine-to-alanine mutation (AtRGS1^{S278A}) affected VPS26a (but not VPS26b) binding (Figure 3B-C), showing an opposite effect of the S278E mutation (Figure 2A). Additionally, the AtRGS1^{S278A}-VPS26 complexes were not affected by flg22 addition (Figure 3B-C). Using quantitative confocal microscopy, we suggest that Ser278 is required for G-protein activation under flg22 elicitation but not for UDP-glucose (Figure 3A), indicating the involvement of the linker region with the CME pathway activated by the presence of pathogens. Consistently, our work provides *in silico* data for the AtRGS1 AlphaFold2 models that indicates a considerable correlation between Ser278 and the serine cluster movement and flexibility (Figure 4). Molecular dynamics simulations also pointed out to several RGSbox residues with close contact with this part of the linker region (Figure 7A),

indicating that the RGSbox position at the membrane may be influenced by the phosphorylation of the linker.

The *in silico* effects of the S278E mutation on the AtRGS1-AtGPA1 heterodimer are also observed. Here, we have provided plausible models for the dimer that are consistent with one of the human crystals (PDB 2GTP). Moreover, short molecular dynamics simulations indicated that the C-terminal tail of AtRGS1 has reduced contacts with the N-terminal helix of AtGPA1, which comprises the phosphosite Thr12 (Figure 5), also induced by phytohormones and immune responses (Xue et al., 2020; Jia et al., 2019; Oliveira et al., 2022).

Based on the phosphorylation of the three cluster residues detected by the pRGS1 antibody, we hypothesized that Ser278 phosphorylation is required for posterior or concomitant cluster phosphorylation, once AtRGS1^{S278A} enriched proteins presented very low signal and no treatment induction for the phosphorylated sites pSer428, pSer435 and pSer436. Unexpectedly, no phosphorylation was detected at the three cluster residues on the S278E phosphomimetic (Figure 6A-B), pointing out to the possible dynamics of other phosphosites on this mutant. The same effect is observed on the phosphorylation of one or more threonine residues detected for the first time *in vivo*, suggesting that the two RGSbox threonines that are phosphorylated by BRL3 *in vitro* are linked to the cluster and liker phosphorylation (Figure 6A-D). Also, the contacts of the conserved residues Thr375 and Thr379 with the cytoplasmic loop of the 7TM domain (Figure 6D) are altered in the AtRGS1^{S278E} model simulation (Figure 7). And, the key contact residues are conserved among land plants, but not in green algae ancient organisms (Figure 8, Figure S3). Finally, RNAseq and proteomic analysis presented here may indicate that BAK1 is the kinase for Ser278 (Figure S4), raising the hypothesis of posterior threonine phosphorylation by BRL3 in order to attenuate the ROS burst elicited by flg22 (Tunc-Ozdemir and Jones, 2017).

In conclusion, our data displays strong evidence of Ser278 influence on G-protein activation during specific bacterial responses. Thus, based on *in silico* and *in vivo* phosphorylation, Ser278 may regulate the availability of other intrachain phosphosites by positioning the intracellular domains at the plasma membrane for kinase and/or adaptor accessibility, as well as AtGPA1 binding regulation.

REFERENCES

Albrecht, C., Boutrot, F., Segonzac, C., Schwessinger, B., Gimenez-Ibanez, S., Chinchilla, D., Rathjen, J. P., de Vries, S. C. and Zipfel, C. (2012). Brassinosteroids inhibit pathogen-associated molecular pattern-triggered immune signaling independent of the receptor kinase BAK1. Proc Natl Acad Sci USA 109, 303–308.

Ashkenazy, H., Abadi, S., Martz, E., Chay, O., Mayrose, I., Pupko, T. and Ben-Tal, N. (2016). ConSurf 2016: an improved methodology to estimate and visualize evolutionary conservation in macromolecules. Nucleic Acids Res. 44, W344-50.

Belkhadir, Y., Yang, L., Hetzel, J., Dangl, J. L. and Chory, J. (2014). The growth-defense pivot: crisis management in plants mediated by LRR-RK surface receptors. Trends Biochem. Sci. 39, 447–456.

Bohnert, H. J. and Sheveleva, E. (1998). Plant stress adaptations — making metabolism move. Curr. Opin. Plant Biol. 1, 267–274.

Bologna, Z., Teoh, J.-P., Bayoumi, A. S., Tang, Y. and Kim, I.-M. (2017). Biased G Protein-Coupled Receptor Signaling: New Player in Modulating Physiology and Pathology. Biomol Ther (Seoul) 25, 12–25.

Bradford, W., Buckholz, A., Morton, J., Price, C., Jones, A. M. and Urano, D. (2013). Eukaryotic G protein signaling evolved to require G protein-coupled receptors for activation. Sci. Signal. 6, ra37.

Brown, N. P., Leroy, C. and Sander, C. (1998). MView: a web-compatible database search or multiple alignment viewer. Bioinformatics 14, 380–381.

Cao-Pham, A. H., Urano, D., Ross-Elliott, T. J. and Jones, A. M. (2018). Nudge-nudge, WNK-WNK (kinases), say no more? New Phytol. 220, 35–48.

Chakravorty, D., Gookin, T. E., Milner, M. J., Yu, Y. and Assmann, S. M. (2015). Extra-Large G Proteins Expand the Repertoire of Subunits in Arabidopsis Heterotrimeric G Protein Signaling. Plant Physiol. 169, 512–529.

Chen, J.-G. and Jones, A. M. (2004). AtRGS1 function in Arabidopsis thaliana. Meth. Enzymol. 389, 338–350.

Chen, J.-G., Willard, F. S., Huang, J., Liang, J., Chasse, S. A., Jones, A. M. and Siderovski, D. P. (2003). A seven-transmembrane RGS protein that modulates plant cell proliferation. Science 301, 1728–1731.

Chen, Y., Ji, F., Xie, H. and Liang, J. (2006). Overexpression of the regulator of G-protein signalling protein enhances ABA-mediated inhibition of root elongation and drought tolerance in Arabidopsis. J. Exp. Bot. 57, 2101–2110.

Choudhury, S. R. and Pandey, S. (2015). Phosphorylation-Dependent Regulation of G-Protein Cycle during Nodule Formation in Soybean. Plant Cell 27, 3260–3276.

Clapham, D. E. and Neer, E. J. (1997). G protein beta gamma subunits. Annu. Rev. Pharmacol. Toxicol. 37, 167–203.

Colaneri, A. C., Tunc-Ozdemir, M., Huang, J. P. and Jones, A. M. (2014). Growth attenuation under saline stress is mediated by the heterotrimeric G protein complex. BMC Plant Biol. 14, 129.

Deuschle, K., Chaudhuri, B., Okumoto, S., Lager, I., Lalonde, S. and Frommer, W. B. (2006). Rapid metabolism of glucose detected with FRET glucose nanosensors in epidermal cells and intact roots of Arabidopsis RNA-silencing mutants. Plant Cell 18, 2314–2325.

Exton, J. H. (2013). G protein signaling regulators. In Encyclopedia of biological chemistry, pp. 492–495. Elsevier.

Fu, Y., Lim, S., Urano, D., Tunc-Ozdemir, M., Phan, N. G., Elston, T. C. and Jones, A. M. (2014). Reciprocal encoding of signal intensity and duration in a glucose-sensing circuit. Cell 156, 1084–1095.

Ghusinga, K. R., Paredes, F., Jones, A. M. and Colaneri, A. (2021). Reported differences in the flg22 response of the null mutation of AtRGS1 correlates with fixed genetic variation in the background of Col-0 isolates. Plant Signal. Behav. 16, 1878685.

Gómez-Gómez, L. and Boller, T. (2000). FLS2: an LRR receptor-like kinase involved in the perception of the bacterial elicitor flagellin in Arabidopsis. Mol. Cell 5, 1003–1011.

Gómez-Gómez, L., Felix, G. and Boller, T. (1999). A single locus determines sensitivity to bacterial flagellin in Arabidopsis thaliana. Plant J. 18, 277–284.

Gurevich, V. V. and Gurevich, E. V. (2019). GPCR signaling regulation: the role of grks and arrestins. Front. Pharmacol. 10, 125.

Hospital, A., Andrio, P., Fenollosa, C., Cicin-Sain, D., Orozco, M. and Gelpí, J. L. (2012). MDWeb and MDMoby: an integrated web-based platform for molecular dynamics simulations. Bioinformatics 28, 1278–1279.

Huang, J.-P., Tunc-Ozdemir, M., Chang, Y. and Jones, A. M. (2015). Cooperative control between AtRGS1 and AtHXK1 in a WD40-repeat protein pathway in Arabidopsis thaliana. Front. Plant Sci. 6, 851.

Hurowitz, E. H., Melnyk, J. M., Chen, Y. J., Kouros-Mehr, H., Simon, M. I. and Shizuya, H. (2000). Genomic characterization of the human heterotrimeric G protein alpha, beta, and gamma subunit genes. DNA Res. 7, 111–120.

Ingram, J. and Bartels, D. (1996). THE MOLECULAR BASIS OF DEHYDRATION TOLERANCE IN PLANTS. Annu. Rev. Plant Physiol. Plant Mol. Biol. 47, 377–403.

Jean-Charles, P.-Y., Kaur, S. and Shenoy, S. K. (2017). G Protein-Coupled Receptor Signaling Through β-Arrestin-Dependent Mechanisms. J. Cardiovasc. Pharmacol. 70, 142–158.

Jiang, H., Galtes, D., Wang, J. and Rockman, H. A. (2022). G Protein-Coupled Receptor Signaling: Transducers and Effectors. Am J Physiol, Cell Physiol.

Jia, H., Song, G., Werth, E. G., Walley, J. W., Hicks, L. M. and Jones, A. M. (2019). Receptor-Like Kinase Phosphorylation of Arabidopsis Heterotrimeric G-Protein Gα -Subunit AtGPA1. Proteomics 19, e1900265.

Jiménez-Góngora, T., Kim, S.-K., Lozano-Durán, R. and Zipfel, C. (2015). Flg22-Triggered Immunity Negatively Regulates Key BR Biosynthetic Genes. Front. Plant Sci. 6, 981.

Jumper, J., Evans, R., Pritzel, A., Green, T., Figurnov, M., Ronneberger, O., Tunyasuvunakool, K., Bates, R., Žídek, A., Potapenko, A., et al. (2021). Highly accurate protein structure prediction with AlphaFold. Nature 596, 583–589.

Kleczkowski, L. A. (1996). Back to the drawing board: redifining starch synthesis in cereals. Trends Plant Sci. 1, 363–364.

Klopffleisch, K., Phan, N., Augustin, K., Bayne, R. S., Booker, K. S., Botella, J. R., Carpita, N. C., Carr, T., Chen, J.-G., Cooke, T. R., et al. (2011). Arabidopsis G-protein interactome reveals connections to cell wall carbohydrates and morphogenesis. Mol. Syst. Biol. 7, 532.

Kuriata, A., Gierut, A. M., Oleniecki, T., Ciemny, M. P., Kolinski, A., Kurcinski, M. and Kmiecik, S. (2018). CABS-flex 2.0: a web server for fast simulations of flexibility of protein structures. Nucleic Acids Res. 46, W338–W343.

Latorraca, N. R., Masureel, M., Hollingsworth, S. A., Heydenreich, F. M., Suomivuori, C.-M., Brinton, C., Townshend, R. J. L., Bouvier, M., Kobilka, B. K. and Dror, R. O. (2020). How GPCR Phosphorylation Patterns Orchestrate Arrestin-Mediated Signaling. Cell 183, 1813-1825.e18.

Liang, X., Ding, P., Lian, K., Wang, J., Ma, M., Li, L., Li, L., Li, M., Zhang, X., Chen, S., et al. (2016). Arabidopsis heterotrimeric G proteins regulate immunity by directly coupling to the FLS2 receptor. eLife 5, e13568.

Liang, X., Ma, M., Zhou, Z., Wang, J., Yang, X., Rao, S., Bi, G., Li, L., Zhang, X., Chai, J., et al. (2018). Ligand-triggered de-repression of Arabidopsis heterotrimeric G proteins coupled to immune receptor kinases. Cell Res. 28, 529–543.

Liggett, S. B. (2011). Phosphorylation barcoding as a mechanism of directing GPCR signaling. Sci. Signal. 4, pe36.

Li, B., Tunc-Ozdemir, M., Urano, D., Jia, H., Werth, E. G., Mowrey, D. D., Hicks, L. M., Dokholyan, N. V., Torres, M. P. and Jones, A. M. (2018). Tyrosine phosphorylation switching of a G protein. J. Biol. Chem. 293, 4752–4766.

Li, B., Ferreira, M. A., Huang, M., Camargos, L. F., Yu, X., Teixeira, R. M., Carpinetti, P. A., Mendes, G. C., Gouveia-Mageste, B. C., Liu, C., et al. (2019). The receptor-like kinase NIK1 targets FLS2/BAK1 immune complex and inversely modulates antiviral and antibacterial immunity. Nat. Commun. 10, 4996.

Li, S., Han, X., Lu, Z., Qiu, W., Yu, M., Li, H., He, Z. and Zhuo, R. (2022). MAPK cascades and transcriptional factors: regulation of heavy metal tolerance in plants. Int. J. Mol. Sci. 23,.

Lomize, A. L., Todd, S. C. and Pogozheva, I. D. (2022). Spatial arrangement of proteins in planar and curved membranes by PPM 3.0. Protein Sci. 31, 209–220.

Lu, D., Wu, S., Gao, X., Zhang, Y., Shan, L. and He, P. (2010a). A receptor-like cytoplasmic kinase, BIK1, associates with a flagellin receptor complex to initiate plant innate immunity. Proc Natl Acad Sci USA 107, 496–501.

Lu, D., Wu, S., He, P. and Shan, L. (2010b). Phosphorylation of receptor-like cytoplasmic kinases by bacterial flagellin. Plant Signal. Behav. 5, 598–600.

Marcec, M. J. and Tanaka, K. (2021). Crosstalk between Calcium and ROS Signaling during Flg22-Triggered Immune Response in Arabidopsis Leaves. Plants 11,.

Mergner, J., Frejno, M., List, M., Papacek, M., Chen, X., Chaudhary, A., Samaras, P., Richter, S., Shikata, H., Messerer, M., et al. (2020). Mass-spectrometry-based draft of the Arabidopsis proteome. Nature 579, 409–414.

Mirdita, M., Schütze, K., Moriwaki, Y., Heo, L., Ovchinnikov, S. and Steinegger, M. (2022). ColabFold: making protein folding accessible to all. Nat. Methods 19, 679–682.

Nelson, D. E., Shen, B. and Bohnert, H. J. (1998). Salinity tolerance — mechanisms, models and the metabolic engineering of complex traits. In Genetic Engineering (ed. Setlow, J. K.), pp. 153–176. Boston, MA: Springer US.

Oldham, W. M. and Hamm, H. E. (2008). Heterotrimeric G protein activation by G-protein-coupled receptors. Nat. Rev. Mol. Cell Biol. 9, 60–71.

Oliveira, C. C., Jones, A. M., Fontes, E. P. B. and Reis, P. A. B. D. (2022). G-Protein Phosphorylation: Aspects of Binding Specificity and Function in the Plant Kingdom. Int. J. Mol. Sci. 23,.

Peres, A. L. G. L., Soares, J. S., Tavares, R. G., Righetto, G., Zullo, M. A. T., Mandava, N. B. and Menossi, M. (2019). Brassinosteroids, the Sixth Class of Phytohormones: A Molecular View from the Discovery to Hormonal Interactions in Plant Development and Stress Adaptation. Int. J. Mol. Sci. 20,.

Pettersen, E. F., Goddard, T. D., Huang, C. C., Couch, G. S., Greenblatt, D. M., Meng, E. C. and Ferrin, T. E. (2004). UCSF Chimera—a visualization system for exploratory research and analysis. J. Comput. Chem. 25, 1605–1612.

Pirasteh-Anosheh, H., Saed-Moucheshi, A., Pakniyat, H. and Pessarakli, M. (2016). Stomatal responses to drought stress. In Water stress and crop plants: A sustainable approach (ed. Ahmad, P.), pp. 24–40. Chichester, UK: John Wiley & Sons, Ltd.

Sheik Amamuddy, O., Glenister, M., Tshabalala, T. and Tastan Bishop, Ö. (2021). MDM-TASK-web: MD-TASK and MODE-TASK web server for analyzing protein dynamics. Comput. Struct. Biotechnol. J. 19, 5059–5071.

Siderovski, D. P. and Willard, F. S. (2005). The GAPs, GEFs, and GDIs of heterotrimeric G-protein alpha subunits. Int. J. Biol. Sci. 1, 51–66.

Smeekens, S., Ma, J., Hanson, J. and Rolland, F. (2010). Sugar signals and molecular networks controlling plant growth. Curr. Opin. Plant Biol. 13, 274–279.

Song, G., Brachova, L., Nikolau, B. J., Jones, A. M. and Walley, J. W. (2018). Heterotrimeric G-Protein-Dependent Proteome and Phosphoproteome in Unstimulated Arabidopsis Roots. Proteomics 18, e1800323.

Soundararajan, M., Willard, F. S., Kimple, A. J., Turnbull, A. P., Ball, L. J., Schoch, G. A., Gileadi, C., Fedorov, O. Y., Dowler, E. F., Higman, V. A., et al. (2008). Structural diversity in the RGS domain and its interaction with heterotrimeric G protein alpha-subunits. Proc Natl Acad Sci USA 105, 6457–6462.

Tunc-Ozdemir, M. and Jones, A. M. (2017). BRL3 and AtRGS1 cooperate to fine tune growth inhibition and ROS activation. PLoS ONE 12, e0177400.

Tunc-Ozdemir, M., Urano, D., Jaiswal, D. K., Clouse, S. D. and Jones, A. M. (2016). Direct Modulation of Heterotrimeric G Protein-coupled Signaling by a Receptor Kinase Complex. J. Biol. Chem. 291, 13918–13925.

Tunc-Ozdemir, M., Li, B., Jaiswal, D. K., Urano, D., Jones, A. M. and Torres, M. P. (2017). Predicted functional implications of phosphorylation of regulator of G protein signaling protein in plants. Front. Plant Sci. 8, 1456.

Urano, D. and Jones, A. M. (2014). Heterotrimeric G protein-coupled signaling in plants. Annu. Rev. Plant Biol. 65, 365–384.

Urano, D., Phan, N., Jones, J. C., Yang, J., Huang, J., Grigston, J., Taylor, J. P. and Jones, A. M. (2012). Endocytosis of the seven-transmembrane RGS1 protein activates G-protein-coupled signalling in Arabidopsis. Nat. Cell Biol. 14, 1079–1088.

Waadt, R., Seller, C. A., Hsu, P.-K., Takahashi, Y., Munemasa, S. and Schroeder, J. I. (2022). Plant hormone regulation of abiotic stress responses. Nat. Rev. Mol. Cell Biol.

Watkins, J. M., Ross-Elliott, T. J., Shan, X., Lou, F., Dreyer, B., Tunc-Ozdemir, M., Jia, H., Yang, J., Oliveira, C. C., Wu, L., et al. (2021a). Differential regulation of G protein signaling in Arabidopsis through two distinct pathways that internalize AtRGS1. Sci. Signal. 14,.

Watkins, J. M., Clark, N. M., Song, G., Oliveira, C. C., Mishra, B., Brachova, L., Seifert, C. M., Mitchell, M. S., Reis, P. A. B. dos, Urano, D., et al. (2021b). Phosphorylation dynamics in a flg22-induced, heterotrimeric G-protein dependent signaling network in Arabidopsis thaliana reveals a candidate PP2A phosphatase involved in AtRGS1 trafficking. BioRxiv.

Xiao, K. and Sun, J. (2018). Elucidating structural and molecular mechanisms of β-arrestin-biased agonism at GPCRs via MS-based proteomics. Cell. Signal. 41, 56–64.

Xue, J., Gong, B.-Q., Yao, X., Huang, X. and Li, J.-F. (2020). BAK1-mediated phosphorylation of canonical G protein alpha during flagellin signaling in Arabidopsis. J. Integr. Plant Biol. 62, 690–701.

Zelazny, E., Santambrogio, M. and Gaude, T. (2013). Retromer association with membranes: plants have their own rules! Plant Signal. Behav. 8,.

Zhang, X., Henriques, R., Lin, S.-S., Niu, Q.-W. and Chua, N.-H. (2006). Agrobacterium-mediated transformation of Arabidopsis thaliana using the floral dip method. Nat. Protoc. 1, 641–646.

Zhou, Z., Zhao, Y., Bi, G., Liang, X. and Zhou, J.-M. (2019). Early signalling mechanisms underlying receptor kinase-mediated immunity in plants. Philos. Trans. R. Soc. Lond. B Biol. Sci. 374, 20180310.

Zipfel, C., Robatzek, S., Navarro, L., Oakeley, E. J., Jones, J. D. G., Felix, G. and Boller, T. (2004). Bacterial disease resistance in Arabidopsis through flagellin perception. Nature 428, 764–767.

SUPPLEMENTARY MATERIAL

Supplemental Table 1 - Oligonucleotides used for cloning, site-directed mutagenesis, and RT-qPCR.

Gene	Oligonucleotide ID	Sequence (5'→3')	Application
AtRGS1	AtRGS1-Fwd-GW	AAAAAGCAGGCTTCACAATGGCGAG TGGATGTGC	pDONR221 cloning
	AtRGS1-Rvs-NS-GW	AGAAAGCTGGGTCACCGGGACTACT GCAT	pDONR221 cloning
	AtRGS1-Fwd-GW	CACCATGGCGAGTGGATGTGCTCTAC AT	pENTR D-TOPO cloning
	AtRGS1-NS-HiBiT-Rvs-GW	GCTAATCTTCTTGAACAGCCGCCAGC CGCTCACACCGGGACTACTGCATCTG	pENTR D-TOPO cloning HiBiT tagging
	AtRGS1-S278D-Fwd	CATTCCCGATgacGGATTATTATTTCG	Site-directed mutagenesis
	AtRGS1-S278E-Fwd	CATTCCCGATgagGGATTATTATTTCG GAAG	Site-directed mutagenesis
	AtRGS1-S278A-Fwd	CATTCCCGATgccGGATTATTATTTCG	Site-directed mutagenesis
	AtRGS1-S278-Rvs	CCTAGAGCTTGACCCATTC	Site-directed mutagenesis
	AtRGS1-S417D-Fwd	AGAAGAAGAAgacTGCCACGAGG	Site-directed mutagenesis
	AtRGS1-S417E-Fwd	AGAAGAAGAAgagTGCCACGAGGCAA TG	Site-directed mutagenesis
	AtRGS1-S417A-Fwd	AGAAGAAGAAgccTGCCACGAGG	Site-directed mutagenesis
	AtRGS1-S417-Rvs	TTGAACTTGATGAAGTAGATG	Site-directed mutagenesis
	AtRGS1-S431A-Fwd	CAGTTTTTCAgctCCAAGACTGAG	Site-directed mutagenesis
	AtRGS1-S431-Rvs	TATCCTTCCTTATGCATTGC	Site-directed mutagenesis
	AtRGS1-q1-Fwd	caagactggctgCAGTTCAAGGCTCTGATG	Site-directed mutagenesis
	AtRGS1-q1-Rvs	gagctgcaaaatcGTATCCTTCCTTATGCAT TG	Site-directed mutagenesis
	AtRGS1-q2-Fwd	caagactggctgCAGTTCAAGGCTCTGATG	Site-directed mutagenesis
	AtRGS1-q2-Rvs	gagctgcaaactcGTATCCTTCCTTATGCAT TG	Site-directed mutagenesis
	AtRGS1-q3-Fwd	caagactggctgCAGTTCAAGGCTCTGATG	Site-directed mutagenesis
	AtRGS1-q3-Rvs	gatctgcaaaagcGTATCCTTCCTTATGCAT TG	Site-directed mutagenesis
	AtRGS1-q4-Fwd	caagactggctgCAGTTCAAGGCTCTGATG	Site-directed mutagenesis
	AtRGS1-q4-Rvs	gctctgcaaaagcGTATCCTTCCTTATGCAT TG	Site-directed mutagenesis
	AtRGS1-q5-Fwd	caagactggatgCAGTTCAAGGCTCTGATG	Site-directed mutagenesis
	AtRGS1-q5-Rvs	gagctgcaaaagcGTATCCTTCCTTATGCAT TG	Site-directed mutagenesis
	AtRGS1-q6-Fwd	caagactggaagCAGTTCAAGGCTCTGATG	Site-directed mutagenesis
	AtRGS1-q6-Rvs	gagctgcaaaagcGTATCCTTCCTTATGCAT TG	Site-directed mutagenesis

	AtRGS1-q1q3q5-Fwd	caagactggatgCAGTTCAAGGCTCTGATG	Site-directed mutagenesis
	AtRGS1-q1q3q5-Rvs	gatctgcaaaatcGTATCCTTCCTTATGCATTG	Site-directed mutagenesis
	AtRGS1-q2q4q6-Fwd	caagactggaagCAGTTCAAGGCTCTGATG	Site-directed mutagenesis
	AtRGS1-q2q4q6-Rvs	gttctgcaaactcGTATCCTTCCTTATGCATTG	Site-directed mutagenesis
	AtRGS1-clusterA-Fwd	caagactggctgCAGTTCAAGGCTCTGATG	Site-directed mutagenesis
	AtRGS1-clusterA-Rvs	gagctgcaaaagcGTATCCTTCCTTATGCATTG	Site-directed mutagenesis
	AtRGS1-quadA-Fwd	caagactggctgCAGTTCAAGGCTCTGATG	Site-directed mutagenesis
	AtRGS1-quadA-Rvs	gagctgaaaaagcGTATCCTTCCTTATGCATTG	Site-directed mutagenesis
	qRT-AtRGS1-Fwd	TCTCTTGGCTTCAGGTTGCT	RT-qPCR
	qRT-AtRGS1-Rvs	ACAACGACGAGAATCCCACC	RT-qPCR
AtUBQ10	qRT-UBQ10-Fwd	GGCCTTGTATAATCCCTGATGAATAAG	RT-qPCR
	qRT-UBQ10-Rvs	AAAGAGATAACAGGAACGGAAACATAGT	RT-qPCR

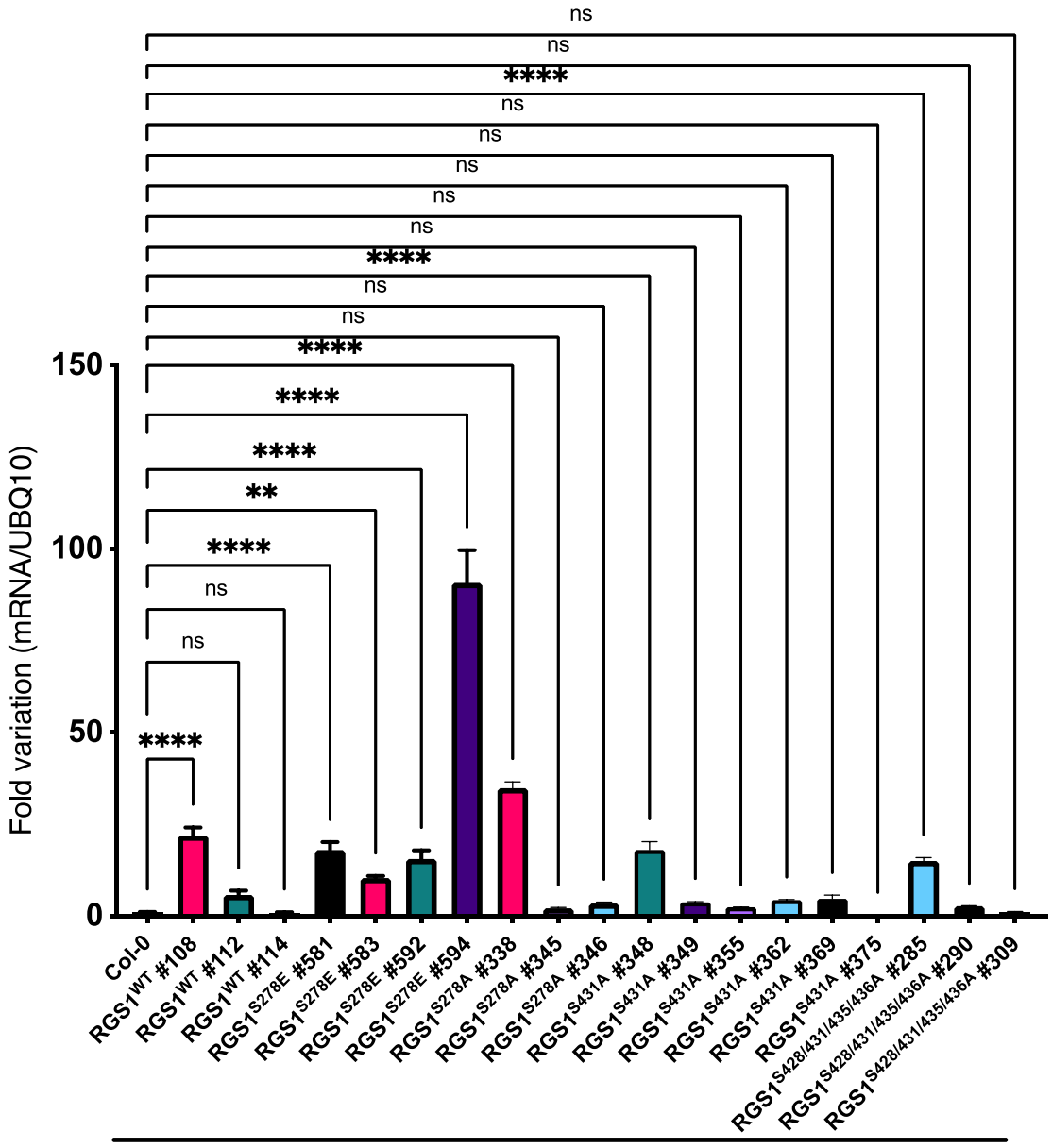

Supplemental Figure 1 - Gene expression profiling of *rgs1-2* complemented lines. Single insertion agrobacterium-transformed lines were selected and genotyped for AtRGS1 expression. Fold variation indicates relative expression of transgenic plants over the wild-type control (Col-0). Error bars = SEM, n ≈ 3. Significance levels: ** <0.01, **** <0.0001, ns = not significant as determined by a two-way ANOVA with post-hoc Dunnett's multiple comparison test.

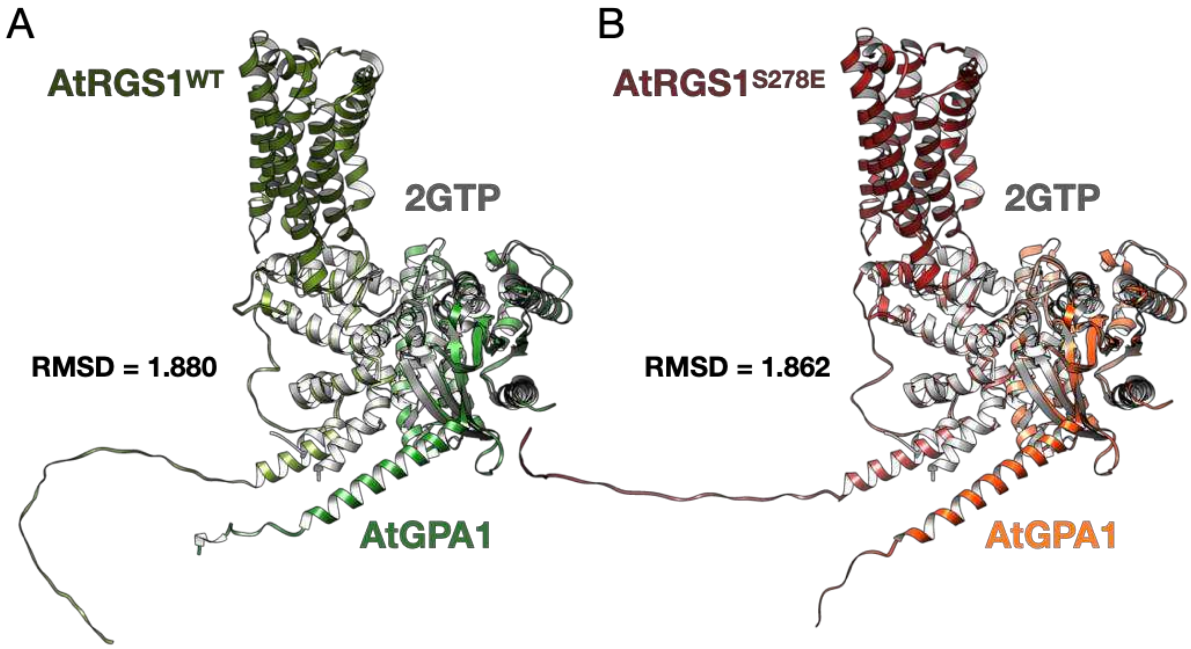

Supplemental Figure 2 - AtRGS1-AtGPA1 complex model overlaps the crystal structure 2GTP. AlphaFold2 model of AtRGS1 (olive green/red) and AtGPA1 (forest green/orange) heterodimer overlapping the crystal structure of the heterodimeric complex of human RGS1 and activated Gi alpha 1 2GTP (grey). RMSD values are indicated on the left.

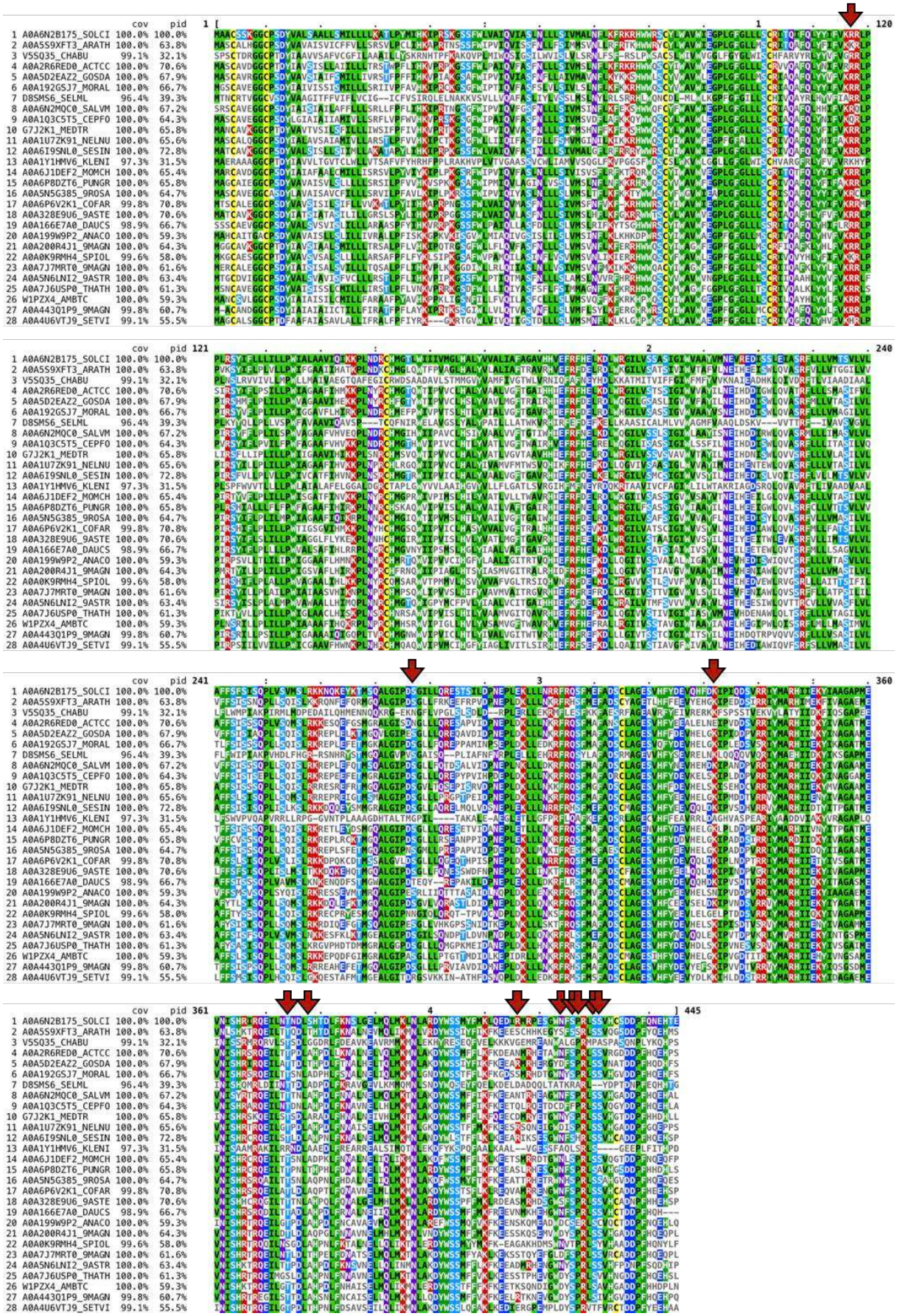

Supplemental Figure 3 - Multiple sequence alignment of AtRGS1 orthologs. AtRGS1 representative sequences were aligned with MAFFT. MView was used for representation

(Brown et al., 1998). Red arrows indicate AtRGS1 residues of interest Lys118, Ser278, Lys333, Thr375, Thr379, Ser417, Ser428, Ser430, Ser431, Ser435 and Ser436, respectively.

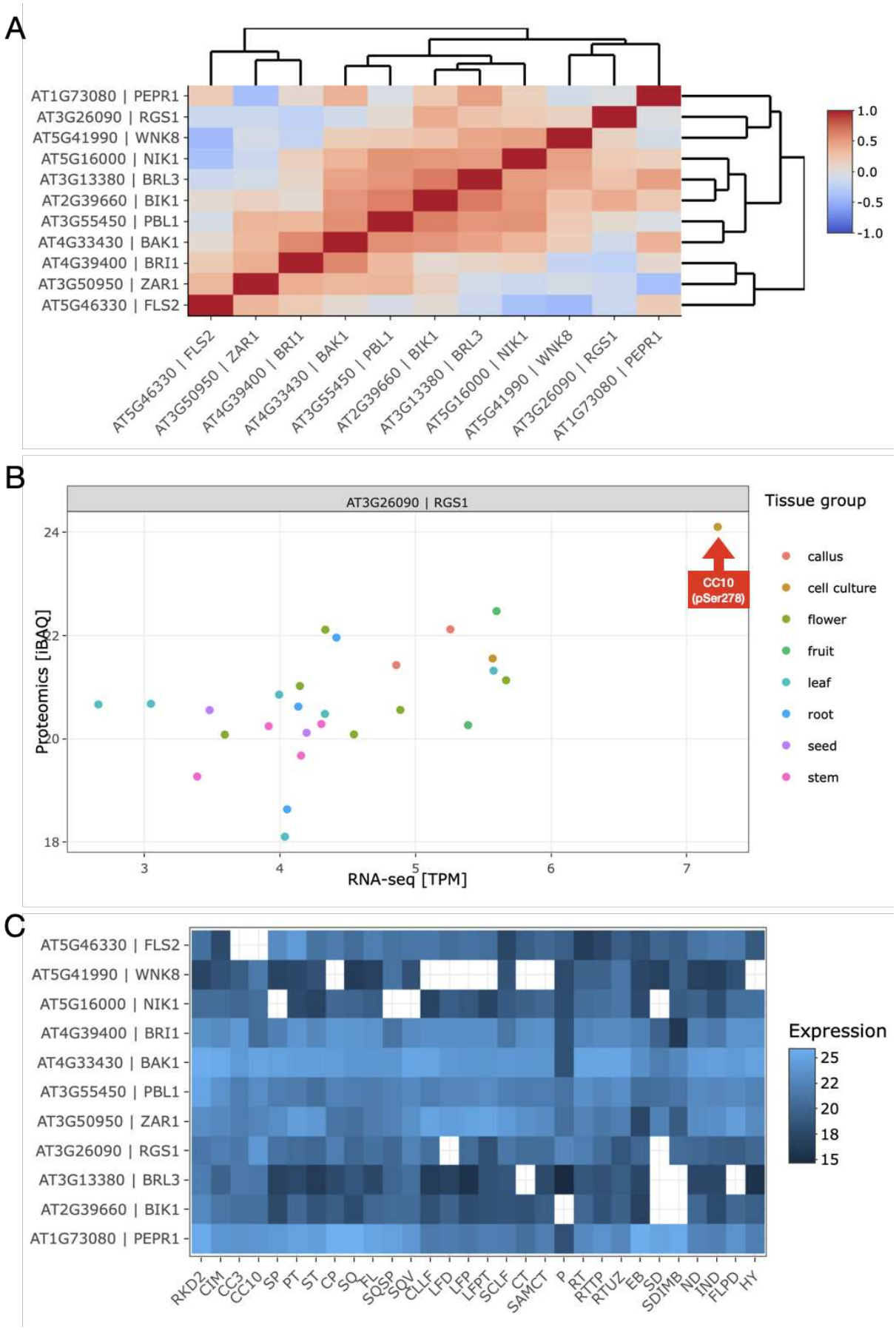

Supplemental Figure 4 - Protein and mRNA expression profiling of AtRGS1 and related kinases. (A) AtRGS1, RLKs and cytoplasmic kinases expression profiles indicate a strong

correlation of the 7TM protein with the LRR-RLKs BRL3, involved in growth inhibition and ROS activation, and NIK1, which acts on viral and bacterial defense responses. The cytoplasmic kinases with strong correlation are the WNK8 and BIK1, involved on sugar signaling and pathogen responses, respectively. **(B)** Tissue specific RNAseq and proteomics profiling indicate the lower Protein/mRNA ratio of AtRGS1 on root cell culture (CC10, red arrow), the only tissue with pSer278 signal detected under normal conditions. **(C)** Root cell culture displays higher protein expression for BAK1, required for flg22-induced phosphorylation of AtRGS1. Figures and raw data were obtained from the ATHENA database (Mergner et al., 2020).

GENERAL CONCLUSION

The sessility of plants is compensated with a complex system that coordinates development while maintaining the homeostasis of the cell (Žádníková et al., 2015). Accordingly, the large family plant of Leucine-Rich Repeats Receptor-Like Kinases (LRR-RLKs) play an essential role in signal recognition and transduction (Dufayard et al., 2017). As the repertoire of plant heterotrimeric G-protein subunits is considerably limited compared to the mammalian one (Mohanasundaram et al., 2022), post-translational modifications at residues inside the core may be the primary regulation mechanism in most bikonts (Bradford et al., 2013; Li et al., 2018; Tunc-Ozdemir et al., 2017). Therefore, the prominent role of AtRGS1 over AtGPA1 nucleotide-status is strongly influenced by the phosphorylation status of both proteins, which defines the four-state model of G-protein activation (Ghusinga et al., 2022).

As the only transmembrane protein of the core, mapping the interactions of AtRGS1 with Gα, Gβ, and with the β-arrestin-like candidate adaptors VPS26a and VPS26B (Watkins et al., 2021) was a crucial step for screening sites of interest that are detected *in vivo* at conserved and non-conserved regions of the seven-transmembrane (7TM) regulator. Thus, since *rgs1-2* knockouts only present significant phenotypes under atypical conditions, the creation of AtRGS1 phosphomimetic and phosphonull mutants allowed us to identify residues that are required for activation during specific conditions, such as bacterial elicitation and sugar responses. Among the tested residues, codon changes at the Ser278 position, as well as molecular dynamics simulations of the phosphomimetic protein, revealed the influence of the linker region over the serine cluster phosphorylation status, and, as a consequence, over AtGPA1 dissociation.

Additionally, we have shown that AtRGS1 undergoes threonine phosphorylation in a mechanism that is dependent on the linker and C-terminal sites. This interpretation is consistent with the changes in global structure that were observed *in silico* for the phosphomimetic S278E, including changes in contacts of two *in vitro*-detected RGSbox phosphothreonine with the 7TM cytoplasmic loop, and the variation of a plausible hydrogen bond that is predicted to link Ser278 with RGSbox residues. Moreover, most of AtRGS1 phosphosites, and other residues of interest identified in the structural model, are significantly conserved in plant 7TM-RGS proteins, but not on the algae proteins at the base of the phylogenetic tree.

Our data implicate in a mechanism that was evolved in land plants in order to drive signal plasticity via the phosphorylation of a relatively low number of signaling proteins. In this model, the phosphorylation status of the linker region of AtRGS1 regulates the membrane positioning of the cytoplasmic domain, changing the accessibility of other regions for

phosphorylation and circumstantial interactions. The phosphorylation of multiple components at the plant G-protein core drives the core formation and their distinct downstream functions. Finally, this initial elucidation of the G-protein phosphorylation “bar-code” is the first step to create G-protein transgenic lines with great agroeconomic interest based on stress resistance and growth efficiency.

REFERENCES

Bradford, W., Buckholz, A., Morton, J., Price, C., Jones, A. M. and Urano, D. (2013). Eukaryotic G protein signaling evolved to require G protein-coupled receptors for activation. Sci. Signal. 6, ra37.

Dufayard, J.-F., Bettembourg, M., Fischer, I., Droc, G., Guiderdoni, E., Périn, C., Chantret, N. and Diévart, A. (2017). New Insights on Leucine-Rich Repeats Receptor-Like Kinase Orthologous Relationships in Angiosperms. Front. Plant Sci. 8, 381.

Ghusinga, K. R., Elston, T. C. and Jones, A. M. (2022). Towards resolution of a paradox in plant G-protein signaling. Plant Physiol. 188, 807–815.

Li, B., Tunc-Ozdemir, M., Urano, D., Jia, H., Werth, E. G., Mowrey, D. D., Hicks, L. M., Dokholyan, N. V., Torres, M. P. and Jones, A. M. (2018). Tyrosine phosphorylation switching of a G protein. J. Biol. Chem. 293, 4752–4766.

Mohanasundaram, B., Dodds, A., Kukshal, V., Jez, J. M. and Pandey, S. (2022). Distribution and the evolutionary history of G-protein components in plant and algal lineages. Plant Physiol. 189, 1519–1535.

Tunc-Ozdemir, M., Li, B., Jaiswal, D. K., Urano, D., Jones, A. M. and Torres, M. P. (2017). Predicted functional implications of phosphorylation of regulator of G protein signaling protein in plants. Front. Plant Sci. 8, 1456.

Watkins, J. M., Ross-Elliott, T. J., Shan, X., Lou, F., Dreyer, B., Tunc-Ozdemir, M., Jia, H., Yang, J., Oliveira, C. C., Wu, L., et al. (2021). Differential regulation of G protein signaling in Arabidopsis through two distinct pathways that internalize AtRGS1. Sci. Signal. 14,.

Žádníková, P., Smet, D., Zhu, Q., Van Der Straeten, D. and Benková, E. (2015). Strategies of seedlings to overcome their sessile nature: auxin in mobility control. Front. Plant Sci. 6, 218.